Chapter 1
Thermodynamics, Phases, and Phase Diagrams

In this chapter, we will briefly go through the basics of chemical thermodynamics. It is assumed that the reader is somewhat familiar with the fundamental concepts, and therefore, they are not discussed in great detail. The emphasis of the chapter is to build a thermodynamic foundation that can be utilized in the later chapters for diffusion kinetic analyses. We will put special emphasis on the use of different types of diagrams to represent thermodynamic data. Therefore, we introduce phase diagrams, potential diagrams, and Gibbs free energy diagrams in considerable detail. These "tools" are then used extensively in diffusion kinetic analysis later on in the book. We will conclude the chapter by introducing some commonly used thermodynamic conventions.

Classical thermodynamics is a phenomenological theory which deals with the physical properties of macroscopic systems under equilibrium conditions and the relations between them. The great importance of classical thermodynamics lies in its exactness as well as in its generality. It does not make any assumptions concerning the atomic structure of the system nor the interactions between the atoms. Even though this can be regarded as being beneficial in many applications, this can also be regarded as a weakness, especially in the case of solids and their solutions and compounds. Statistical thermodynamics, on the other hand, strives to obtain thermodynamic relationships based on the molecular behavior of matter. It provides additional information that cannot be achieved with classical thermodynamics. Firstly, statistical thermodynamics shows that the laws of thermodynamics are a direct consequence of the principles of quantum theory combined with one very general statistical postulate. Secondly, statistical thermodynamics provides general relations that cannot be derived from the laws of thermodynamics. Most importantly, by utilizing statistical thermodynamics, it is possible to obtain a physical understanding of the properties of solutions and about the reasons for their behavior. Thus, it is beneficial to utilize both of the approaches described above to obtain a more fundamental understanding of the behavior of different material combinations. The subject of thermodynamics is vast, and there are a large number of excellent books available [1–5]. The following seeks to summarize those parts of thermodynamics that are considered essential for a basic understanding of energetics in materials science. Further, the topics in Chap. 1 are

A. Paul et al., *Thermodynamics, Diffusion and the Kirkendall Effect in Solids*,
DOI: 10.1007/978-3-319-07461-0_1,

chosen in such a way to be closely correlated to the use of thermodynamics in the diffusion calculations from subsequent chapters. The treatment utilized in Chap. 1 partly follows the approach presented in the comprehensive textbook written by Kivilahti [6].

1.1 Thermodynamics System and Its State

The *system* is a clearly defined part of a macroscopic space, distinguished from the rest of the space by a physical boundary. The rest of the space (taking only the part that can be regarded to interact with the system) is defined as the *environment*. The system can be *isolated, closed,* or *open* depending on its interactions with the environment. An isolated system cannot exchange energy or matter, a closed system can exchange energy, but not matter, and an open system can exchange both energy and matter with the environment. A system can be homogeneous, thus thoroughly uniform, or heterogeneous. A homogeneous system is defined as a *phase*, which can be either a pure component (element or chemical compound) or a solution phase. A heterogeneous system, on the other hand, is a phase mixture. Thermodynamics aims to determine the state of the system under investigation. From experiment, it is known that when a certain number of macroscopic variables of the system have been fixed, the values of all other variables are also fixed and the state of the system becomes fully determined. In thermodynamics, the variables can be *extensive*, *intensive,* and *partial*. Extensive properties depend on the size of the system, whereas the intensive properties do not. Partial properties are the molar properties of a component. Those variables which are chosen to represent the system are called independent variables. A *macrostate* of the system is characterized, for example, by its temperature (T), pressure (p), and composition (n_i) or temperature (T), volume (V), and composition (n_i). A macrostate does not change over time if its observable properties do not change. The system can, however, go through changes in its state for a number of different reasons. These changes can be *reversible* or *irreversible*. A reversible change is a change that can be reversed by an infinitesimal modification of a variable, whereas irreversible processes have a definite direction which cannot be reversed. In a system, the energy of that system is constantly being redistributed among the particles of that system. The particles in liquids and gases are constantly redistributing in location as well as changing in quanta value (the individual amount of energy that each molecule has). Every specific arrangement of the energy of each molecule in the whole system at one instant is called a *microstate*. The nature of every microstate implicitly contains the important concept of *fluctuations* in it. It is evident that a given macrostate can be represented by number of different microstates.

1.2 The Laws of Thermodynamics

Thermodynamics is based on a few empirical generalizations, which are stated in the form of the following laws.

The zeroth law defines *temperature* such that if two systems are independently in equilibrium with a third system, they must also be in equilibrium with each other. Then, they have a common state variable—temperature.

The first law states the principle of conservation of energy such that the macrostate of a system can be characterized with an extensive variable, called internal energy E, which is constant in an isolated system. When the system interacts with the environment and transfers from one macrostate to another, the infinitesimal change in the internal energy can be stated as

$$E = dq + dw \tag{1.1}$$

where dq and dw are the heat and work transferred into the system during the change. When the system receives heat from the environment, $dq > 0$, and when the system gives up heat, $dq < 0$. The same is, of course, true for the work transferred. If the system does work, $dw < 0$, and if work is done on the system, $dw > 0$.If the external pressure acting on the systems' straight interface is p, then $dw = -pdV$, if the expansion work is the only form of work. The internal energy of the system is a state function. This means that dE is an *exact differential*. During a change, its value is, therefore, independent of the path between the initial and the final states. It is to be noted that dq and dw are not exact differentials, but infinitesimal quantities of heat and work, and thus, they are *path functions*. Their value, when integrated, depends on the path between the initial and final states.

The second law gives the criteria for the spontaneous change in nature that allows the macrostate in equilibrium to be characterized by a variable S, the entropy, which has the following properties

(i) Entropy, which is defined as

$$S = \left(\frac{dq}{T}\right)_{\text{rev}} \tag{1.2}$$

is a state function. In Eq. 1.2, the subscript rev refers to a reversible process. Entropy can be expressed as a function of the independent state variables of the system as $S = S(E, V_i, n_i)$. The infinitesimal entropy change of a closed system in an arbitrary reversible process can be thus written as

$$dS = \left(\frac{\partial S}{\partial E}\right) dE + \left(\frac{\partial S}{\partial V}\right) dV \tag{1.3}$$

By utilizing the first law $(dE)_{V,n_i} = dq$ and Eq. 1.2, we obtain

$$\left(\frac{\partial S}{\partial E}\right)_{V,n} = \frac{1}{T} \tag{1.4}$$

where T is the absolute temperature.

(ii) The entropy of the system is an extensive property.
(iii) The entropy of the system can change for one of two reasons, either as a result of the transfer of entropy between the system and the environment or by the creation of entropy within the system. The entropy change can be written as

$$dS = d_e S + d_i S \tag{1.5}$$

where $d_i S$ is the entropy created within the system. From the experiment, it is known that this quantity is *always positive*. During a totally reversible change, the entropy change can be zero. When the system is isolated, its entropy can never be decreased

$$dS = (dS)_{E,V} = d_i S \geq 0 \tag{1.6}$$

Hence, in real irreversible processes, the entropy of an isolated system always increases and reaches its maximum at the equilibrium state.

The third law states that the entropy of the system has a property that $S \to S_o$ when $T \to 0$, where S_o is a constant independent of the structure of the system. At absolute zero, the entropy of pure, defect-free, crystalline elements has the same value, S_o, which has been chosen to be zero.

Thus, the thermodynamics of closed and isolated systems is based on the following equations

$$\begin{aligned} dE &= dq + dw \quad \text{(for all changes)} \\ dS &= \frac{dq}{T} \quad \text{(for reversible changes)} \\ dS &\geq 0 \quad \text{(for changes in isolated systems)} \end{aligned}$$

These equations can be combined to give the fundamental equation for a closed homogeneous system

$$\begin{aligned} dE &= TdS + dw \quad \text{or} \\ dE &= TdS - pdV \end{aligned} \tag{1.7}$$

if only expansion work is considered.

Note The concept of entropy is highly ambiguous. Several interpretations have been given to entropy. The entropy law is a consequence of the fact that matter is composed of interacting particles that are in motion and which constantly show a tendency to muddle up and thereby to mix both matter and energy. Thus, it has been proposed that entropy is the measure of the systems mixed-upness (Gibbs), or the degree of disorder (Planck). According to Guggenheim, entropy is the measure of the spread of energy and matter. Shannon, on the other hand, has defined entropy as the lack of information or data [6].

The above equations are valid for closed systems with fixed composition. In order to extend the treatment to open heterogeneous systems, we need to choose a third variable, one that describes the composition and quantity of the system. This is the n_i being the number of moles of component i.

1.3 Heterogeneous Systems

A heterogeneous system is composed of several homogeneous subsystems, meaning phases which each have their own energy E^{ϕ}, entropy S^{ϕ}, and composition n_i^{ϕ} ($i = 1, 2, \ldots k$). Consequently, the energy, the entropy, and the number of moles of substance of the phase mixture are

$$E = \sum_{\phi} E^{\phi} \tag{1.8}$$

$$S = \sum_{\phi} S^{\phi} \tag{1.9}$$

$$n = \sum_{\phi} n^{\phi} = \sum_{\phi} \sum_{i} n_i^{\phi} \tag{1.10}$$

To exactly determine the state of the phase mixture requires that each phase that it contains must be described accurately. If we choose the variables (S, V, and n_i) to describe the state of a given phase, all other properties are then necessarily functions of the chosen variables. This means that especially the internal energy of a phase can be expressed as $E^{\phi}(S^{\phi}, V^{\phi}, n_i^{\phi})$. Its exact differential for an arbitrary change can be written as

$$dE = \left(\frac{\partial E}{\partial S}\right) dS + \left(\frac{\partial E}{\partial V}\right) dV + \sum_i \left(\frac{\partial E}{\partial n_i}\right) dn_i \tag{1.11}$$

When the composition of the phase does not change, Eq. 1.7 is valid and the first two partial derivatives in Eq. 1.11 are temperature of the phase (T) and its pressure (p). The last term is defined as the chemical potential of a component i. The chemical potential is defined formally in the following [1]: "If to any homogeneous mass we suppose an infinitesimal quantity of any substance to be added and its entropy and volume remaining unchanged, the increase of the energy of the mass divided by the quantity of the substance added is the (chemical) *potential* for that substance in the mass considered."

Consequently, we obtain an equation for the change in the phase internal energy

$$dE^{\phi} = T^{\phi} dS^{\phi} - p^{\phi} dV^{\phi} + \sum_i \mu_i^{\phi} dn_i^{\phi} \tag{1.12}$$

This equation is the fundamental equation for the independent variables S, V, and n_i. The internal energy E is their characteristic function, the thermodynamic potential of the phase. In a thermodynamic system, each phase has such a potential.

Next, a new thermodynamic function is defined with the help of internal energy and entropy

$$F = E - TS \tag{1.13}$$

By differentiating the function and by substituting Eq. 1.13 into the differential form of 1.12, we obtain

$$dF^{\phi} = -S^{\phi} dT^{\phi} - p^{\phi} dV^{\phi} + \sum_i \mu_i^{\phi} dn_i^{\phi} \tag{1.14}$$

This equation defines the Helmholtz free energy F, which is a function of the independent variables T, V, and n_i. The properties of this free energy function shall be discussed in more detail in Sect. 1.5.

Let us further examine the function E^{ϕ} with independent variables (S^{ϕ}, V^{ϕ}, and n_i^{ϕ}). Because T, p, and μ_i are intensive variables, they are not dependent on the amount of phase ϕ. From this, it follows that as the intensive variables remain constant, Eq. 1.12 can be integrated. This gives the thermodynamic potential of phase ϕ as

$$E^{\phi} = TS^{\phi} - pV^{\phi} + \sum_i \mu_i^{\phi} n_i^{\phi} \tag{1.15}$$

Next, we define two new functions, the enthalpy (H) and the Gibbs free energy (G)

$$H \equiv E + pV \tag{1.16}$$

$$G \equiv H - TS \tag{1.17}$$

By recalling the definition of Helmholtz free energy (1.13), Eq. 1.15 (together with 1.16 and 1.17) yields a function

$$G^{\phi} = \sum_i \mu_i^{\phi} n_i^{\phi} \tag{1.18}$$

This function (Gibbs free energy) is also a thermodynamic potential of a phase, and it is an extensive variable. Therefore, the Gibbs free energy of a phase mixture is given as

$$G = \sum_{\phi} \sum_i \mu_i^{\phi} n_i^{\phi} \tag{1.19}$$

When the Gibbs free energy function for a phase is known, all other thermodynamic properties of a given phase can be expressed with the help of this potential and its derivatives. The properties of the Gibbs free energy function are discussed in more detail in Sect. 1.5.

1.4 Commonly Used Terms and First Glance at Phase Diagrams

Thermodynamics is an exact discipline. Therefore, it is of great importance to define a few more key terms which will be frequently encountered later on in the text. *A component* refers to independent species in the system under investigation, giving the minimum number of substances which must be available in the laboratory in order to make up any chosen equilibrium mixture of the system in question. *A phase* is a region of uniformity in a system under investigation, as already stated. It is a region of uniform chemical composition and uniform physical properties. A phase is also distinguished from other dissimilar regions by an interface.

To illustrate the concepts of *compound* and a *phase,* we will consider a simple example H_2O. Ice, water, and water vapor are all different phases of the compound H_2O that exist in different temperature and pressure ranges, as shown in Fig. 1.1. The diagram shown in Fig. 1.1 is called a *unary phase diagram* and is shown for water in the figure. The point marked as C is called the critical point. When temperature rises above that critical point, the gas phase (water vapor) cannot be liquefied by increasing the pressure. The curve TC gives the equilibrium vapor pressure of the liquid as a function of temperature up to the critical point. At point *T* (called the triple point), all three phases of water are in equilibrium with each other.

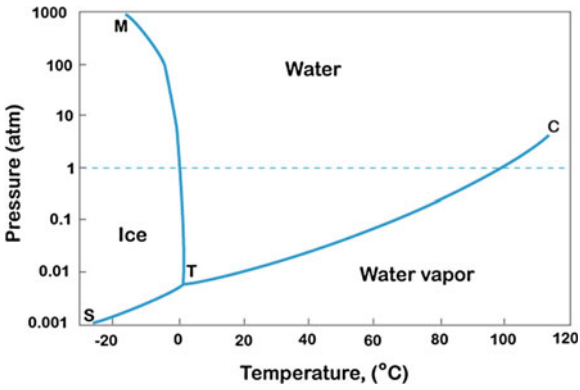

Fig. 1.1 The pressure–temperature diagram of H_2O

Based on the Gibbs phase rule (derived later on) at this point, the number of degrees of freedom is zero. The equilibrium can therefore be attained only at a specific temperature and pressure. The curve ST gives the equilibrium vapor pressure of the solid (ice) as a function of temperature. The curve TM gives the change in the melting point of ice as a function of pressure. It is to be noted here that the curve TM for the system H_2O is highly unusual as the TM curve here is descending, whereas in most of the systems, it is ascending. This is a result of the fact that the molar volume of solid water (ice) is larger than that of liquid water (in Sect. 1.7 is introduced the Clausius–Clapeyron equation that can be used to calculate this). In most systems, however, the opposite is true. Another unary system exhibiting this type of behavior (i.e., larger volume in solid than in liquid) is bismuth (Bi).

Different pure elements, for example, Cu or Ni, also have three different phases: solid, liquid, and gas. Similarly, two allotropic forms, solid gray tin and white tin, which have a different crystal structure and properties, are considered as distinct phases. To show the example of phases with two different components, we consider the Ag–Cu *binary phase diagram*, which is shown in Fig. 1.2. All phases are made of the two components, Ag and Cu. The different phases α, β, and liquid are stable within a certain *temperature* and *composition* (expressed here as weight percentage) range. Note that the phase diagram shown in Fig. 1.2 is determined at constant pressure. The α-phase is basically a solid solution Ag(Cu), that is, Ag (with its face-centered cubic (FCC) structure) with a limited amount of dissolved Cu, whereas the β-phase is a solid solution Cu(Ag), that is, Cu (with FCC structure) with a limited amount of dissolved Ag. Different notations (α and β) are used to differentiate solid solutions from pure elements. The *solvus* curve separates the single solid-phase region α from the solid two-phase region $\alpha + \beta$. Similarly, another solvus curve separates the one-phase solid region β from that of the solid two-phase region $\alpha + \beta$. The *solidus* curve separates the solid one-phase α-region from the two-phase region where the solid α and the liquid are in equilibrium. Similarly, another solidus curve separates the solid one-phase region β from the two-phase region β + liquid. The *liquidus* curve, on the other hand, separates the two-phase α + liquid and β + liquid areas from the liquid one-phase area L. In

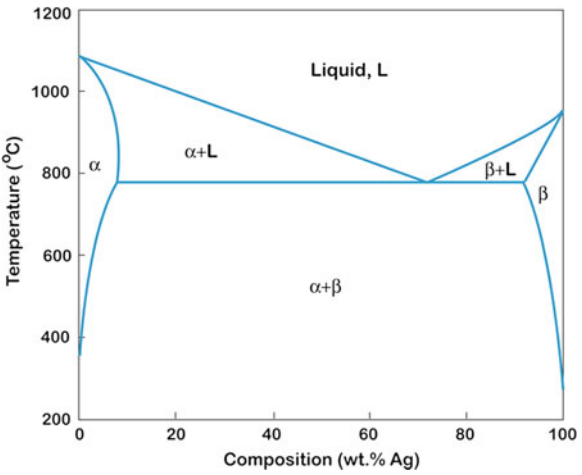

Fig. 1.2 Binary phase diagram of Ag–Cu

Fig. 1.2, there is a horizontal line of specific importance. It represents the so-called eutectic reaction, where liquid L reacts to form two new solid phases α and β. At the line, there are three phases L, α, and β which are in equilibrium with each other. According to the Gibbs phase rule (note that here the pressure is constant), such an equilibrium in a binary system can exist only at a specific temperature and only with specific compositions of the three phases participating in the equilibrium. It is common practice to show the stability of phases in a single-component system in different temperature and pressure ranges as shown in Fig. 1.1. In a binary system case, the stability of the phases is shown in a different temperature and composition range under constant pressure. Unless mentioned, a binary phase diagram (shown in Fig. 1.2) is commonly determined at atmospheric pressure. Note that at different pressure, the binary temperature–composition phase diagram will be different since the equilibrium transition temperature between different phases changes with pressure. It is also to be noted that typically, especially in the case of metals, the vapor region is not shown in the binary phase diagram as it typically exists at relatively high temperatures under atmospheric pressure. Finally, it is important to realize that one cannot obtain any information about kinetics or the morphology of the phase mixture from the phase diagram. The diagram only gives information about the phases that can be in equilibrium under certain composition–temperature combinations. Although there are three different species present in a system, there are times when the phase diagram is presented as a binary phase diagram. For example, as Fig. 1.3 shows, the $MgO–Al_2O_3$ phase diagram is presented as a binary phase diagram, where MgO and Al_2O_3 are considered as the components. The reason for this is clear. Even though there are three species (Mg, O, and Al) in the system, there are only two components (MgO and Al_2O_3). Only the amounts of these components can be changed *independently*. This is called a pseudobinary phase diagram.

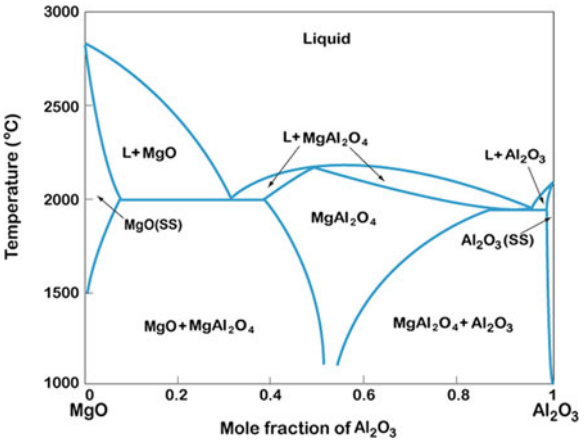

Fig. 1.3 Pseudobinary phase diagram of MgO and Al_2O

In a ternary system (Fig. 1.4), where three elements are mixed, the phase diagrams take the standard form of a prism which combines an equilateral triangular base (ABC) with three binary system "walls" (A–B, B–C, and C–A). This three-dimensional form allows the three independent variables to be specified (two-component concentrations and temperature). In practice, determining different sections of the diagram from these kinds of graphical models is difficult and, therefore, horizontal (isothermal) sections through the prism are used (Fig. 1.4b). The isothermal section is a triangle at a given temperature, where each corner represents the pure element, each side represents relevant binary systems, and areas of different phases can be determined inside the triangle. In addition to the isothermal section, also vertical sections (isopleths) can be taken from a space diagram of a given ternary system. We will return to these diagrams and their uses in Sects. 1.12 and 1.13.

Another commonly used term, as already mentioned, is *composition*. Composition can be expressed in terms of mole fraction, atomic fraction or atomic percentage, and weight fraction or weight percentage. It should be pointed out that in a binary (not pseudobinary) or multicomponent system, the mole fraction is equal to the atomic fraction. This can be shown very easily for a system of total 1 mol, where X_A and X_B are mole fractions of A and B, respectively. This can be written as

$$X_A + X_B = 1 \tag{1.21}$$

If n_A and n_B are the total number of atoms of A and B, respectively, we can write

$$X_A = n_A/N_o \quad \text{and} \quad X_B = n_B/N_o \tag{1.22}$$

where N_o (=6.022 $\times$ 10^{23} atoms/mole) is the Avogadro number.

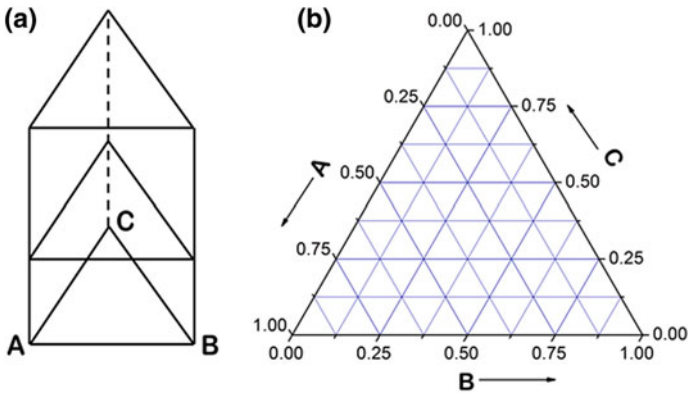

Fig. 1.4 **a** Ternary system, and **b** isothermal section at $T = x$ °C

This means that the atomic fraction of A (N_A) and B (N_B), with the help of Eq. 1.21, can be expressed as

$$N_A = \frac{n_A}{n_A + n_B} = \frac{X_A N_o}{X_A N_o + X_B N_o} = \frac{X_A}{X_A + X_B} = X_A \tag{1.23a}$$

$$N_B = \frac{n_B}{n_A + n_B} = \frac{X_B N_o}{X_A N_o + X_B N_o} = \frac{X_B}{X_A + X_B} = X_B \tag{1.23b}$$

Although in the previous example, we considered the one-mole system (which will be useful in the proceeding section), it can be shown that the mole fraction is always equal to the atom fraction, even if the system has a total more or less than one mole of atoms. For example, we consider the system of total x mole, where the mole of A and B are x_A and x_B, respectively. This can be written as

$$x_A + x_B = x \tag{1.24}$$

The mole fraction of A, X_A, can be expressed as

$$X_A = \frac{x_A}{x} = \frac{x_A}{x_A + x_B} \tag{1.25}$$

Consequently, the atomic fraction of A, N_A, can be expressed as

$$N_A = \frac{n_A}{n_A + n_B} = \frac{x_A N_o}{x_A N_o + x_B N_o} = \frac{x_A}{x_A + x_B} = x_A \tag{1.26}$$

A similar expression can be derived for B.

Concentration can be expressed as *molal concentration,* that is, c_i = number of moles (g-atoms, g-ions, etc.) of the solute i per 1,000 g of solution, or as *volume concentration,* that is, the number of moles per cubic meter (m^3). It is to be noted that the latter definition is valid only at constant temperature. When describing the composition of the liquid solution, for example, it is expedient to use as the two other independent variables (in addition to composition regardless of how it is expressed) temperature and pressure, so that differentiation with respect to temperature implies constant pressure. Thus, we have

$$\left(\frac{\partial C}{\partial T}\right) = -\alpha C_S$$

where α is the thermal expansivity and C_s is the concentration of the species of interest. The relation above shows that if C_s is chosen as a variable, it will not be an independent variable [2]. Further, when we consider the solid state, it becomes evident that in order to use volume concentrations, we should have knowledge about the molar volume as a function of composition of the phase under investigation. This is why volume concentrations are not always convenient variables and, for this reason, will not typically be used later on in the text.

1.5 Spontaneous Change

Entropy is the basic fundamental concept when the direction of natural change is considered as discussed in Sect. 1.2. Unfortunately, the use of entropy as the criteria for spontaneous change requires that changes in both the system and the environment are investigated. As the environment is not always easily defined, the entropy criterion is not convenient to use in many practical cases. However, if we concentrate on the system, we may lose some generality but gain a lot in the sense that the environment no longer needs to be considered. Next, we will look in greater detail how this can be achieved. Consider a system in thermal equilibrium with its surroundings at a temperature T. When a change in the system occurs, the second law of thermodynamics states (the Clausius inequality)

$$dS - \frac{dq}{T} \geq 0 \tag{1.27}$$

Depending on the conditions under which the process occurs, this inequality can be developed in two ways.

(i) Heat transfer at constant volume

In the absence of non-expansive work, it is possible to write $dq_V = dE$. This is because as volume is kept constant and only expansion work is considered, the work done by or to the system must be zero. Thus, we can write

$$dE = dq$$

and utilizing Eq. 1.27, the following is obtained

$$dS - \frac{dE}{T} \geq 0 \tag{1.28}$$

It is to be noted that here the criteria of spontaneity is expressed in terms of state functions only. Equation 1.28 can be rearranged as

$$TdS \geq dE \quad (V \text{ constant, no additional work}) \tag{1.29}$$

At either constant internal energy ($dE = 0$) or constant entropy ($dS = 0$), Eq. 1.29 can be expressed as

$$dS_{E,V} \geq 0 \quad \text{or} \quad dE_{S,V} \leq 0$$

The first inequality states that entropy increases in a spontaneous change in a system with constant volume and constant internal energy. The second inequality states that given the constant entropy and volume of a system, its internal energy decreases during spontaneous change. This is, in fact, a statement about entropy since it states that if the entropy of the system remains unchanged in the transformation, there must be an increase in the entropy of the environment caused by the outflow of heat from the system.

(ii) Heat transfer at constant pressure

Again, in the absence of non-expansive work, we may write $dq_p = dH$ and obtain

$$TdS \geq dH \quad (p \text{ constant, no additional work}) \tag{1.30}$$

At constant enthalpy or entropy, the following inequalities are obtained

$$dS_{H,p} \geq 0 \quad \text{or} \quad dH_{S,p} \leq 0$$

which can be interpreted in a similar fashion as inequalities concerning heat transfer at constant V.

Unfortunately, transformations where E and V, H and p, S and V, or S and p are constant are rare. Far more frequently, transformations take place under conditions where V and T, or even more typically, p and T, are constant.

Equations 1.29 and 1.30 can be written as

$$dE - TdS \leq 0 \quad \text{and} \quad dH - TdS \leq 0 \tag{1.31}$$

The Helmholtz and Gibbs free energy functions were defined as follows (Sect. 1.3)

$$F = E - TS \text{ and } G = H - TS \tag{1.32}$$

At constant temperature, the differentials of the functions F and G are

$$(dF)_{T,V} = dE - TdS \tag{1.33}$$

$$(dG)_{T,p} = dH - TdS \tag{1.34}$$

where the entropies of the phases have been replaced by the temperature of the system. We get two new inequalities for a spontaneous change with frequently observed variables

$$(dF)_{T,V} \leq 0 \tag{1.35}$$

$$(dG)_{T,p} \leq 0 \tag{1.36}$$

(iii) Expansion work is not the only form of work

How shall the above-derived conditions for spontaneity change if the expansion work is no longer the only form of work? The second law of thermodynamics states that $dE = dq + dw_{\text{tot}}$, where $dw_{\text{tot}} = dw' - pdV$ is the total work and dw' takes into account all other forms of work except expansion work. By solving dq, we get

$$dq = dE - dw' + pdV \tag{1.37}$$

and utilizing the fact that $dq - TdS \leq 0$, we obtain

$$dE - TdS - dw' + pdV \leq 0 \tag{1.38}$$

By utilizing the definition of the Helmholtz free energy, we obtain

$$(dF)_T \leq dw' - pdV = dw_{\text{tot}} \tag{1.39}$$

Thus, at constant T, change occurs spontaneously when the change in Helmholtz energy is smaller than the total amount of work. If the volume is constant $dV = 0$, then

$$(dF)_{T,V} \leq dw' \tag{1.40}$$

which is equal to Eq. 1.39 when the expansion work is the only form of work.

From the definition of enthalpy ($H = E + \text{pV}$) and from $dE = dq + dw' - pdV$ under constant pressure, it follows that

$$(dH)_p = dE + pdV = dq + dw' - pdV + pdV \tag{1.41}$$

which gives

$$dq_p = (dH)_p - dw' \tag{1.42}$$

Combining this with Eq. 1.31 results in

$$dH - TdS - dw' \leq 0 \text{ (constant pressure)} \tag{1.43}$$

and finally,

$$(dG)_{T,p} \leq dw' \tag{1.44}$$

At constants T and p, the change is spontaneous if the change in Gibbs energy is less than the additional work done. Equations 1.44 and 1.40 can be stated also as *$-\Delta G$is the maximum amount of work (other than expansion work) that the system can release during spontaneous change at constant temperature and pressure. The value $-\Delta F$is the maximum amount of total work that the system can release during spontaneous change at constant temperature.*

Given that $G = G(T, P, n_1, n_2, \ldots)$ in an open system, with n_i being the number of moles of component i, the derivative of the Gibbs energy function yields

$$dG = -SdT + Vdp + \sum_i \mu_i dn_i \tag{1.45}$$

where μ_i is the chemical potential of component i. At a constant value of the independent variables P, T, and $n_j (j \neq i)$, the chemical potential equals the partial molar Gibbs free energy, $(\partial G/\partial n_i)_{P,T,j\neq i}$. The chemical potential (partial Gibbs energy) has an important function analogous to temperature and pressure. A temperature difference determines the tendency of heat to flow from one body into another, while a pressure difference, on the other hand, determines the tendency toward a bodily movement. A chemical potential can be regarded as the cause of a chemical reaction or the tendency of a substance to *diffuse* from one phase to another.

As shown before in Eq. 1.17, the Gibbs free energy can be expressed as

$$G = H - TS$$

where H (J/mole) is the enthalpy, T (Kelvin, K) is the absolute temperature, and S (J/mole K) is the entropy of the system. Further, H, the total heat content or total energy of the system, was defined in Eq. 1.16 as

$$H = E + pV$$

where E is the internal energy, P is the pressure, and V is the volume of the system.

In general, the contribution of PV in Eq. 1.16 is very small in the solid and liquid states if the pressure is not exceptionally high. Therefore, while working with condensed phases (solid and liquid), the PV term can, in most cases, be neglected. Hence, the change in internal energy of the system can be approximated to be equal to its enthalpy

$$H = E \tag{1.46}$$

The internal energy of the system consists of the potential and kinetic energies of the atoms within the system. The kinetic energy of solids and liquids is caused by the vibration of atoms at their position. In liquids and gases, the translational and rotational movement of the atoms (or molecules), within the system, provides an additional contribution to the kinetic energy. Every atom vibrates with different energy at its position with degrees of freedom in x, y, and z directions with very high frequency that is temperature dependent. The frequency spectrum starts from 0 and goes up to a maximum value of v_D, which is called the Debye frequency. By utilizing the vibration frequencies, it is possible to calculate the heat capacity of a given solid. Above a certain temperature (θ_D, the Debye temperature), all atoms are essentially vibrating with their corresponding maximum Debye frequency. For metals at room temperature, they are typically above their Debye temperature, which makes it possible to use single (maximum) frequency values when considering the diffusion of atoms, for instance. The average total energy ($=3NkT$ where k is the Boltzmann constant and N is the number of atoms in a crystal) of atoms is fixed with respect to a particular temperature. Moreover, the vibration of any atom depends on the vibration of neighboring atoms because of inter-atomic bonding. This coupling produces an elastic wave with quantized energy. The quantum of energy in an elastic wave is called a phonon. For example, sound waves and thermal vibrations in crystals are phonons. The other part of internal energy in solids, the potential energy, depends on the inter-atomic bonding between the atoms. In a single-component system, the potential energy depends on one type of bonding, but, in a binary or multicomponent system, the potential energy depends on the type, number, and magnitude of the different bonds between the atoms within the system. This is explored further in Sect. 1.9 for binary systems cases. The entropy of a crystal is composed of two terms: *thermal entropy* and the *configurational entropy*. The first part is concerned with the distribution of energy over the available energy states in the crystal (system) and the latter part with the distribution of atoms or particles within the crystal (system).

Note By utilizing the Gibbs free energy, all forms of work (excluding expansion work) can be taken into account $\mathbf{-(\Delta G)_{p,T} \geq w' = \Sigma \mu_i n_i + \gamma A + zFU + \cdots}$, where the first term is the chemical part, the second is the surface energy contribution, the third is the electrical component, etc. Thus, Gibbs energy gives the amount of maximum additional (non-expansion) work that the system can perform. For all spontaneous processes, the change in Gibbs energy must be negative. It should also be noted that the temperature and pressure of the system do not have to be constant during the whole process. It is adequate that they are the same at the initial and final stages. An example is an exothermic reaction taking place at temperature T, where the reaction heat is transferred to the environment at the end of the reaction, thus making T_{initial} equal to T_{final}. This is, of course, a consequence of the fact that the Gibbs energy is a state function and its value is only dependent on the initial and final states, not the path between them.
The Helmholtz free energy of a closed system, on the other hand, is a function of *temperature* and *volume*. Helmholtz free energy (F) is maximum free energy, which can be used to do work at constant volume and temperature and can be expressed as

$$F = E - TS$$

where E is the internal energy. The main difference between Gibbs free energy (i.e., the change in energy at constant pressure and temperature) and Helmholtz free energy (i.e., the change in energy at constant volume and temperature) is "PV". This comes from the fact that there is need for extra work to accommodate the volume change. Thus, the Helmholtz free energy is the maximum amount of any kind of work the system can do and is, therefore, sometimes called the maximum work function. The change in Helmholtz free energy must also always be negative for a spontaneous change.

With the help of the Gibbs free energy function derived above, the equilibrium state of the system can be investigated. There is the relation between the chemical potential of components and the total Gibbs energy of the system, as expressed in Eq. 1.19 (Sect. 1.3) through

$$G_{\text{tot}} = \sum_{\phi} \sum_{i} \left(\mu_i^{\phi} n_i^{\phi} \right)$$

The Gibbs energy function can be utilized from the component level to the system level and back again. Hence, Eq. 1.19 provides the very important connection between component and system level properties.

Three stable equilibrium states to be considered here are (i) complete or global thermodynamic equilibrium, (ii) local thermodynamic equilibrium, and (iii) partial thermodynamic equilibrium. When the system is at *complete equilibrium,* its Gibbs free energy (G) function has reached its minimum value

$$dG = 0 \quad \text{or} \quad \mu_i^{\alpha} = \mu_i^{\beta} = \cdots = \mu_i^{\phi}, \quad (i = \mathrm{A}, \mathrm{B}, \mathrm{C}, \ldots) \tag{1.47}$$

and then, the system is in mechanical, thermal, and chemical equilibrium with its surroundings. Consequently, there are no gradients inside the individual phases and no changes in the macroscopic properties of the system are to be expected.

Local equilibrium, on the other hand, is defined in such a way that the equilibrium exists only at the interfaces between the different phases present in the system. This means that the thermodynamic functions are continuous across the interface and the compositions of the phases right at the interface are very close to those indicated by the equilibrium phase diagram. This also indicates that there are activity gradients in the adjoining phases. These gradients, together with the diffusivities, determine the diffusion of components in the various phases of a joint region.

Partial equilibrium means that the system is in equilibrium only with respect to certain components. It is generally found that some processes taking place in the system can be rapid, while others are relatively slow. If the rapid ones occur quickly enough to fulfill the requirements for stable equilibrium (within the limit of error) and the slow ones are slow enough that they can be ignored, then it is quite proper to treat the system as being in equilibrium with respect to the rapid processes alone [7].

It is also possible that the global energy minimum of the system is not accessible owing to different restrictions. In such cases, we are dealing with metastable equilibrium, which can be defined as a local minimum of the total Gibbs energy of the system. In order to obtain global stable equilibrium, some forms of activation (e.g., thermal energy) must be brought into the system. It is to be noted that metastable equilibrium can also be complete, local, or partial; the local metastable equilibrium concept, in any case, will be used frequently in the following sections. Very often, one or more interfacial compounds, which should be thermodynamically stable at a particular temperature, are not observed between two materials and, then, these interfaces are in local metastable equilibrium. Another situation commonly encountered occurs in solid/liquid reaction couples, where during the few first seconds, the solid material is in local metastable equilibrium with the liquid containing the dissolved atoms, before the intermetallic compound(s) is formed at the interface. In fact, a principle commonly known as *Ostwald's rule* states that, when a system undergoing reaction proceeds from a less stable state, the most stable state is not formed directly but rather the next more stable state is formed, and so on, step by step until (if ever) the most stable is formed. It is a fact that most materials used in everyday life have not been able to reach their absolute minimum energy state and are, therefore, in metastable equilibrium. It should be noted that a system at metastable equilibrium has thermodynamic properties, which are exactly determined, just as a system at stable equilibrium.

1.6 Free Energy and Phase Stability of Single-Component System

Different phases of a single element can be stable at a different temperature range under a particular pressure (we consider atmospheric pressure). For example, below the melting point, a solid phase is stable, whereas above the melting point, a liquid phase is stable. In general, at a particular temperature, the phase with the lowest Gibbs free energy will be the stable one. If at a particular temperature, the free energy of two phases is the same, then both phases are stable at that temperature. This takes place, for example, at the melting point where the solid and the liquid phases exist together. This also means that the system is in equilibrium and there is no driving force for change. To explain the stability of phases at different temperatures, we need to know the change in their free energies as a function of temperature. Consequently, (following Eq. 1.18) in order to determine free energy at a particular temperature, it is necessary to determine the enthalpy and the entropy at that particular temperature. Both properties can be determined from the knowledge of specific heat at constant pressure, C_P. The specific heat or specific heat capacity C_P (J/mole K) is defined as the amount of heat required to increase the temperature of a system by one Kelvin under constant pressure.

The absorption or release of heat, *dq,* in a reversible process, at constant pressure from the system to the surrounding area is equal to the enthalpy change, *dH,* of the system. We can write

$$dq = dH \tag{1.48}$$

Further, from the definition of C_p, the equation can be written

$$C_p = \frac{dq}{dT} \tag{1.49}$$

From Eqs. 1.48 and 1.49, follows

$$dH = C_p dT \tag{1.50}$$

By integrating Eq. 1.50, it can be expressed as

$$\begin{aligned} \int_o^H dH &= \int_o^T C_P dT \\ H_T &= H_o + \int_o^T C_P dT \end{aligned} \tag{1.51}$$

where H_T and H_o are enthalpy at temperature T and 0 K, respectively.

The enthalpy at room temperature 298 K is often known, and Eq. 1.51 can be written as

$$H_T = H_{298} + \int_{298}^{T} C_P dT \tag{1.52}$$

Further, from the definition of entropy for a reversible process, we know

$$dS = \frac{dq}{T} = \frac{C_P dT}{T} \tag{1.53}$$

By integrating Eq. 1.53, we get

$$S_T = S_o + \int_{o}^{T} \frac{C_P}{T} dT = \int_{o}^{T} \frac{C_p}{T} dT \tag{1.54}$$

where S_o is the entropy at 0 K. However at 0 K, the entropy of a defect-free pure element is, by definition, zero (according to the third law of thermodynamics). Moreover, if the entropy at 298 K is known, then Eq. 1.54 can be written as

$$S_T = S_{298} + \int_{298}^{T} \frac{C_P}{T} dT \tag{1.55}$$

Note We have considered above a pure element with a defect-free structure. However, it is to be emphasized that it is impossible to obtain a defect-free structure at temperatures above 0 K. There will always be a certain amount of point defects, such as vacancies and impurities present in the structure under the equilibrium condition. The free energy of a phase including the contribution from defects can be expressed as

$$G_m = G + \Delta G_d$$

G_m is the free energy of a single-component material with point defects; G is the free energy of the defect-free material, and ΔG_d is the free energy change because of the presence of defects. As will be shown later on, vacancies, for instance, are always present with a certain equilibrium concentration above 0 K. However, since the concentration of defects, in general, is small compared to the number of atoms, we can in many cases neglect the contribution from ΔG_d.

In general, the C_P values for different phases can be experimentally determined and are available in the literature. The way that C_P typically varies with temperature is shown in Fig. 1.5a. From the knowledge of C_P, it is possible to calculate H and S at a particular temperature T and consequently determine the variation of free energy G as a function of temperature. If there are phase transformations within the temperature range of interest, the enthalpies and entropies of the corresponding transformation must be added, at the appropriate T, and the integration must continue with the C_p value of the new phase, to obtain the correct H and S at the required temperature. The enthalpy of the formation of all pure elements under atmospheric pressure and with their most stable form at room temperature (298 K) has been defined to be zero at all temperatures. These are called the standard enthalpies of formation. And from these, the enthalpy change as a function of temperature can be determined as $H_T = \int_{298}^{T} C_P dT$. The typical change in enthalpy, entropy, and free energy is shown in Fig. 1.5b. There are a few important points that should be noted here. It is clear from Eq. 1.50 that the slope of the enthalpy curve dH/dT is equal to C_P. Since the value of C_P always increases with temperature, the slope of the enthalpy curve will also increase continuously with rising temperature. Further, from standard thermodynamic relation, we know that $dG = Vdp - SdT$. Since transformations at constant pressure are under consideration, we can write $dG = -SdT$. Hence, the slope of the free energy curve dG/dT is equal to $-S$. Since entropy always increases with temperature, the slope of the free energy, G, should always decrease with rising temperature.

Now, let us consider the stability of the solid and liquid phases of a metal. To do this, we will first need to determine the change in free energy with temperature for both solid and liquid phases separately. From Eqs. 1.17, 1.50, and 1.55, we can write the expressions for free energy for solid and liquid phases as

$$G^S = H_0^S + \int_0^T C_P^S dT - T\int_0^T \frac{C_P^S}{T} dT \tag{1.56a}$$

$$G^L = H_0^L + \int_0^T C_P^L dT - T\int_0^T \frac{C_P^L}{T} dT \tag{1.56b}$$

The superscripts "S" and "L" are denoted for solid and liquid phases, respectively. In general, the C_P of the liquid phase at a particular temperature is higher than that of the solid phase. The typical variation of C_P for solid and liquid phases is shown in Fig. 1.6a. The corresponding changes in enthalpy and free energy as a function of temperature of the phases are shown in Fig. 1.6b.

As already discussed, the pV term for both solid and liquid phases is very small and the enthalpy can be taken to be practically equal to E. Therefore, the Gibbs energy function can be written as $G = E - TS$, making the free energy low for a

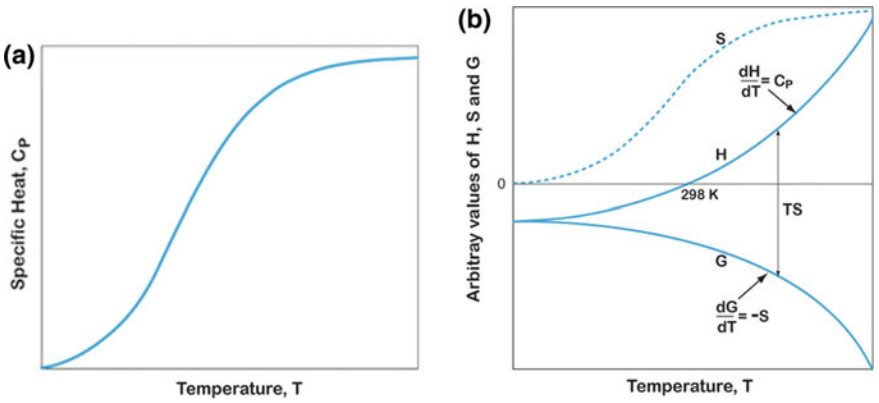

Fig. 1.5 **a** Typical change of C_P with temperature. **b** Arbitrary values of H, S, and G with temperature. Note that in many metals, the enthalpy is zero at room temperature, 298 K

phase with a low internal energy E and/or high entropy S. It is also apparent that at low temperature, the E term will dominate, whereas at higher temperature, the term becomes more and more significant. In general, the solid phases have higher bonding energies compared to those of liquid phases. So the internal energy, i.e., enthalpy, of the solid phase is lower than the liquid phase. Further, the entropies of liquids are typically larger than those of solids. Thus, at higher temperatures, the liquid phase becomes stable. From Fig. 1.6b, it can be seen, for instance, that below the melting point the solid phase is stable, whereas above the melting point the liquid phase is stable. At the melting point, their Gibbs energies are the same, as discussed in the beginning of this section.

Now, let us turn to consider solid-state transformation between gray tin to white tin. Gray tin has a diamond crystal structure which is very brittle. White tin, on the other hand, which is commercially available with a metallic luster has a BCT (body-centered tetragonal) structure. The Gibbs energy curves for both structures are shown in Fig. 1.7.

In Fig. 1.7, the molar Gibbs energy of the BCT-Sn has been set at zero for all temperatures. Thus, the BCT-Sn is the *reference state*. The Gibbs energies of different forms of Sn are then compared against this self-chosen reference value. As can be seen from Fig. 1.7, BCT-Sn should be stable between 13 and 232 °C. Below 13 °C, Sn with a diamond structure is the most stable form of tin, and above 232 °C, the liquid Sn is the most stable form of tin. It is to be noted that even though the transition temperature between the diamond and body-centered tetragonal structures is 13 °C, in practice the transformation requires undercooling to about −30 °C. This is because at 13 °C, the two crystal structures are in equilibrium and their Gibbs energies are the same. Thus, the driving force for the transformation is zero. As temperature decreases, the driving force for the transformation increases and the kinetics becomes slower. Thus, the optimum conditions for the transformation are found at −30 °C. This occurrence of the low

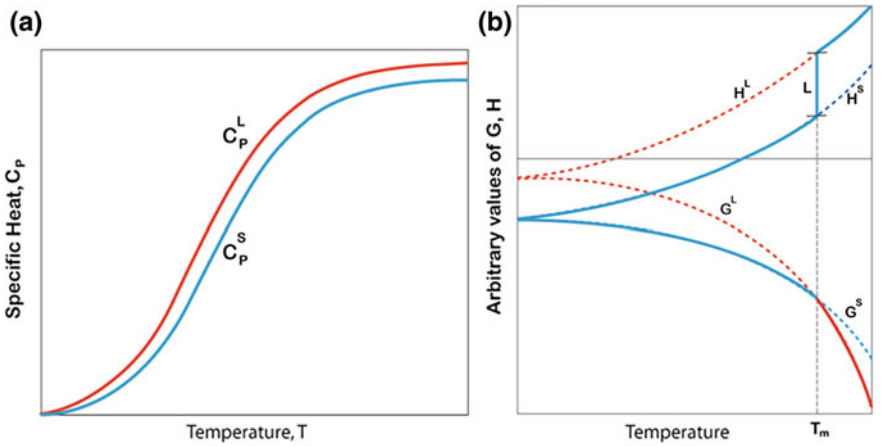

Fig. 1.6 **a** Arbitrary values of specific heat at constant pressure solid and liquid phase. **b** The change of enthalpy (H^S-enthalpy of solid phase, H^L-enthalpy of liquid phase) and free energy (G^S-free energy of solid phase, G^L-free energy of liquid phase) of solid and liquid phases with temperature. L is the latent heat of fusion. Solid line follows the change of enthalpy and free energy of the system with temperature

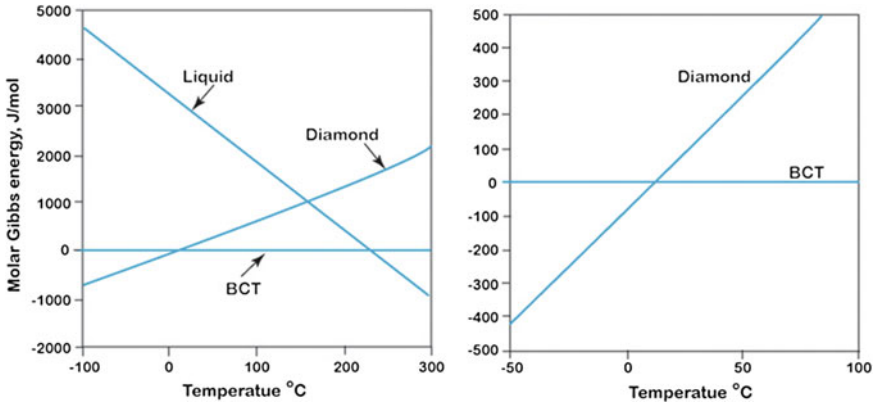

Fig. 1.7 The molar Gibbs energies of different phases of Sn as a function of temperature at 1 atm pressure. The figure on the right shows an enlarged part of the figure on the left

temperature diamond form of Sn should be avoided as it will lead to a phenomenon called tin pest. Owing to the much larger molar volume of Sn with the diamond structure (in comparison with the smaller BCT-Sn), the transition fractures (or even pulverizes) the tin objects going through the transition. One can also determine the hypothetical melting point of the diamond Sn from the intersection point of the metastable part of the diamond Gibbs energy curve with that of the liquid phase. It turns out to be about 160 °C.

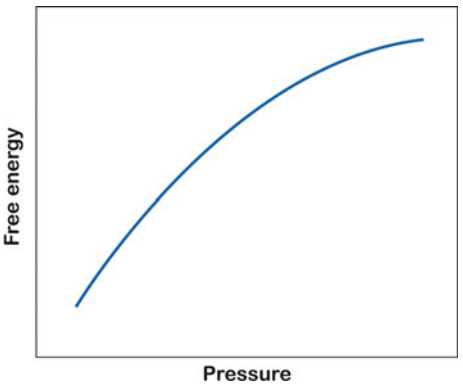

Fig. 1.8 The variation of molar Gibbs free energy g with increase in pressure

The increasing importance of the entropy term (−TS) is the reason why in many metals, we find the phase with a relatively closely packed structure is stable at a lower temperature, whereas a relatively loosely packed structure is stable at higher temperature. The reason for this lies in a more loosely packed structure where there is a higher degree of vibrational freedom. For instance, α-Ti with an HCP structure is stable at low temperature, whereas β-Ti with a BCC structure is stable at high temperature.

1.7 Pressure Effect of Single-Component Phase Diagram

Until now, as mentioned earlier, it has been assumed that all transformations occur under constant, typically atmospheric, pressure. If we consider the Gibbs free energy at constant temperature but under different pressure, for example, at higher pressure, then the freedom for vibration of atoms will be decreased in comparison with the normal pressure. This will result in an increase in free energy, as shown in Fig. 1.8. We know from the standard thermodynamic relation $dG = Vdp - SdT$ that the slope of the free energy versus pressure curve is equal to volume *V,* at constant temperature. Since the volume of matter generally decreases with increasing pressure, the slope of the free energy versus pressure curve will be positive, but it will decrease continuously with increasing pressure. Consequently, the equilibrium transition temperature from one phase to another will be different under different pressures and depending on the conditions, the transition temperature with increasing pressure might increase or decrease. This can be understood as being based on the Clausius–Clapeyron relation, which can be derived by considering the equilibrium transition temperature between the α- and γ-phases in an iron system. By using a standard thermodynamic relation, it is possible to write for the molar Gibbs energy

$$dg^{\alpha} = v_m^{\alpha} dP - s^{\alpha} dT \tag{1.57a}$$

$$dg^{\gamma} = v_m^{\gamma} dP - s^{\gamma} dT \tag{1.57b}$$

Since the equilibrium transition between these two phases is under consideration at equilibrium temperature, one has $g^{\alpha} = g^{\gamma}$ and further, $dg^{\alpha} = dg^{\gamma}$. By equating Eqs. 1.57a and 1.57b, the following is obtained

$$\left(\frac{\partial P}{\partial T}\right)_{eq} = \frac{s^{\gamma} - s^{\alpha}}{v_m^{\gamma} - v_m^{\alpha}} = \frac{\Delta s}{\Delta v_m} \tag{1.58}$$

From Eqs. 1.17, we can write

$$g^{\gamma} = h^{\gamma} - Ts^{\gamma} \tag{1.59a}$$

$$g^{\alpha} = h^{\alpha} - Ts^{\alpha} \tag{1.59b}$$

From Eqs. 1.59a and 1.59b and from the consideration of equilibrium transition, we can write

$$\Delta g = g^{\gamma} - g^{\alpha} = 0 = (h^{\gamma} - h^{\alpha}) - T(s^{\gamma} - s^{\alpha}) = \Delta h - T\Delta s \tag{1.60}$$

Further, we can write at the transition temperature (T_{tr})

$$\Delta s = \frac{\Delta h}{T} \tag{1.61}$$

By introducing Eq. 1.61 in Eq. 1.60, we arrive at the following

$$\left(\frac{dP}{dT}\right) = \frac{\Delta h}{T\Delta v_m} \tag{1.62}$$

Equation 1.62 is the Clausius–Clapeyron equation, which can be used to calculate, for example, the TM curve shown in Fig. 1.1. We know that the α-phase has a BCC structure and the γ-phase has an FCC structure. Since FCC is a more closely packed structure, we can write for the transition $\alpha \rightarrow \gamma$, $\Delta v = v_m^{\gamma} - v_m^{\alpha} < 0$. On the other hand, we have seen previously that the enthalpy of a phase which is stable at higher temperature is higher (less negative) than that of a phase which is stable at lower temperature. This becomes $\Delta h = h^{\gamma} - h^{\alpha} > 0$. From Eq. 1.63, it follows that $\left(\frac{dP}{dT}\right)_{\mathrm{eq}} < 0$ for the equilibrium transformation from the α-phase to the γ-phase. This is the reason why the equilibrium transition temperature decreases with increasing pressure. Let us consider the case of the equilibrium transition between the γ- to δ-phase. Since the γ-phase has an FCC structure, whereas the δ-phase has a BCC structure, it is possible to write for the transition $\gamma \rightarrow \delta$ $\Delta v = v_m^{\delta} - v_m^{\gamma} > 0$.

Further, from our previous explanation, we can write $\Delta h = h^{\delta} - h^{\gamma} > 0$. So $\left(\frac{dP}{dT}\right)_{\text{eq}} > 0$ for this transition and equilibrium transition temperature increases with increasing pressure.

1.8 Free Energy and Stability of Phases in a Binary System

In the previous sections, we have considered mainly single-component systems (i.e., pure elements). It is common knowledge that most materials in nature consist of several phases and that these phases themselves are never pure elements. In fact, based on the second law of thermodynamics, a pure substance exists only in our minds and represents a limiting state, which we may asymptotically approach but never actually obtain. Thus, the thermodynamic description of multicomponent systems is of great importance from the theoretical as well as from the practical point of view. In the treatment of multicomponent open systems, the most common process considered in defining the thermodynamic functions for a solution is called the mixing process, which Guggenheim defines as [2]:

> The mixing process is the change in state experienced by the system when appropriate amounts of the 'pure' components in their reference states are mixed together forming a homogeneous solution brought to the same temperature and pressure as the initial state.

It is to be noted that although the mixing process is strongly influenced by interaction forces between atoms and molecules (i.e., Δh), the fundamental cause behind mixing is the entropy (Δs) change of the system.

For our analysis, we shall consider a system with a total of one mole of atoms, where X_{A} is the mole fraction of element A and X_{B} is the mole fraction of element B. This translates into

$$X_{\text{A}} + X_{\text{B}} = 1 \tag{1.63}$$

We define the free energies of pure elements A as G_{A} and that of B as G_{B} at a particular temperature. The total molar free energy g_0 of a *purely mechanical mixture* can be written as

$$g_0 = X_{\text{A}} g_{\text{A}} + X_{\text{B}} g_{\text{B}} \tag{1.64}$$

Now, if we allow interdiffusion to taken place between the elements A and B, there will be change in the free energy because of mixing, g_{mix}. Consequently, the total free energy of the system after mixing can be written as

$$g = g_0 + \Delta g_{\text{mix}} \tag{1.65}$$

From Eqs. 1.17 and 1.65, we find the expression for the free energy change because of mixing as

$$\begin{aligned} \Delta G_{\text{mix}} &= g - g_0 = h - Ts - h_0 + Ts_0 = (h - h_0) - T(s - s_0) \\ \Delta g_{\text{mix}} &= \Delta h_{\text{mix}} - T\Delta s_{\text{mix}} \end{aligned} \tag{1.66}$$

where h_o and h are the total enthalpy of the system before and after mixing. The values s_o and s are the entropies of the system before and after mixing. The value $\Delta h_{\text{mix}} = (h - h_0)$ is the change in enthalpy, and $\Delta s_{\text{mix}} = (s - s_0)$ is the change in entropy due to mixing. The enthalpy of mixing can be zero, negative, or positive depending on the system; the entropy of mixing, on the other hand, is always positive. We shall first briefly discuss the mixing process in general and then look a little closer at where the different terms in Eq. 1.66 arise.

1.8.1 Change in Free Energy in an Ideal System

Note that in the case of an ideal solution, $\Delta h_{\text{mix}} = 0$ and the free energy of the system can be written as

$$g = g_0 + \Delta g_{\text{mix}} = g_0 - T\Delta s_{\text{mix}} \tag{1.67}$$

The change in free energy with composition is shown in Fig. 1.9a at one particular temperature T. The straight dotted line represents the total free energy $(g_0 = X_{\text{A}} g_{\text{A}} + X_{\text{B}} g_{\text{B}})$ of the elements A and B before any mixing (i.e., a purely mechanical mixture of A and B). The solid curved line represents the free energy of the system after mixing $(g = g_0 - T\Delta s_{\text{mix}})$. Further, the change in free energy with composition at higher temperature, T_1, is shown in Fig. 1.9b. The change in free energy caused by mixing in an ideal solution $\Delta g_{\text{mix}} = -T\Delta s_{\text{mix}}$ is naturally larger at the higher temperature.

Entropy of mixing (Δs_{mix})

The entropy of mixing originates from two different contributions, thermal and configurational. If we consider that there are no volume and enthalpy changes caused by mixing, then the only contribution to the entropy will configurational. Configurational entropy comes from the possibility of arranging the atoms A and B in different ways for a particular macrostate. Following statistical thermodynamics, the configurational entropy can be expressed as

$$S = k \ln w \tag{1.68}$$

where w is a thermodynamic probability, a kind of measure of randomness. This means that the molar entropy of mixing can be written as

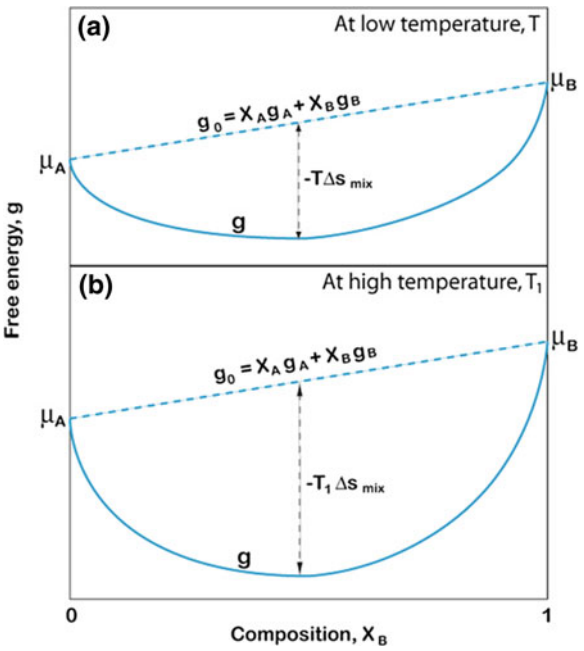

Fig. 1.9 Free energy versus composition diagram in an ideal case at **a** low temperature, T, and **b** high temperature, T_1

$$\Delta s_{\text{mix}} = s - s_0 = k \ln w - k \ln 1 = k \ln w \tag{1.69}$$

where, as explained before, s_0 is the entropy before mixing and s is the entropy after mixing. Since in the case of a pure element, there is only one way by which atoms can be arranged (if vacancies are neglected), we can write $w = 1$. If we consider the random solid solution, then the number of different ways by which atoms A and B can be arranged is

$$w = \frac{(n_{\text{A}} + n_{\text{B}})!}{n_{\text{A}}! n_{\text{B}}!} \tag{1.70}$$

where n_{A} and n_{B} are the total number of atoms of A and B, respectively.

According to Stirling's approximation,

$$\ln N! = N \ln N - N \tag{1.71}$$

Following Stirling's approximation, Eq. 1.69 can be written as

$$\begin{aligned} \Delta S_{\text{mix}} &= k \ln w \\ &= [(n_{\text{A}} + n_{\text{B}}) \ln(n_{\text{A}} + n_{\text{B}}) - (n_{\text{A}} + n_{\text{B}})] - [n_{\text{A}} \ln n_{\text{A}} - n_{\text{A}}] - [n_{\text{B}} \ln n_{\text{B}} - n_{\text{B}}] \end{aligned} \tag{1.72}$$

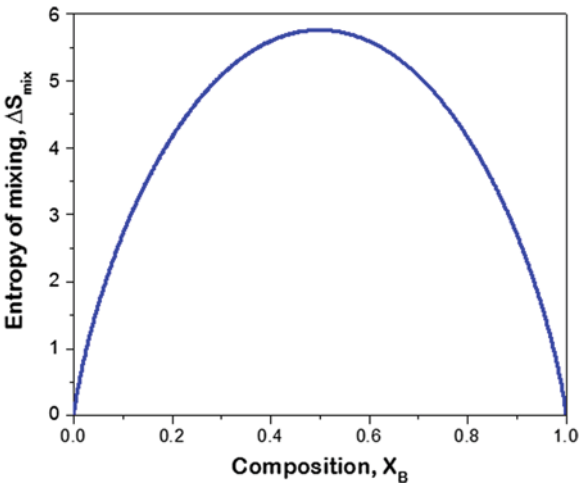

Fig. 1.10 The change in entropy of mixing with the change in composition

From the definition of the mole fraction, we can write

$$n_A = X_A N_0; \quad n_B = X_B N_0; \quad X_A + X_B = 1 \tag{1.73}$$

Substituting Eq. 1.73 in Eq. 1.72, we get

$$\begin{aligned} \Delta s_{mix} &= -kN_0[X_A \ln X_A + X_B \ln X_B] \\ &= -R[X_A \ln X_A + X_B \ln X_B] \end{aligned} \tag{1.74}$$

It is, therefore, clearly apparent from Eq. 1.74 that the entropy of mixing is always positive and will vary, as shown in Fig. 1.10. It can also be seen that the entropy of mixing reaches its maximum at $X_B = 0.5$. To find the slope at different compositions, we can differentiate Eq. 1.74 (note that $X_A + X_B = 1$).

$$\begin{aligned} \frac{d\Delta s_{mix}}{dX_B} &= -R\left[-\ln(1-X_B) - (1-X_B)\frac{1}{(1-X_B)} + \ln X_B + X_B \frac{1}{X_B}\right] \\ &= -R \ln \frac{X_B}{(1-X_B)} \end{aligned} \tag{1.75}$$

So the slope at $X_B = 0.5$ is equal to zero, whereas the slope at $X_B = 0$ or 1 is infinity. Thus, it is evident from the above discussion why a pure substance is just a limit which we can approach but never achieve—as stated at the beginning of this section. As the slope goes to infinity at $X_B = 0$, it states that in order to remove the last B impurity from A, an infinite amount of energy must be used.

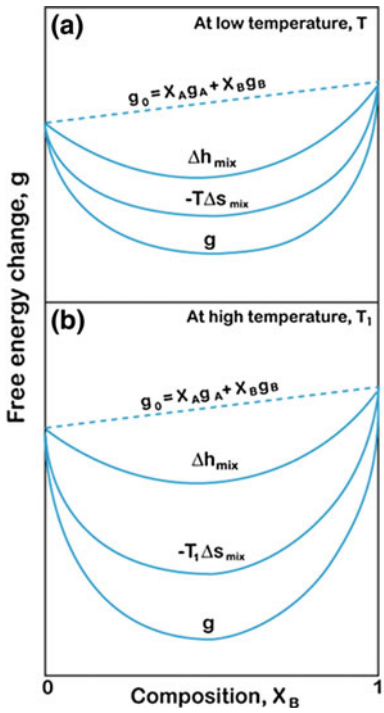

Fig. 1.11 Free energy versus composition diagram for a system with exothermic transformation at **a** low temperature, T, and **b** high temperature, T_1

1.8.2 Change in Free Energy in a System with Exothermic Transformation

As discussed above, the enthalpy of mixing in an exothermic transformation is negative. The free energy of mixing for such a case at different compositions at a particular temperature T is shown in Fig. 1.11a. The free energy curves at higher temperature T_1 are shown in Fig. 1.11b. At higher temperature, the $T\Delta s_{\text{mix}}$ term will be higher, making Δg_{mix} higher after mixing. In consequence, the total free energy of the system will change far more drastically with composition compared to at lower temperature.

1.8.3 Change in Free Energy in a System with Endothermic Transformation

In endothermic transformation, the enthalpy of mixing $\Delta h_{\text{mix}} > 0$. So, if the temperature under consideration is reasonably low, the negative contribution to the Gibbs energy of mixing from $T\Delta s_{\text{mix}}$ may be smaller than the positive contribution from the enthalpy of mixing Δh_{mix} within a certain composition range. In that case,

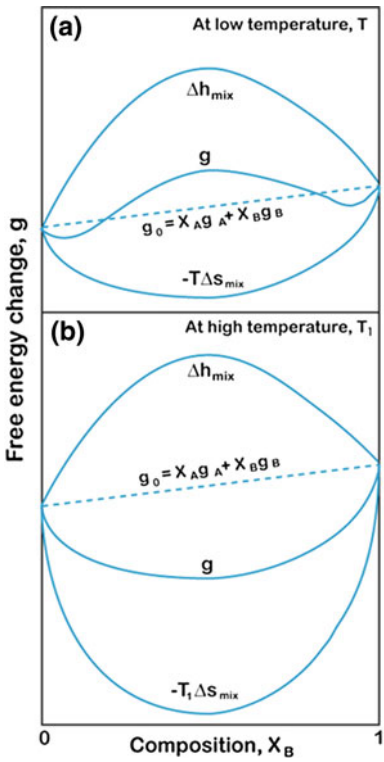

Fig. 1.12 Free energy versus composition diagram in a system with endothermic transformation at **a** low temperature, T, and **b** high temperature, T_1

the free energy of mixing will be positive at a certain composition range and the total free energy change can vary, for example, as shown in Fig. 1.12 resulting in a formation of a miscibility gap. However, at higher temperature, T_1 at all compositions Δh_{mix} will be smaller than $T\Delta s_{\text{mix}}$ and the free energy of mixing is always negative, as can be seen in Fig. 1.12b. The next section considers the origin of the enthalpy of mixing.

Note We have considered a very simplified model to establish the relation of free energy after mixing in a binary system. We have not considered the elastic strain that could play an important role. In some systems, where the size of the atoms is very similar, this factor can be disregarded. However, in some systems because of a large difference in atomic size, the elastic strain might play a significant role. Calculations, however, become extremely complicated if we are to consider the effect of elastic strain and so it is left outside the scope of this book. It must, nevertheless, be remembered that the elastic energy (as other forms of work) can be incorporated into the Gibbs free energy of the system.

1.9 Thermodynamics of Solutions and Phase Diagrams

In the following section, the thermodynamic background necessary for understanding the phase diagrams introduced briefly in Sect. 1.4 is discussed. After that the binary and ternary phase diagrams are discussed in greater detail.

1.9.1 The Chemical Potential and Activity in a Binary Solid Solution

For any heterogeneous system at equilibrium, the chemical potential of a component i has the same value in all phases of the system, where the component has accessibility. A general problem for dealing with solutions thermodynamically can be regarded as one of properly determining the chemical potentials of the components. Usually, the treatment utilizes the activity function introduced by Lewis and Randall [8]. The value of the treatment lies in its close relation to composition; with appropriate choice of reference state, the activity approaches the mole fraction as the mole fraction approaches unity. Most commonly in the thermodynamics of solutions, it is not the activity which is used, but rather the activity coefficient which is defined as the ratio of the activity a_i to the mole fraction X_i

$$\gamma_i = \frac{a_i}{X_i} \tag{1.76}$$

In terms of the chemical potential, the activity can be expressed

$$\mu_i^j - \mu_i^o = RT \ln a_i^j = RT \ln X_i^j + RT \ln \gamma_i^j \tag{1.77}$$

where μ_i^o is the chemical potential of pure i in the reference or standard state, μ_i^j the chemical potential of i in phase j, a_i^j the activity of component i in phase j, R the gas constant, T the temperature, and (i = A, B,…; $j = \alpha, \beta, \ldots$). In the limiting case of ideal solutions, where the enthalpy ($\Delta h = 0$) and volume change ($\Delta v = 0$) of mixing are zero and the only contribution to Gibbs free energy of mixing arises from the configurational entropy term

$$\Delta s_m = \sum_{i=\mathrm{A}} X_i \ln X_i \tag{1.78}$$

the activity coefficient in Eq. 1.77 is unity and the activity of the component equals its mole fraction (i.e., Raoultian behavior, see discussion below). If the equality is valid for all compositions, the solution is called perfect. Thus, the activity coefficient represents deviation of the real solutions from this limiting behavior. The use of activity coefficient instead of activity in Eq. 1.77 clearly indicates the

excess energy term $RT \ln \mu_i^j$ to be responsible for the non-ideal behavior. This issue is addressed in more detail in the next section.

As only relative values of thermodynamic functions can be determined, an agreed reference state has to be established for each element or species in order to make thermodynamic treatment quantitative (see Fig. 1.7 and related discussion). In principle, the choice of the reference state is arbitrary as long as the chosen state is used consequently throughout the analysis. The chosen state is then defined to be zero and all other possible states of the element are compared against the reference state to obtain their relative stabilities. It should be noted that there are some uncertainties related to the usage of reference states in the literature.

1.9.2 Free Energy of Solutions

In Sect. 1.9, we briefly discussed the so-called mixing process as well as the binary solution phases. In the beginning of this section, we also introduced the concept of activity, which describes the deviation of the behavior of a solution from ideal behavior. A statistical approach can be used to provide more insight into the properties of the phases. The simplest model is one in which the total energy of the solution is given by a summation of interactions between the nearest neighbor atoms. If we have a binary system with two types of atoms (A and B), there will be three interaction energy terms. These are the energy of the A–A pairs, that of the B–B pairs, and that of the A–B pairs. Here, we assume that the total energy of the solution arises from the interactions between the nearest neighbors. The binding energy may be defined by considering that the change in energy as the distance between a pair of atoms is decreased from infinity to an equilibrium separation. The change in energy during this process is the binding energy, which for a pair of A atoms is given as $-2\varepsilon_{\mathrm{AA}}$, for B atoms as $-2\varepsilon_{\mathrm{BB}}$, and so forth. Thus, the bond energies are negative quantities.

The simplest model for real solution phases based on the above-defined nearest neighbor interaction approach is the so-called regular solution model. It is based on the following assumptions: (i) Mixing among accessible lattice spaces is completely random $p_i = \frac{N_i}{N} = X_i$, (ii) atoms interact only with their nearest neighbors, (iii) the bond energy between dissimilar atoms ε_{ij} is independent of composition and temperature, and (iv) there is no change in volume upon mixing.

Let us examine a solution which is formed by two metals (A and B) with an identical crystal structure. Let us further assume that the system as defined above is in equilibrium with its surroundings. We will presume that metal A has N_{A} atoms and metal B has N_{B} atoms and that $\varepsilon_{\mathrm{AA}}$ and $\varepsilon_{\mathrm{BB}}$ are the bond energies of the AA and BB atom pairs according to the assumptions (ii) and (iii). Then, the configuration energies of pure metals, with the coordination number z, are $E_{\mathrm{A}}^0 = zN_{\mathrm{A}}^0\varepsilon_{\mathrm{AA}}/2$ and $E_{\mathrm{B}}^0 = zN_{\mathrm{B}}^0\varepsilon_{\mathrm{BB}}/2$, when the atoms are at rest at their equilibrium lattice points. The number two in the nominator in the above equations is

introduced in order to prevent calculating the A–A and B–B interactions twice. The formation of the solution phase starts by removing one atom from each metal and transferring them to an infinite distance from the metal (and each other). The work associated with this process is $-z(\varepsilon_{AA} + \varepsilon_{BB})$. By returning an atom A to metal B and an atom B to metal A, the pure metals are transformed into solutions with infinite dilution. The total number of A–B bonds with bond energy ε_{AB} in these solutions is $2z$. The energy associated with this mixing process (per interchange) can be described as

$$dE = 2z\left[\varepsilon_{AB} - \frac{1}{2}(\varepsilon_{AA} + \varepsilon_{BB})\right] = -2zI_{AB} \tag{1.79}$$

where I_{AB} (per bond) is the interchange energy.

As the energy change associated with the formation of a mixture with a number of N_{AB} bonds is $\Delta E = N_{AB}I_{AB}$, the internal energy of the solution phase is

$$E = \left(\frac{z}{2}\right)N_A(\varepsilon_{AA}) + \left(\frac{z}{2}\right)N_B(\varepsilon_{BB}) + N_{AB}I_{AB} \tag{1.80}$$

The next step is to identify what the most probable number of AB bonds (N_{AB}) is with the nominal composition of X_B^o. This problem can be resolved by utilizing the first assumption of the regular solution model, i.e., that the mixing among the lattice sites is completely random. This means that the probability that an atom A is in position 1 equals $p_{A(1)} = (N_A/N)$ and that atom B is in position 2 equals $p_{B(2)} = (N_B/N)$. However, since $p_{A(1)}p_{B(2)} = (N_A N_B/N^2)$ and because $p_{A(1)}p_{B(2)} = p_{A(2)}p_{B(1)}$, we get

$$p_{AB}^{(1,2)} = \frac{2N_A N_B}{N^2} \tag{1.81}$$

In the solution phase, we have total of $0.5zN$ adjacent lattice site pairs and therefore,

$$\bar{p}_{AB} = p_{AB}^{(1,2)} = \frac{2N_A N_B}{N^2}\left(\frac{zN}{2}\right) = z\left(\frac{N_A N_B}{N_A + N_B}\right) \tag{1.82}$$

Thus, the internal energy of the solution phase can be written as

$$E = \left(\frac{z}{2}\right)N_A(\varepsilon_{AA}) + \left(\frac{z}{2}\right)N_B(\varepsilon_{BB}) + z\left(\frac{N_A N_B}{N_A + N_B}\right)I_{AB} \tag{1.83}$$

By assuming that the chemical potentials of pure metals A and B can be approximated as $\mu_A^0 \cong \frac{1}{2}Z(\varepsilon_{AA})$ and $\mu_B^0 \cong \frac{1}{2}Z(\varepsilon_{BB})$ and utilizing the definition of the chemical potential, the Gibbs energy of the regular solution phase becomes

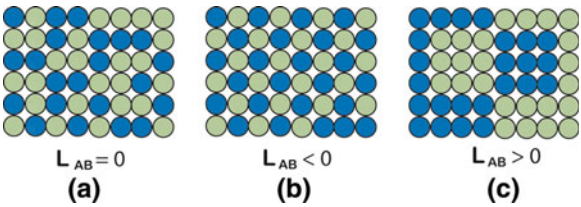

Fig. 1.13 Schematic presentation of the effect of the sign of the enthalpy of mixing and that of the interaction parameter on the formation of a solution phase

$$G = N_A\mu_A^o + N_B\mu_B^o + kT\sum_i N_i \ln\left(\frac{N_i}{N_A + N_B}\right) + z\left(\frac{N_A N_B}{N_A + N_B}\right)I_{AB} \tag{1.84}$$

from which the molar Gibbs energy is obtained as

$$g = X_A^o\mu_A + X_B^o\mu_B + RT\sum_i X_i \ln X_i + L_{AB}X_A X_B \tag{1.85}$$

where L_{AB} ($=zNI_{AB}$) is the molar interaction energy, i.e., the *interaction parameter*.

The relationship between activity and the interaction parameter can be written as

$$a_i = \gamma_i X_i = X_i \exp\left[\frac{L_{ij}(1 - X_i)^2}{RT}\right] \tag{1.86}$$

Consequently, the sign of the interaction parameter determines whether the formation of mixture is favored or hindered. When $|\varepsilon_{AA} + \varepsilon_{BB}| < |2\varepsilon_{AB}|$ and the interaction parameter is negative (remember that the bonding energies are negative), the solution will have a larger than random probability of bonds between unlike atoms, and thus, mixing or compound formation is favored, as in Fig. 1.13. The converse is true when the interaction parameter is positive ($|\varepsilon_{AA} + \varepsilon_{BB}| > |2\varepsilon_{AB}|$) since atoms then prefer to be neighbors to their own kind and form clusters. From Eq. 1.86, it is also seen how the activity coefficient depends on both the sign and magnitude of the interaction parameter. Activity is eventually determined by the interactions between different types of atoms in the solution phase. It is also helpful to notice that the excess term in Eq. 1.86 $L_{AB}X_A X_B$ can be identified with the enthalpy of mixing in Eq. 1.66.

Justification of Eq. 1.86
Deviations from ideal behavior are commonly expressed in the form of excess functions. The excess Gibbs energy of mixing can be expressed as $\Delta g_{mix}^{xs} = \Delta h_{mix}^{xs} - T\Delta s_{mix}^{xs}$. This is the extra energy of mixing resulting from the formation of a real instead of an ideal solution. In a regular solution model, the entropy of mixing is defined to be the same as that of an ideal solution.

Thus, the excess entropy of mixing $\Delta s^{xs}_{\text{mix}}$ is zero and $\Delta g^{xs}_{\text{mix}} = \Delta h^{xs}_{\text{mix}}$ in the case of regular solutions. Therefore, the expression $L_{\text{AB}}X_{\text{A}}X_{\text{B}}$ in Eq. 1.86 can be equated to the excess enthalpy of mixing. It is to be noted that the expression $L_{\text{AB}}X_{\text{A}}X_{\text{B}}$ is also the simplest possible expression for the excess energy of mixing, as it is required that the excess energy of mixing goes to zero when $X_{\text{A}} = 0$ or $X_{\text{A}} = 1$. There is a standard relation between the partial molar properties of a component and the total properties of a phase that can be expressed for the excess enthalpy of mixing and the partial excess enthalpy of the mixing of component B as

$$\Delta h^{xs}_{\text{B,mix}} = \Delta h^{xs}_{\text{mix}} + X_{\text{A}} \frac{d\Delta h^{xs}_{\text{mix}}}{dX_{\text{B}}}$$

We have the above-defined $\Delta h^{xs}_{\text{mix}} = L_{\text{AB}}X_{\text{A}}X_{\text{B}} = L_{\text{AB}}(1 - X_{\text{B}})X_{\text{B}} = L_{\text{AB}}(X_{\text{B}} - X_{\text{B}}^2)$
Thus,

$$\frac{d\Delta h^{xs}_{\text{mix}}}{dX_{\text{B}}} = L_{\text{AB}}(1 - 2X_{\text{B}})$$

and we obtain

$$\begin{aligned}\Delta h^{xs}_{\text{B,mix}} &= L_{\text{AB}}X_{\text{A}}X_{\text{B}} + X_{\text{A}}L_{\text{AB}}(1 - 2X_{\text{B}}) \\ &= X_{\text{A}}L_{\text{AB}}(X_{\text{B}} + 1 - 2X_{\text{B}}) = X_{\text{A}}L_{\text{AB}}(1 - X_{\text{B}}) = L_{\text{AB}}X_{\text{A}}^2\end{aligned}$$

The excess enthalpy of the mixing of component B can also be equated (in the case of regular solution model) to $RT \ln \gamma_{\text{B}}$ as discussed above.
Thus, we can write as follows:

$$\begin{aligned}RT \ln \gamma_{\text{B}} &= L_{\text{AB}}X_{\text{A}}^2 \\ \gamma_{\text{B}} &= \exp\left[\frac{L_{\text{AB}}(1 - X_{\text{B}})^2}{RT}\right]\end{aligned}$$

As $a_{\text{B}} = X_{\text{B}}\gamma_{\text{B}}$, we finally obtain

$$a_{\text{B}} = X_{\text{B}}\gamma_{\text{B}} = X_{\text{B}} \exp\left[\frac{L_{\text{AB}}(1 - X_{\text{B}})^2}{RT}\right]$$

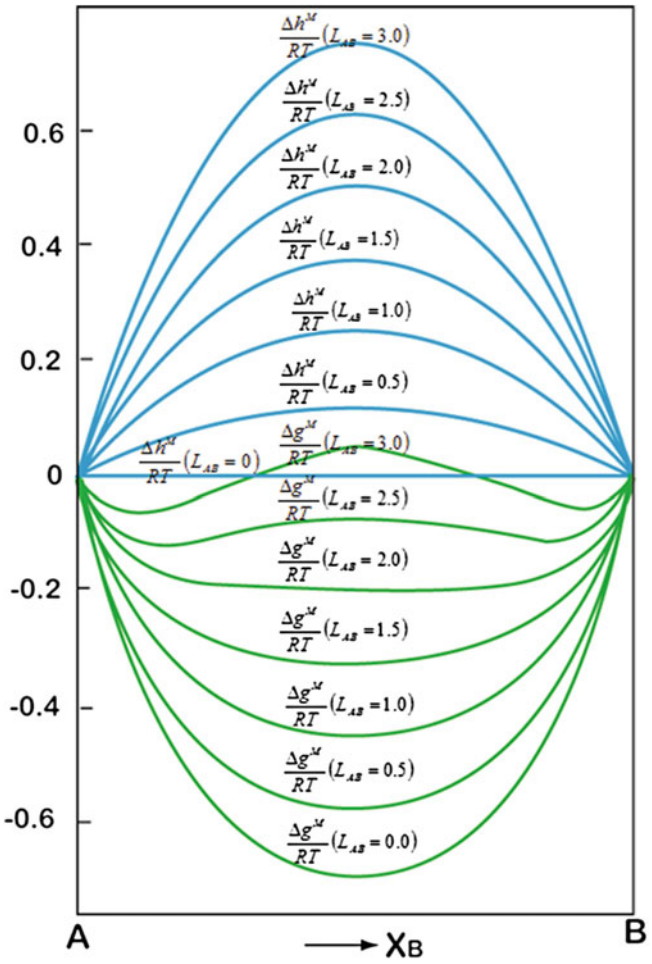

Fig. 1.14 The effect of interaction parameter on the stability of a solution phase [9]

In Fig. 1.14, the effect of the sign and magnitude of the interaction parameter on the formation of a solution phase is shown [9]. When there is no preferred interaction between the atoms in the system, the interaction parameter $L_{AB} = 0$ ($\varepsilon_{AA} + \varepsilon_{BB} = 2\varepsilon_{AB}$), the integral heat of mixing is zero, and the free energy of mixing is given by curve I. As the interaction parameter is made more positive, it can be seen how the enthalpy of mixing becomes more positive and the free energy of mixing becomes less negative. When a certain magnitude of positive interaction is reached, it can be seen that the system is about to enter the state where the solution phase becomes unstable. When L_{AB} is increased to even more positive values, one can see how the Gibbs energy curve changes its sign of curvature at the middle region and the so-called miscibility gap is formed. This is associated with the formation of two separate phase regions—one rich in A and another rich in B.

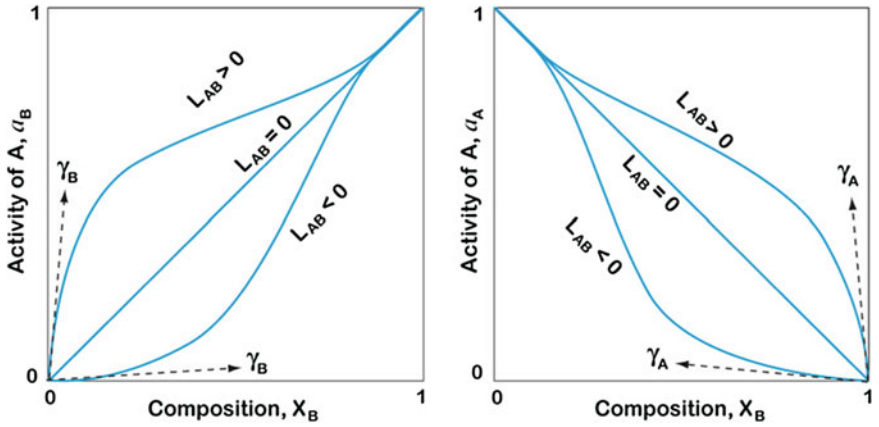

Fig. 1.15 Raoult's and Henry's laws in a binary solution

It was shown that one may find a situation where the interaction parameter is zero and there is no net interaction between A and B (i.e., $\varepsilon_{AA} + \varepsilon_{BB} = 2\varepsilon_{AB}$). This type of behavior is associated with the above-defined ideal systems and is described by Raoult's law. The Raoultian solution was shown above to be the one where the activity coefficient (Eq. 1.76) is unity and the activity of the component equals its mole fraction. Such behavior is shown in Fig. 1.15. If Raoult's law is obeyed by the solution phase through the whole composition range, the solution is called perfect. This type of solution does not exist in reality, but it does provide a convenient reference state to which the behavior of real solutions can be compared. In Fig. 1.15, another limiting law (Henry's law) is also shown. This limiting law can be understood by utilizing the regular solution model and Eq. 1.86. When one approaches the limit where $X_i \rightarrow 0$, i.e., the solution becomes dilute, it can be seen from Eq. 1.87 that the activity coefficient becomes concentration independent as

$$^{\infty}\gamma_i = \exp\left[\frac{L_{ij}}{RT}\right] \tag{1.87}$$

This defines the Henry's law line seen in Fig. 1.15. The limiting laws shown in Fig. 1.15 provide the reference states to which real solutions can be compared. As we approach pure substance ($X_i \rightarrow 1$), the solution behavior necessarily approaches Raoultian behavior no matter how "non-ideally" it otherwise behaves. This is true also for Henry's law, as all solutions approach it as the solution becomes dilute enough. It is also to be noted that if the solute follows Henry's law, then the solvent necessarily follows Raoult's law. Furthermore, whereas perfect solutions do not exist, ideal solution behavior is commonly encountered in practice within restricted composition limits.

Historically, activity measurements have been carried out mainly by measuring the changes in the partial pressure of a given substance upon alloying with respect to the values of the pure component. As this type of approach also gives an easily accessible alternative route to derive the above-defined limiting laws, we shall briefly consider Raoult's and Henry's laws from this point of view. Consider a pure liquid A in a closed vessel (initially evacuated) at temperature T. It will spontaneously evaporate until the pressure in the vessel is equal to the saturated vapor pressure of liquid A (p^o_{A}) at temperature T. At this point, the rate of evaporation $r_{\mathrm{e(A)}}$ and the rate of condensation $r_{c(\mathrm{A})}$ are equal. In order for an atom to escape the surface of the liquid and enter the gas phase, it must overcome the attractive forces exerted on it by its neighbors (i.e., overcome the activation energy E^* barrier). The magnitude of E^* determines the intrinsic evaporation rate. The condensation rate is proportional to the number of A atoms in the vapor phase, which strike (and stick) the liquid surface in unit time. For a fixed temperature, the condensation rate is proportional to the pressure of the vapor $r_{c(\mathrm{A})} = kp^o_{\mathrm{A}}$ which is equal to $r_{e(\mathrm{A})}$ at equilibrium. A similar situation holds for a liquid B. If we now add a small amount of liquid B to liquid A, what happens? If the mole fraction of A in the resulting binary mixture is X_{A} and assuming that the atomic diameters of A and B are comparable and there is no surface excess, the fraction of the surface area occupied by A atoms is X_{A}. It is a natural assumption that atom A can evaporate only from a site where it is present and, therefore, $r_{e(\mathrm{A})}$ is decreased by a factor of X_{A} and the equilibrium pressure exerted by A is decreased from p^o_{A} to p_{A}

$$r_{e(\mathrm{A})}X_{\mathrm{A}} = kp_{\mathrm{A}} \tag{1.88}$$

and by utilizing the above-defined equality between evaporation rate and equilibrium pressure, we obtain

$$p_{\mathrm{A}} = X_{\mathrm{A}}p^o_{\mathrm{A}} \tag{1.89}$$

which is Raoult's law. A similar equation holds for component B. The law states that the vapor pressure exerted by a component i in a solution is equal to the product of the mole fraction of i in the solution and the vapor pressure of i at the temperature of the solution.

While deriving Raoult's law, it was assumed that there is no change in the intrinsic evaporation rates. This requires that the magnitudes of the A–A, B–B, and A–B interactions are balanced so that the depth of the potential energy well of an atom at the surface site is independent of the types of atoms surrounding it (see discussion below). If we take that the A–B interaction is much stronger than that between identical atoms and consider a solution of A in B which is sufficiently dilute in such a way that every A atom is surrounded only by B atoms, in this case, the activation energy for an A atom to evaporate from the surface is higher than without B and thus, the intrinsic evaporation rate will be smaller ($r'_{e(\mathrm{A})} < r_{e(\mathrm{A})}$) and equilibrium occurs when

$$r'_{e(\mathrm{A})} X_{\mathrm{A}} = k p_{\mathrm{A}} \tag{1.90}$$

which results in

$$p_{\mathrm{A}} = \frac{r'_{e(\mathrm{A})}}{r_{e(\mathrm{A})}} X_{\mathrm{A}} p^{o}_{\mathrm{A}} \tag{1.91}$$

and as $\left(r'_{e(\mathrm{A})} < r_{e(\mathrm{A})}\right)$, p_{A} is a smaller quantity than that in Eqs. 1.88, 1.91 can be written as

$$p_{\mathrm{A}} = k'_{\mathrm{A}} X_{\mathrm{A}} \tag{1.92}$$

If the X_{A} of the solution is increased, it becomes more probable that not all of the A atoms at the surface are surrounded only by the B atoms. This will have an effect on the activation energy (depth of the potential energy well), and thus, after a certain critical value of X_{A}, the intrinsic evaporation rate becomes composition dependent and Eq. 1.93 no longer holds. Equation 1.93 is, of course, Henry's law (a similar equation holds for B atoms also). Note also that Raoultian and Henrian activity coefficients have different reference states. More information about the use of these standard states as well as changing between them can be found, for example, from Refs. [10, 11].

1.10 Lever Rule and the Common Tangent Construction

When two materials, especially metals, are mixed together, they either form a homogeneous solution or separate into a mixture of phases, as already discussed. Let us consider an alloy X in Fig. 1.16 in the binary system A–B to separate into a mixture of two phases α and β (under a particular temperature and pressure).

We shall assume that there are N atoms of alloy X and that the fraction of atoms in the α-phase is $(1-x)$ and in the β-phase is x. The number of B atoms in alloy X is n^{X}_{B}, the number of B atoms in the α-phase is n^{α}_{B}, and the number of B atoms in the β-phase is n^{β}_{B}. We can change these to atomic fractions by dividing by the total number of atoms N to get

$$\begin{aligned} X_{\mathrm{B}} &= \frac{n^{x}_{\mathrm{B}}}{N} \\ X^{\alpha}_{\mathrm{B}} &= \frac{n^{\alpha}_{\mathrm{B}}}{N(1-x)} \\ X^{\beta}_{\mathrm{B}} &= \frac{n^{\beta}_{\mathrm{B}}}{Nx} \end{aligned} \tag{1.93}$$

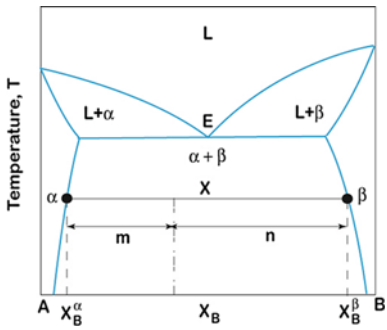

Fig. 1.16 The lever rule

Since $n_B^X = n_B^\alpha + n_B^\beta$, then

$$NX_B = NX_B^\alpha(1-x) + NX_B^\beta x \tag{1.94}$$

where

$$x = \frac{X_B - X_B^\alpha}{X_B^\beta - X_B^\alpha} = \frac{m}{m+n} \tag{1.95}$$

and

$$1 - x = \frac{X_B^\beta - X_B}{X_B^\beta - X_B^\alpha} = \frac{n}{m+n} \tag{1.96}$$

and

$$\frac{x}{1-x} = \frac{m}{n} \tag{1.97}$$

Equation 1.97 is called the lever rule, which enables us to calculate the relative amounts of phases in a phase mixture in terms of the alloy composition and the phases into which it separates. The free energy of a phase mixture can also be determined by using the lever rule. If alloy X separates into phases α and β, the free energy of an alloy will be unchanged by the separation. The free energy of alloy X is, therefore, equal to the sum of the free energies of the α- and β-phases. Since alloy X consists of an amount of the α-phase equal to $\left(\frac{X_B^\beta - X_B}{X_B^\beta - X_B^\alpha}\right)$ and similarly $\left(\frac{X_B - X_B^\alpha}{X_B^\beta - X_B^\alpha}\right)$ of the β-phase, the molar free energy of alloy X will be

$$g = a\left(\frac{X_B^\beta - X_B}{X_B^\beta - X_B^\alpha}\right) + b\left(\frac{X_B - X_B^\alpha}{X_B^\beta - X_B^\alpha}\right) \tag{1.98}$$

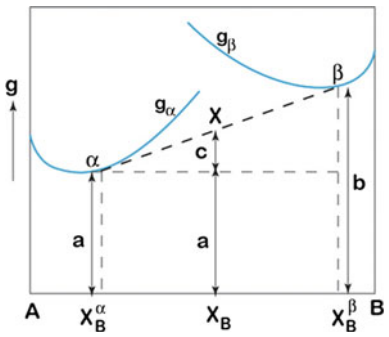

Fig. 1.17 The common tangent construction

where a and b represent the free energies of the α- and β-phases at the given temperature and pressure, as seen from Fig. 1.17. We can further rearrange Eq. 1.98 in order to obtain the free energy of alloy X

$$\begin{aligned} g &= a\left[\frac{(X_B^\beta - X_B^\alpha) - (X_B - X_B^\alpha)}{X_B^\beta - X_B^\alpha}\right] + b\left(\frac{X_B - X_B^\alpha}{X_B^\beta - X_B^\alpha}\right) \\ &= a + (b-a)\left(\frac{X_B - X_B^\alpha}{X_B^\beta - X_B^\alpha}\right) \\ &= a + c \end{aligned} \tag{1.99}$$

Hence, alloy X which separates into two phases of composition X_B^α and X_B^β with the free energies a and b has a free energy given by the point x on the straight line connecting α and β (the common tangent). This is depicted in Fig. 1.17.

As an example of the use of common tangent construction, the calculation of two-phase equilibrium is presented in Fig. 1.18. The condition for chemical equilibrium is that the chemical potentials of the components are equal in the phases that are in equilibrium. In the beginning, the α-phase with composition α1 is contacted with the β-phase with a composition β1. As seen from Fig. 1.18 (at the moment in question), the chemical potential (partial molar Gibbs energy) of component A in the α-phase is $\mu_A^{\alpha 1}$ and in the β-phase $\mu_A^{\beta 1}$, whereas that of component B in the α-phase is $\mu_A^{\alpha 1}$ and in the β-phase it is $\mu_A^{\beta 1}$, which are hardly equal. Thus, there is a driving force $\Delta^1\mu_B(\mu_B^{\alpha 1} - \mu_B^{\beta 1})$ which drives the diffusion of the B atoms to the α-phase (from composition β1 to α1) and $\Delta^1\mu_A(\mu_A^{\beta 1} - \mu_A^{\alpha 1})$ driving the A atoms in the opposite direction. As the diffusion proceeds, the driving force for diffusion gradually decreases ($\Delta^2\mu_B$ and $\Delta^2\mu_A$) and vanishes when the chemical potentials of the components (A and B) become equal in both phases. This takes place when the two Gibbs energy curves for the α- and β-phases have a common tangent and the equilibrium has been established.

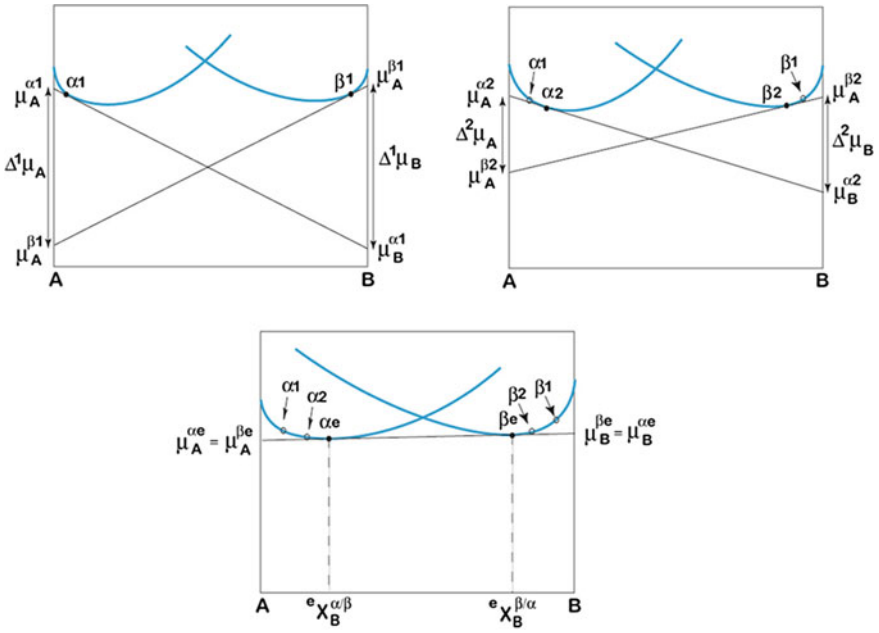

Fig. 1.18 Use of the common tangent construction to determine the phase equilibria

1.11 The Gibbs Phase Rule

The Gibbs phase rule explains the number of phases that will be present in a system in equilibrium and is expressed as

$$F + P = C + N \tag{1.100}$$

where F is the number of degrees of freedom (always ≥ 0), P is the number of phases (liquid phase, α-phase, β-phase), C is the number of components, and N corresponds to the non-compositional variable. In our case, there are two non-compositional variables present, temperature and pressure. This means that Eq. 1.100 can be written as

$$F + P = C + 2 \tag{1.101}$$

Now for the purpose of explaining the stability of the phases in equilibrium, a single-component system that is presented in Fig. 1.19a is considered. First, let us examine the single-phase, solid, liquid or gas phase, region which can be written in this region $C = 1$, $P = 1$. Also from Eq. 1.101, we can write $F = 2$. This means that in this region, there are two degrees of freedom, temperature and pressure. Accordingly, temperature and pressure can be varied independently within the region. Consequently, to determine the state of the phase in a single-phase region,

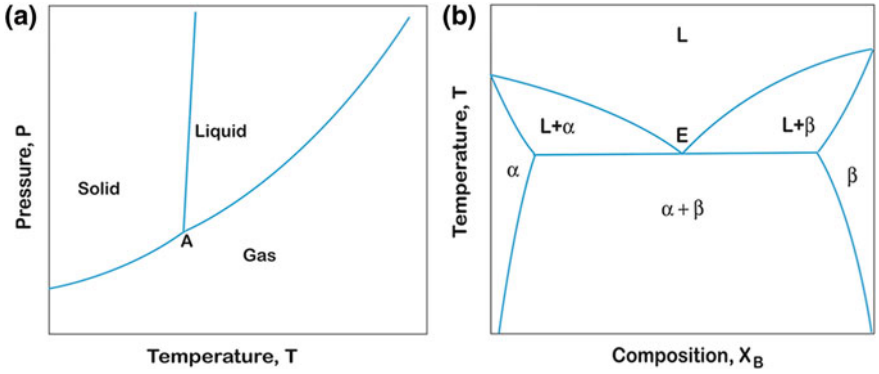

Fig. 1.19 **a** single-component phase diagram **b** binary phase diagram

both temperature and pressure must be fixed. Next, we consider the phase boundary, along which the two phases are in equilibrium. For this can be written $C = 1$, $P = 2$. Further, from Eq. 1.100, we can write $F = 1$, meaning that there is only one degree of freedom and only temperature or pressure can be varied along that tie-line. The other variable is automatically fixed for a particular temperature or pressure. Let us further consider the invariant point A, where all three phases can exist together. At this point, $C = 1$, $P = 3$. Therefore, following Eq. 1.100, $F = 0$, meaning that there are no degrees of freedom at that point and all three phases can exist only at one particular pressure and temperature.

Let us further consider the binary phase diagram shown in Fig. 1.19b. Since binary phase diagrams are measured at constant (in general, atmospheric) pressure, there is only one non-compositional variable present, which is temperature. Equation 1.100 can thus be written as

$$F + P = C + 1 \tag{1.102}$$

Now, if we consider the single-phase region, then we can write $C = 2$, $P = 1$. Following Eq. 1.102, we find $F = 2$ in the single-phase α-region. This means that to determine the state of an alloy inside a single-phase region, both temperature and composition must be fixed. Further, if we consider a two-phase region such as $(L + \alpha)$, then we can write $P = 2$, $C = 2$. So following Eq. 1.102, we find the number of degrees of freedom $F = 1$. To determine the state of an alloy inside this region, we need to fix only one variable, either T, X_A, or X_B. Since, if we fix any one of these variables, other variables will be fixed automatically. Take, for instance, T_2 where the composition of liquid and α-phases have fixed values. Next, if we consider the eutectic point E, where the three phases, α, β, and liquid exist together, we can write $P = 2$, $C = 2$. Following Eq. 1.103, we find $F = 0$, meaning that there are no degrees of freedom and T, X_A, and X_B are all fixed at this point.

The phase rule is a convenient tool to check that experimentally determined phase diagrams are correct. With its help, it is possible to point out anomalies in phase diagrams and to offer corrections.

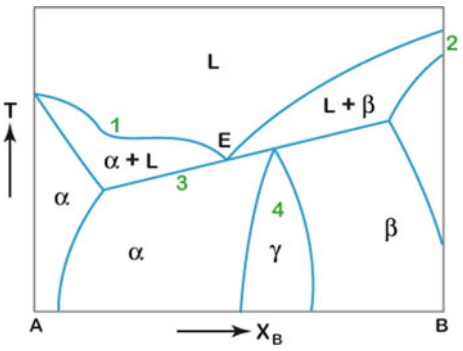

Fig. 1.20 A hypothetical erroneous phase diagram

Let us briefly look at one example. In Fig. 1.20, there is a hypothetical binary A–B phase diagram. It contains four errors. Let us next look what they are and produce two versions of the corrected diagram.

Error 1 Two-phase region in a binary diagram, thus $F = 1$ (pressure is fixed). If the temperature is fixed, the compositions are unambiguously determined. In the diagram, this is not so. If we choose temperature conveniently, the tie-line enters the single-phase region and returns back to the two-phase region. *Correction* remove the bend from the liquidus.

Error 2 Pure element, thus one component $F = 1 + 1 - P = 2 - P$. At the melting point, there are two phases in equilibrium $F = 2 - 2 = 0$. Hence, phase transformation for a pure element takes place at one particular temperature. *Correction*: Liquidus and solidus curves must meet at the same point.

Error 3 Eutectic line represents three-phase equilibrium, thus $F = 0$. Temperature must be constant. *Correction* Eutectic line must be horizontal.

Error 4 There are four phases in equilibrium at the eutectic isotherm, and thus, $F = -1$. The number of degrees of freedom must not be negative and, therefore, four-phase equilibrium in a binary system, with constant pressure, is not possible. *Correction 1* γ-phase must be removed to obtain the necessary degree of freedom to make $F = 0$. *Correction 2* If there is first a two-phase $\alpha + \beta$ region below the eutectic isotherm and after that a peritectoid reaction takes place, we can preserve the γ-phase.

The two versions of the corrected phase diagrams are shown in Fig. 1.21.

1.12 Correlation of Free Energy and Phase Diagram in Binary Systems

We shall first start with the simplest possible binary system, where elements A and B are completely miscible in both solid and liquid state. This requires that the elements A and B have (i) the same crystal structure, (ii) their size difference is less than 15 %, and (iii) their electronegativities have similar values. These are

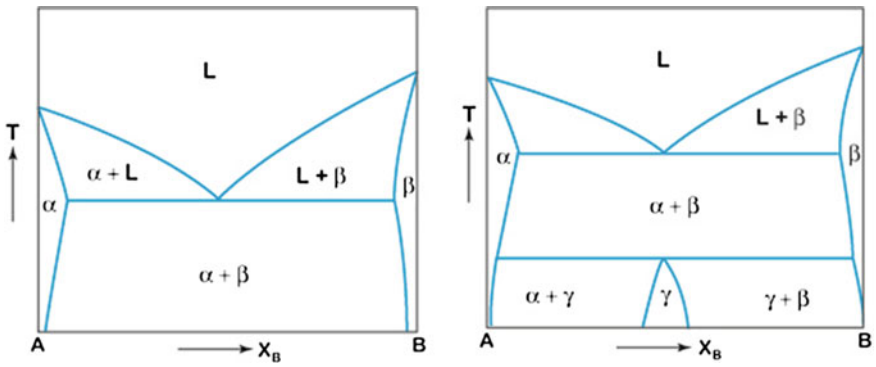

Fig. 1.21 The two correct versions of the diagram shown in Fig. 1.20

known as the Hume-Rothery rules. An example of such a system is Cu–Ni above 355 °C (i.e., above the solid state, miscibility gap caused at least partly by the ferromagnetism of Ni). Thus, the A–B system shown in Fig. 1.22 exhibits ideal behavior and atoms will not have any preference to select neighboring atoms. To give a mental picture of what complete miscibility in solid state means, we can trace the following line of thought. If one begins with pure A, with its own crystal structure, and starts to replace A atoms with B atoms, then, in the case of complete solubility, one can eventually replace all A atoms with B atoms without any change in crystal structure or formation of new phases and reach pure element B, with its own crystal structure (which has to be, by definition, the same as A's). To illustrate this behavior, we have to consider the change in free energy with composition for two different phases, solid (g^s) and liquid (g_L), to find the stability of the phases at different temperatures and compositions. Here, we assume that the melting point of element A (T_m^{A}) is higher than the melting point of element B (T_m^B). First, if we consider a relatively high temperature, as shown in Fig. 1.22a, we know from our previous discussion that the liquid phase will be stable because of a high contribution of entropy. Now, if we start to decrease the temperature to a certain extent, two factors shall be mainly noticed, which shall change in the free energy diagram. We have seen before that the free energy of a liquid phase decreases faster than that of a solid phase. So with the decrease in temperature, the difference in free energy of both liquid and solid phases will decrease. Further, because of the decrease in temperature, the contribution of $\Delta g_{\mathrm{mix}} \approx -T\Delta s_{\mathrm{mix}}$ will decrease, which means that the curvature of both curves will recede. If we decrease the temperature up to the melting point of element A (T_m^A), then we shall find, as shown in Fig. 1.22b, that g^L and g^S will intersect at $X_{\mathrm{B}} = 0$. If the temperature is decreased further, then the curves are found to intersect somewhere in the middle, as shown in Fig. 1.22c. The diagram can be separated into three different composition range of $\left(0 - X_{\mathrm{B}}^S\right)$, $\left(X_{\mathrm{B}}^S - X_{\mathrm{B}}^L\right)$, and $\left(X_{\mathrm{B}}^L - 1\right)$. Here, especially the composition range of $\left(X_{\mathrm{B}}^S - X_{\mathrm{B}}^L\right)$ draws attention for further discussion.

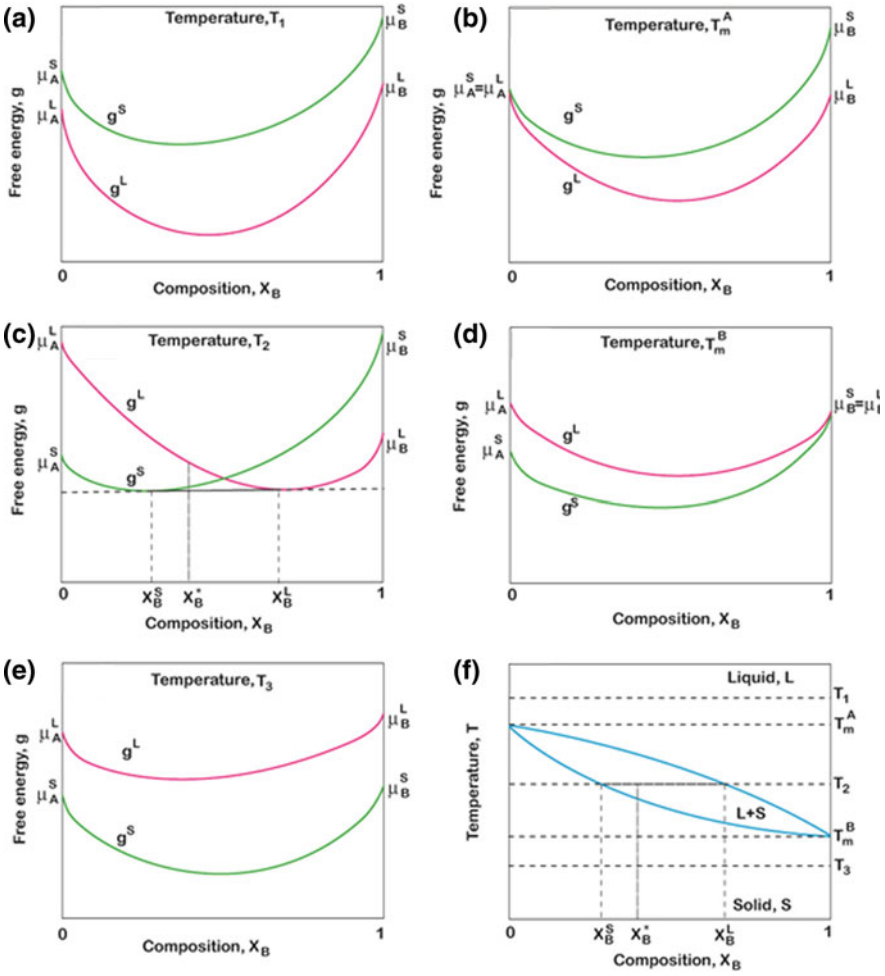

Fig. 1.22 Free energy versus composition diagram at different temperatures **a**–**e** for an isomorphous system and **f** the corresponding phase diagram

For the sake of discussion, if we consider the nominal composition X_B^* in this composition range, then it is apparent that the liquid phase (with this composition) cannot be stable at this temperature, since it does not correspond to the minimum free energy of the system. At the first instance, the solid phase with this composition seems to be the stable one. However, the system always tries to minimize its free energy if possible. In this case, there is a possibility to further minimize the free energy, if both solid and liquid phases exist together, the Gibbs energy value then sits on the common tangent as defined in Sect. 1.10. It is clear from Fig. 1.22c that the system will have minimum free energy when the solid phase with the composition of X_B^S exists with the liquid phase having the composition of X_B^L.

Since X_B^* is the average composition of the alloy, the mole fraction of the solid phase, following the lever rule (defined in Sect. 1.8), will be $(X_B^L - X_B^*)/(X_B^L - X_B^S)$ and the mole fraction of the liquid phase will be $(X_B^* - X_B^S)/(X_B^L - X_B^S)$. It should be noted that with the change in average composition within the range of $(X_B^L - X_B^S)$, the composition of the solid and liquid phases will not change, but, only the relative amount of the phases will change. It can also be understood from Fig. 1.22c that in this range, the liquid and solid phases with the composition X_B^S and X_B^L will exist together, since the chemical potential or activity of elements A and B in both the phases must be the same ($\mu_A^S = \mu_A^L$ and $\mu_B^S = \mu_B^L$). In other words, once solid and liquid phases reach their stable composition, there is no further driving force for change. It is also clear that in the composition range of $\left(0 - X_B^S\right)$, the solid phase will be stable since it has minimum free energy in that composition range, whereas in the composition range of $\left(X_B^L - 1\right)$, only the liquid phase will be stable since it has minimum free energy in that composition range. If we decrease the temperature to T_m^B, the free energy curves of the phases, as depicted in Fig. 1.22d, will intersect at $X_B = 1$. If we decrease the free energy of the system even further, the free energy of the solid phase, as shown in Fig. 1.22e, will be lower than the free energy of the liquid phase in all compositions and the solid phase will be stable. The corresponding phase diagram can be seen from Fig. 1.22f.

Next, let us consider a solution with a positive heat of mixing (endothermic behavior), which means that there is a miscibility gap in the system. Further, it is assumed that the miscibility gap occurs only in the solid state but not in the liquid phase. Thus, at low temperatures, the free energy of the mixing of the solid phase will be positive because of the positive heat of mixing. At higher temperature, however, the free energy of mixing becomes negative, because of the growing importance of the entropy term $(-T\Delta s_{mix})$. At a reasonably high temperature, the free energy of the solid and liquid phases might vary with composition, as shown in Fig. 1.23a.

With a further decrease in temperature to T_m^A, the free energy curves of solid (g^S) and liquid (g^L) phases will intersect, as is presented in Fig. 1.23b. Any further decrease in temperature down to T_2, because of the difference in curvature, g^L intersects g^S at two points, so there are five-phase regions stable at a different composition range, as given in Fig. 1.23c. With a further decrease in temperature to T_3, we shall find that g^S is lower than g^L at all compositions so that only the solid phase is stable at this temperature, as shown in Fig. 1.23d. It also should be noted that because of the endothermic nature of transformation, with the decrease in temperature, the curvature of g^S is decreased very rapidly and with the further decrease in temperature to T_4, the free energy of mixing becomes positive and the curvature of the free energy curve will become positive in a certain composition range in the middle.

This is the reason why in this composition range, the solid cannot be present as a single stable phase but will spontaneously dissociate into two different phases with compositions α_1 and α_2, as can be seen from Fig. 1.23e. The area between compositions α_1 and α_2 in Fig. 1.23e is called the spinodal region. It is to be noted that

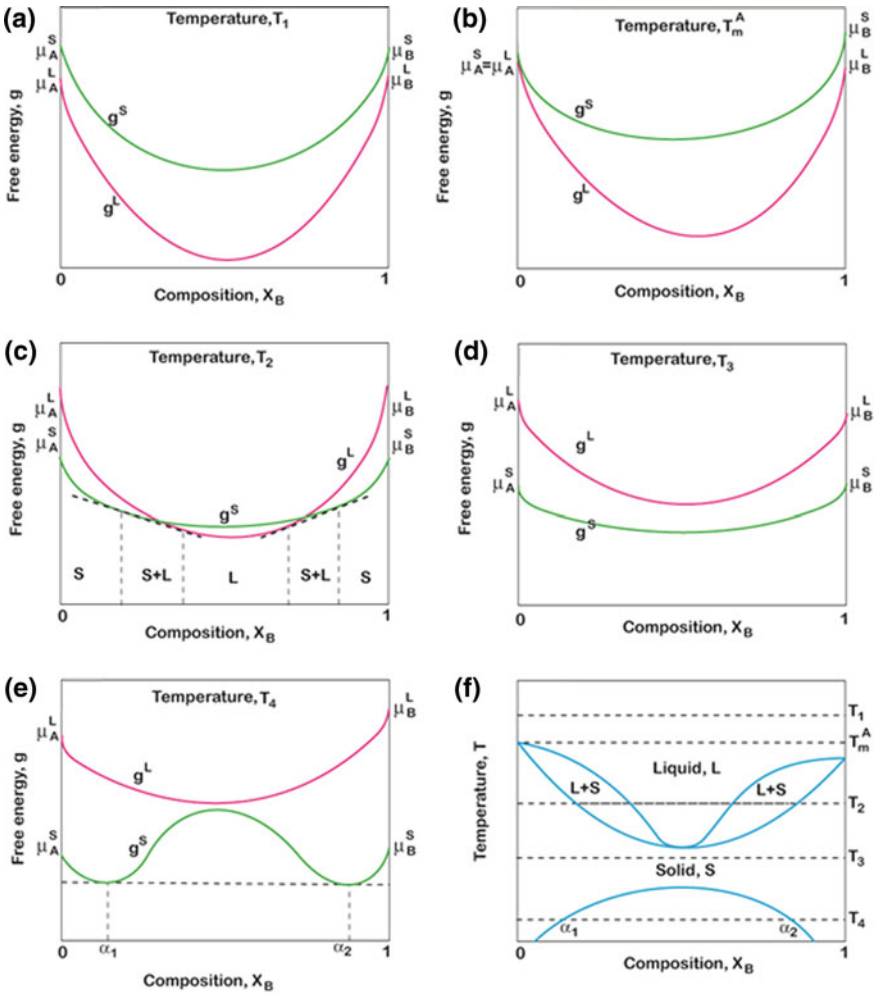

Fig. 1.23 Free energy versus composition diagram of a system which goes through endothermic transformation because of mixing and corresponding phase diagram

decomposition of the phase inside the spinodal does not require nucleation. Only after reaching the inflection points of the Gibbs energy curve, must nucleation precede the formation of a new phase. Figure 1.23f presents the corresponding phase diagram.

There are systems in which the enthalpy of mixing is positive and of such a high magnitude that the free energy curve will have positive curvature within a certain composition range up to a reasonably high temperature. In such cases, the free energy curves of the phases will change as a function of temperature in a way shown in Fig. 1.24a–e. The corresponding phase diagram is presented in Fig. 1.24f. Here, the main difference will be that at temperature T_E and at a particular

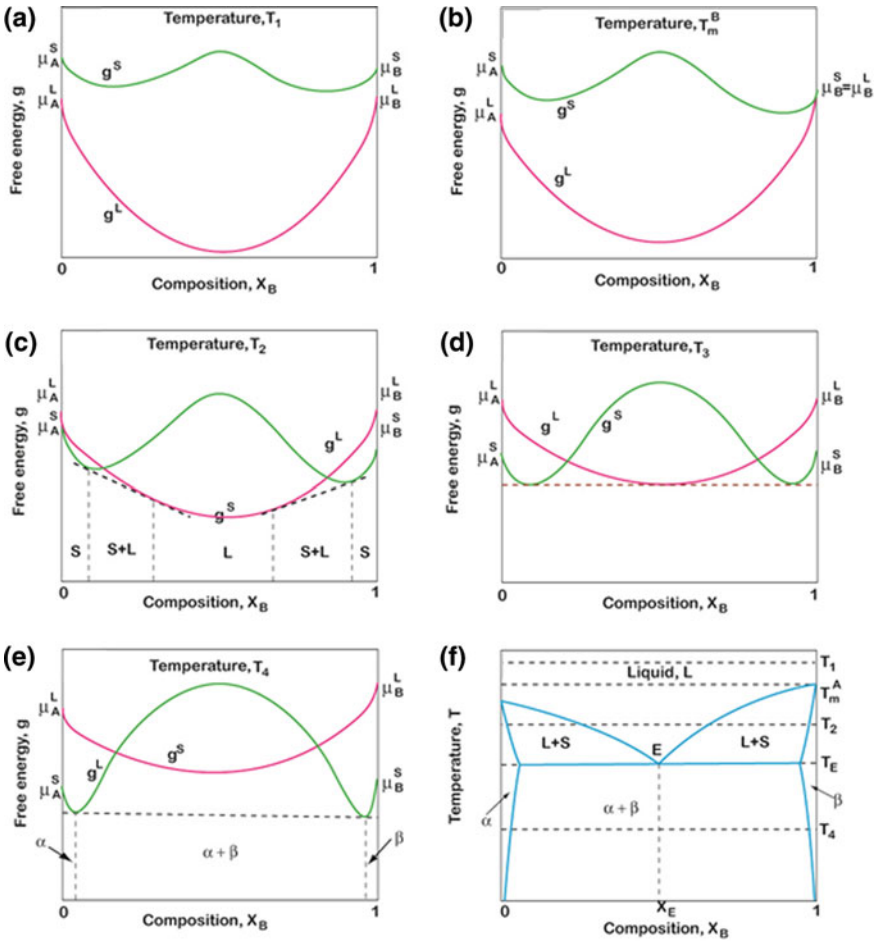

Fig. 1.24 Free energy versus composition diagram of a system which goes through endothermic transformation with very high enthalpy of mixing and corresponding phase diagram

composition X_E, the three phases, α, β, and L, can all exist together. Point E, plotted in Fig. 1.24f, corresponds to eutectic transformation. At the eutectic isotherm, the number of degrees of freedom is zero and thus, the equilibrium can occur only at a specific temperature and with fixed compositions of α, β, and L.

In all the above cases, we have considered systems where the crystal structure of elements A and B were similar and thus, there has been only one free energy curve for the solid phase. However, in a system where the elements have different crystal structure, we need to consider different free energy curves for different elements, as shown in Fig. 1.25. Let us designate, A(B), i.e., element A with a particular crystal structure, alloyed with some B as the α-phase. Similarly, B(A) is

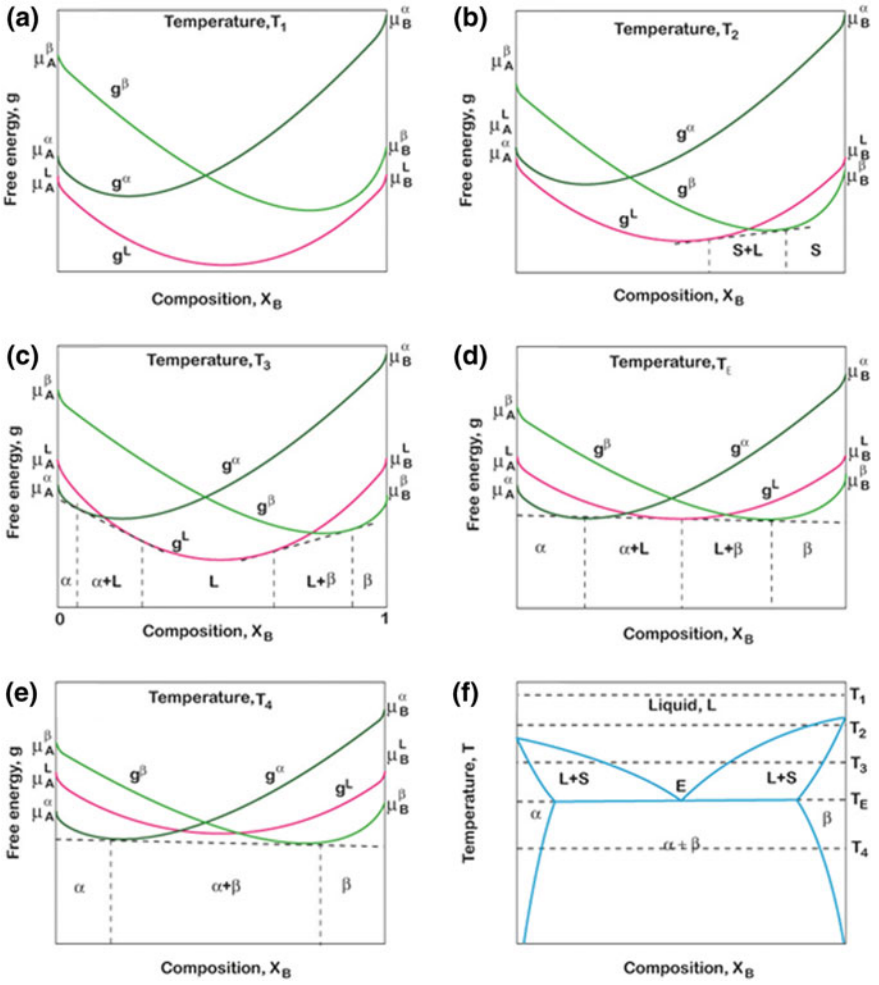

Fig. 1.25 Free energy versus composition diagram of a system where elements have different crystal structures and corresponding phase diagram

designated as the β-phase. Note in Fig. 1.25a that element A with the crystal structure of element B (g_B^{α}) will have a much higher free energy than its stable free energy (g_A^{α}); thus, it is a metastable crystal structure of A. Similarly, g_B^{α} is much higher than g_B^{α}. This system, under our consideration, also has an eutectic transformation as in the previous example.

Let us next consider the case, where the formation of the γ-phase in the system is associated with strong exothermic transformation, as can be noted from Fig. 1.26a. This implies that there is considerable difference in the electronegativities of the elements A and B. Note also that with only a slight change in

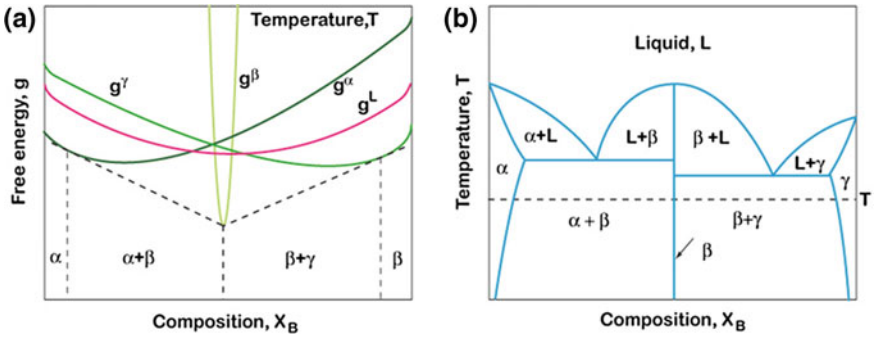

Fig. 1.26 Free energy versus composition diagram and the corresponding phase diagram where the phase (ordered γ-phase) goes through strong exothermic transformation

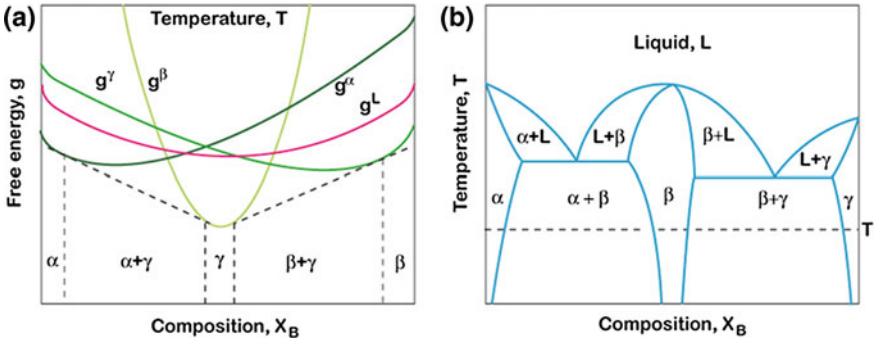

Fig. 1.27 Free energy versus composition diagram and the corresponding phase diagram where the ordered γ-phase has a wide homogeneity range

composition, the free energy of this phase increases very rapidly. Thus, the composition limits of the stability region of this phase are strictly limited. The corresponding phase diagram at a particular temperature T is given in Fig. 1.26b. As will be discussed in Sect. 2.6, different atoms in the ordered phase try to occupy particular lattice positions in the crystal to maximize the number of A–B bonds depending on the average composition of the phase. These ordered phases are known as *intermetallic compound* or *intermediate phases,* and in general, these phases have a different crystal structure than the crystal structure of the pure element. In the example shown in Fig. 1.26, it is to be observed that the γ-phase has a very narrow homogeneity range. However, in some cases, as presented in Fig. 1.27, the ordered phase can, in fact, have a wide homogeneity range, where the change in free energy (because of the small change in composition) is not very striking, unlike as in the previous example. These phases can deviate from their stoichiometric composition because of the presence of defects, as discussed in Sect. 1.11.

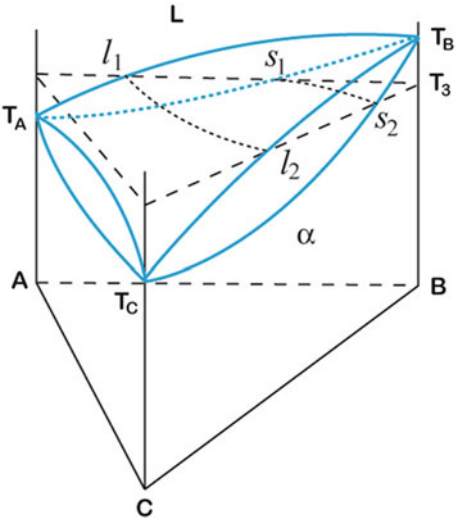

Fig. 1.28 Ternary space diagram with complete solid and liquid solubilities in all three binary systems

1.13 Ternary Phase Diagrams

According to the Gibbs phase rule, the number of degrees of freedom in a homogeneous ternary phase under constant pressure is three. Thus, we need to specify three independent variables (two-component mole fractions and temperature) in order to fix an equilibrium in a ternary solution phase. This leads to a three dimensional (T, X_A, X_B) presentation. As already discussed, it is of common practice to utilize an equilateral triangular (the Gibbs triangle) base (ABC) with three binary system "walls" (A–B, B–C, C–A) and temperature as the vertical axis. Next, we will briefly discuss ternary space diagrams as well as the isothermal and vertical sections taken from those diagrams.

Figure 1.28 shows the simplest possible ternary system, where there is complete solid and liquid solubility in the system (ABC). This ternary space model is very simple and easy to interpret, but as the systems become more complex, the space model becomes harder and harder to use. Therefore, it is common practice to utilize different sections and projections from the space model to yield more easily accessible information. As an example, the liquidus and solidus projections from the ABC system are shown in Fig. 1.29.

These types of projections are typically made with constant temperature intervals and can therefore be interpreted similarly as the contour lines in a map. Accordingly, the closer the spacing of the projection lines, the steeper is the projected surface. Isothermal sections are the most commonly used types of presentation of ternary equilibria. Figure 1.30 shows the isothermal section at temperature T_3 from the ABC system given in Fig. 1.28.

The plane intersects the liquidus surface at T_3 along the curve l_1l_2 and the solidus surface along the curve s_1s_2. On the left-hand side of the curve l_1l_2, there is

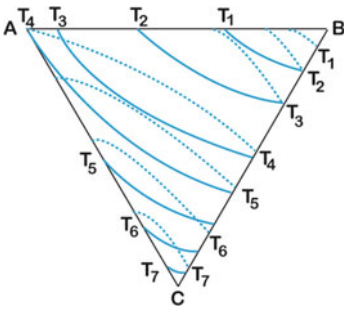

Fig. 1.29 Solidus and liquidus projections from the space diagram in Fig. 1.28

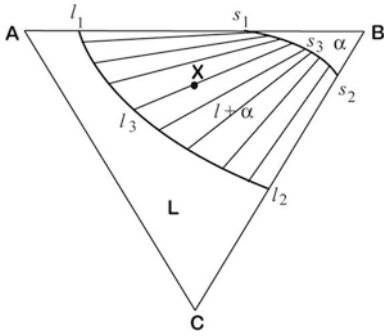

Fig. 1.30 Isothermal section at temperature T from the diagram seen in Fig. 1.28

a single-phase liquid region and on the right-hand side of the curve s_1s_2, there is a single-phase solid region. Between these two curves, there is a two-phase liquid and a solid region. The compositions of the phases in two-phase equilibrium are obtained at the end points of the tie-line and the amounts by the lever rule, as in binary phase diagrams. The directions of the tie-lines lying within the figure vary fan-like, so that there is a gradual transition from the direction of one bounding tie-line to that of the other. No two tie-lines at the same temperature may ever cross. This is a direct result of the Gibbs phase rule. Beyond these considerations, nothing can be said about the direction of tie-lines, except that they must run from liquidus to solidus. Other than those tie-lines on the edges of the diagram, none of them point toward a corner of the diagram unless by mere coincidence or due to a complete lack of solubility with the element at the given corner. Therefore, it is necessary to determine the position and direction of the tie-lines experimentally. It should be noted that the activity of a given component has the same value at each end of a tie-line.

Vertical sections (isopleths) from ternary space diagrams can also be taken. Figure 1.31 presents some ways in which this can be achieved. Afterward, these isopleths are shown in Fig. 1.32.

Even though the isopleths appear quite like binary phase diagrams, they must not be confused with them. In general, tie-lines cannot be used with isopleths and they only show the temperature composition regions of the different phases.

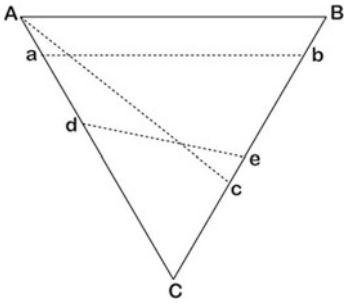

Fig. 1.31 Different ways one can take an isopleth

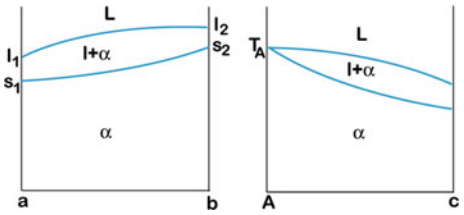

Fig. 1.32 Two isopleths taken along the lines ab and Ac

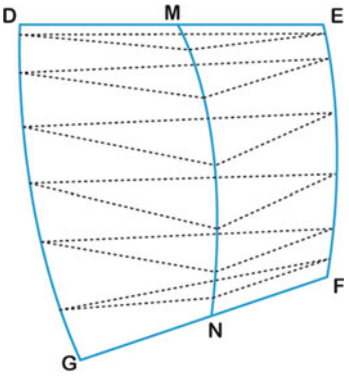

Fig. 1.33 Stack of tie-traingles

When there are three phases in equilibrium in a ternary system under constant pressure, there is still one degree of freedom left. Thus, three-phase equilibrium in a ternary system exists within a certain temperature range and not at a single temperature as in binary systems under constant pressure. Three-phase equilibrium in a ternary phase diagram is represented by a tie-triangle and as the temperature changes these tie-triangles form a "stack" of tie-triangles (Fig. 1.33). The composition of phases participating in the three-phase equilibrium can be found from the corners of the tie-triangle and the amount by applying the lever rule three times.

In this hypothetical ternary system in AC, there is complete solid and liquid solubility, whereas AB and BC are eutectic systems. Point M is the eutectic point of system AB, which is at a higher temperature than *N*, which is the eutectic point of the system BC. Thus, in both binary systems (AB and BC), an eutectic reaction $l \Leftrightarrow \alpha + \beta$ takes place. In Fig. 1.34, the surfaces AMNC ja MNB are the liquidus

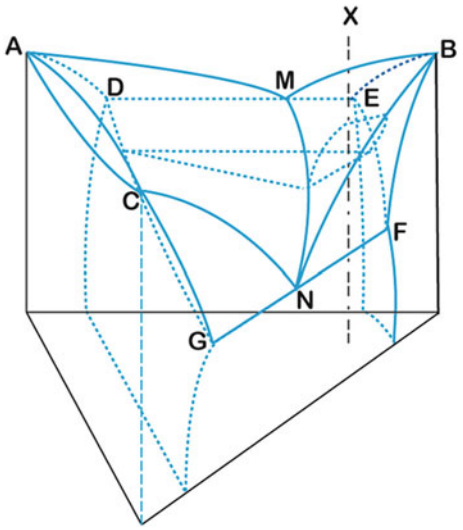

Fig. 1.34 ABC ternary system, where binary system AC has complete solid solubility and binary systems AB and BC are eutectic ones

surfaces and thus determine the solubilities of α and β to liquid. These surfaces meet at the eutectic valley MN. DG and EF are curves joining the points representing the respective compositions of the α and β phases formed in the eutectic reactions in the binary systems. DME and GNF are horizontal lines that represent these eutectic reactions. The surfaces ADGC and BEF are the solidus surfaces. The three curves MN, DG, and EF do not lie in the same plane. The curve MN lies above the surface DEFG, in such a way that there are three curved surfaces DMNG, MEFN, and DEFG, which enclose a three-phase space where α, β, and the liquid are in equilibrium. Each of these surfaces is made up of tie-lines representing $l + \alpha$, $l + \beta$, and $\alpha + \beta$ equilibria. The surfaces DMNG, MEFN, and DEFG separate the three-phase space from the liquid + α, liquid + β , and $\alpha + \beta$ regions, respectively. Where the three-phase region terminates in the binary systems AB and BC, it shrinks to the binary eutectic lines. In a ternary system, the eutectic reaction $l \rightarrow \alpha + \beta$ occurs over a range of temperature. If we have an alloy with nominal composition of X, as in Fig. 1.34, the solidification takes place as follows. During the solidification, the first solid phase to form is primary β, when the liquidus surface is first met. The composition of the liquid then changes along a path on the liquidus surface and that of the solid β along a path on the solidus surface as the temperature decreases. Then, at a certain temperature T_1, before solidification is completed, the liquid composition reaches a point on the curve MN and solid composition a point on the curve EF. The situation at T_1 is given in Fig. 1.35a where a tie-triangle is drawn. At this temperature, the nominal composition is seen to lie on the $l\beta$ tie-line. When the temperature is decreased to T_2, the three-phase equilibrium is established, as the nominal composition now lies inside the tie-triangle Fig. 1.35b. The compositions of the liquid, α, and β are given by the points l_2, α_2, and β_2, and their respective amounts can be obtained by applying the lever rule three times

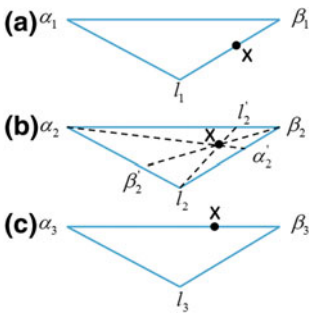

Fig. 1.35 The process of solidification of an alloy with nominal composition X in the system shown in Fig. 1.34 is exemplified in this figure as a function of temperature. **a** Temperature at which liquid composition reaches a point on the curve MN and solid composition a point on the curve EF, **b** temperature where three-phase equilibrium is established, and **c** temperature when solidification ends

$$\%\,\text{liquid}(l_2) = \frac{Xl_2'}{l_2l_2'} \times 100, \quad \%\,\beta_2 = \frac{X\beta_2'}{\beta_2\beta_2'} \times 100 \quad \text{and} \quad \%\,\alpha_2 = \frac{X\alpha_2'}{\alpha_2\alpha_2'} \times 100$$

Solidification ends at T_3 when the $\alpha_3\beta_3$ tie-line is encountered.

As the ternary systems become more complicated, the analysis shown above becomes increasingly difficult. Thus, it is of common practice to utilize different sections taken from the space model to provide information in a more accessible form. Next, we shall consider isothermal sections a little more, as they, in general, provide the most useful information on the ternary system. When working with the isothermal section and naming the phase regions, it is helpful to remember that the sides of the three-phase triangles must always face the two-phase regions, and at the corners of the tie-triangle, single-phase regions exist. These rules are based on the more general Palatnik-Landau theorem. Figure 1.36 contains an example of the AuPbSn system at 200 °C with all the phase regions clearly marked in the figure. It is to be noted that in the case of systems with stoichiometric compounds, the two-phase regions between three-phase regions may be reduced to just a single tie-line.

As an example of utilization of isothermal sections, we shall consider the following case. An interesting behavior has been observed in the Cu/SnBi eutectic system during soldering at temperatures above 200 °C. In particular, when the solder volume is small, reactions can result in drastic changes to the microstructure when soldering times are increased. Since bismuth does not react with Cu, only tin is consumed during the reactions. This will eventually lead to a shift in the liquid solder composition toward the Bi-rich corner. When the isothermal section of the SnBiCu equilibrium phase diagram is investigated, it is to be noted that when the enrichment of liquid with bismuth increases and the composition of the solder is around 60 at-% bismuth, the local equilibrium condition changes, as shown in Fig. 1.37.

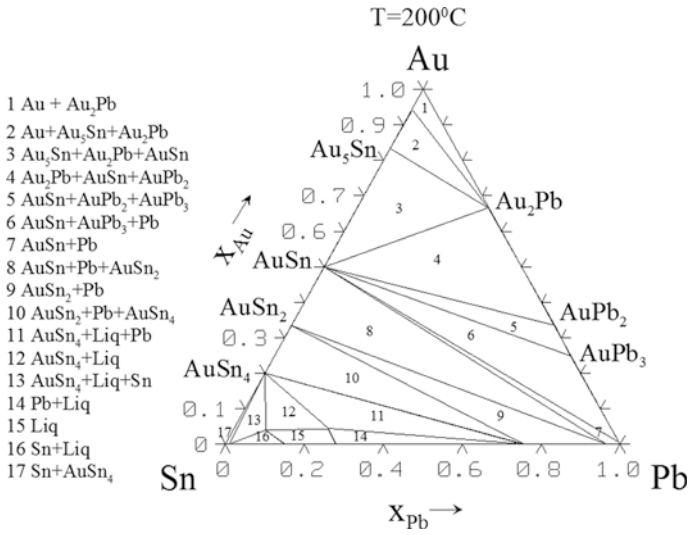

Fig. 1.36 Isothermal section from the Au–Pb–Sn ternary system at 200 °C

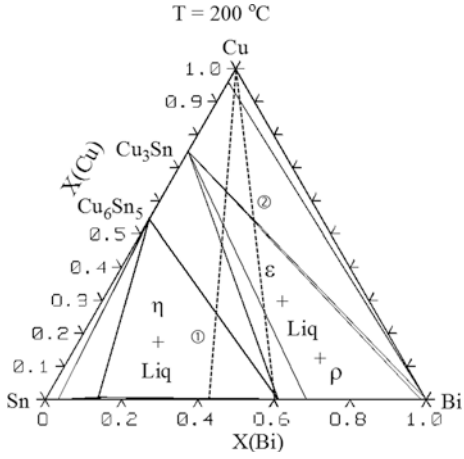

Fig. 1.37 Isothermal section from the Bi–Cu–Sn phase diagram at 200 °C

Cu_6Sn_5 cannot exist in local equilibrium with solder enriched with Bi at this temperature ($\sim$200 °C, shown as contact line 2). Cu_3Sn can, however, exist in local equilibrium even with pure Bi. Therefore, the Cu_6Sn_5 should transform into the Cu_3Sn layer. This has indeed been experimentally verified to take place [12]. The thing of special interest was that the Cu_3Sn layer maintained the original Cu_6Sn_5 morphology that it replaced [12].

From the thermodynamic data, one can also calculate the so-called phase fraction diagram (NP)-diagrams, which can be utilized to investigate, for example,

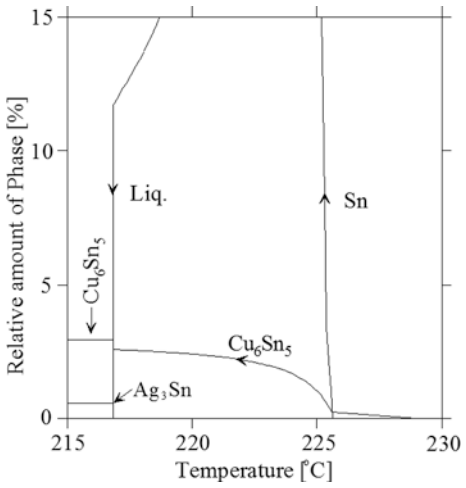

Fig. 1.38 NP-diagram of the phase formation during solidification of a SnAgCu solder, when Cu/(OSP) metallization is used. Note that owing to the high fraction of Sn, the diagram has been enlarged and therefore relative amount of phases goes only up to 15 %

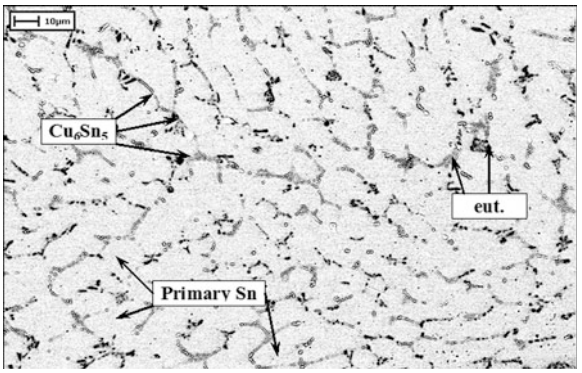

Fig. 1.39 Solder microstructure after reflow when Ni(P) metallization is used [13]

solidification. They show, as a function of temperature, the changes in the fractions of phase with a given nominal composition. An example is shown in Fig. 1.38.

As an example of the use of phase fraction diagrams, let us consider the next case, where identical SnAgCu solder alloy is used to solder components on two types of printed wiring boards (PWB's)—one with an Ni(P)/Au and one with a Cu(OSP) surface finish. Under the reflow conditions typically used in lead-free soldering, the solidification structure is generally cellular, where the small Cu_6Sn_5 and Ag_3Sn phases are dispersed between the large primary Sn grains [13]. If protective Au surface finishes are used, some small needle-like $AuSn_4$ can also be found inside the solder matrix at the high-angle boundaries. An example of the microstructure formed in the interconnections soldered with the Sn0.5Ag0.5Cu alloy on electrochemical Ni(P) with a thin flash Au on top (denoted Ni(P)|Au in the following) is shown in Fig. 1.39.

Both the Cu_6Sn_5 and the Ag_3Sn particles are uniformly distributed around the relatively large Sn grains. Figure 1.40 shows a micrograph taken from a sample

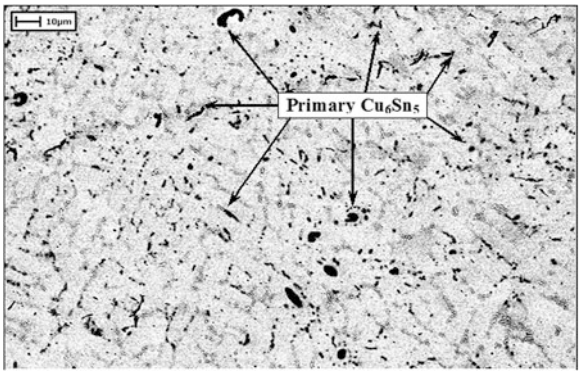

Fig. 1.40 Solder microstructure after reflow when Cu(OSP) metallization is used [13]

soldered with the same solder alloy but this time on the boards with organic solderability preservative (OSP) on the Cu pads (noted Cu|OSP). The resulting microstructure seems to be different even though the same solder alloy was used relative to Ni(P)|Au, interconnections formed on the Cu|OSP contain more and larger Cu_6Sn_5 intermetallic particles dispersed inside the solder.

What is the reason behind these differences observed experimentally? Let us take a closer look at what takes place during soldering. The thin layer of Au on top of Ni(P) dissolves instantly and completely into the molten solder, and the Ni starts dissolving next into the melt. The OSP coating partially evaporates and the rest dissolves into the solder flux during soldering. In the case of the Cu|OSP boards, it is the Cu pad that starts dissolving into the solder alloy. The dissolution rate of Cu in Sn0.5Ag0.5Cu (wt%) is about 0.07 μm/s. Based on this, the amount of Cu dissolution at the entire area of the soldering pad during the typical 40–45 s time above 217 °C is enough to lift the Cu concentration in the soldered interconnections close to 1 wt%, even when taking the amount of Cu bonded into the intermetallic layers on both sides of the interconnections into account. The dissolution rate of Ni is about 50 times smaller than that of Cu and thus, the dissolution of Ni to the solder is insignificant. All Ni that is dissolved at the interface is bonded to the $(Cu, Ni)_6Sn_5$ layer. Taking into account the amount of Cu bonded to the intermetallic layers on both sides of the interconnections, the nominal composition of the interconnections soldered on the Ni(P)|Au-coated pads will result in about Sn0.5Ag0.3Cu, whereas the final composition on the interconnection on Cu was about Sn0.5Ag1.0Cu.

An important consequence of higher Cu content is that solidification process is different in interconnections soldered on Ni from those soldered on Cu. Figures 1.38 and 1.41 present the phase fraction diagrams, where the amount of different phases in the relative number of moles can be presented as a function of temperature. The interconnections soldered on Ni(P)|Au PWB have the Sn0.5Ag0.3Cu composition, whereas the interconnections soldered on Cu|OSP have the Sn0.5Ag1.0Cu.

As can be seen from Fig. 1.41, the solidification of the liquid interconnections soldered on Ni(P)|Au boards starts with the formation of the primary Sn phase when

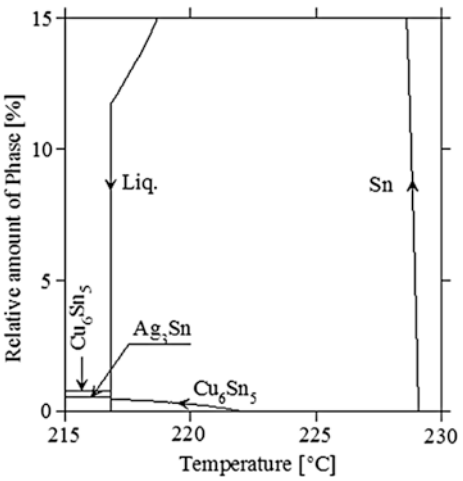

Fig. 1.41 NP-diagram of the phase formation during solidification when Ni(P)/Au metallization is used [13]

the interconnections are cooled down from the peak reflow temperature to below the liquidus temperature of 229 °C. The Cu_6Sn_5 phase does not nucleate until below 222 °C, where the composition of the liquid reaches the eutectic valley. Figure 1.38 presents the phase fraction diagram of the liquid interconnections soldered on Cu|OSP boards. In this case, the solidification begins with the formation of primary Cu_6Sn_5 below 229 °C. However, the nominal composition of the liquid soon meets the curve of two-fold saturation, after which the solidification of the interconnections proceeds by the binary eutectic reaction $L \rightarrow (Sn)eut + (Cu_6Sn_5)eut$. Below the four-phase invariant temperature, there is more than three times as much Cu_6Sn_5 in the Cu|OSP interconnections as in those on the Ni(P)|Au substrate. It is to be noted that the above analysis of solidification has been carried out by considering that the system is in complete equilibrium. As this is not typically the case in practical applications, the above-presented discussion must be taken to represent the ideal situation where kinetics plays no role in the process.

1.14 Stability Diagrams (Activity Diagrams, etc.)

The activity diagram shown in the right-hand side of Fig. 1.42 is one form of many different types of stability diagrams. In such a diagram, the thermodynamic potential of one of the components is plotted as a function of the relative atomic fractions of the other two components. The activity values which are needed in the construction of such a diagram can be calculated from the assessed thermodynamic data. When calculating the activities of the components, the activities of the stoichiometric compounds at equilibrium are regarded to be one. It should be noted that the precision of the calculations is very much dependent on the accuracy and

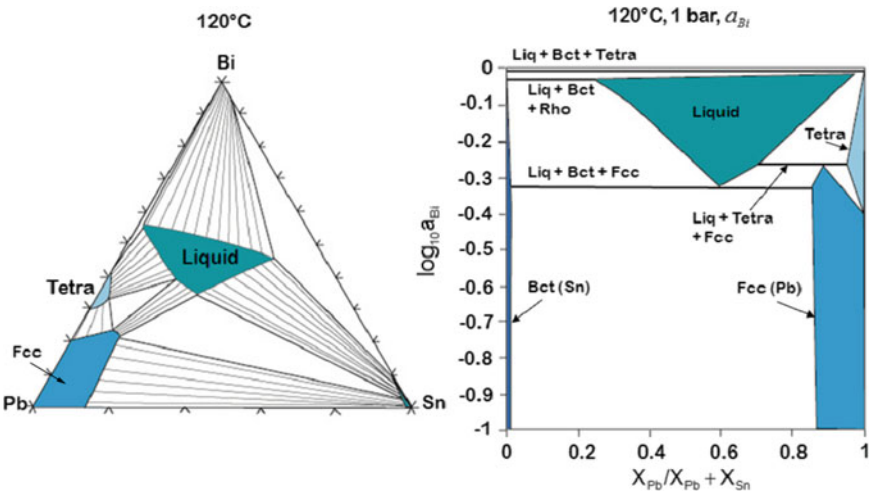

Fig. 1.42 Isothermal section from the Bi–Pb–Sn phase diagram at 120 °C and the corresponding activity diagram at the same temperature

consistence of the thermodynamic data used. Therefore, great care should be exercised when using data from different sources.

The edges of the diagram shown in Fig. 1.42 represent the binary systems (Sn–Bi, Sn–Pb, and Pb–Bi). The ternary phase relations are represented by the inside of the diagram. The stoichiometric single-phase regions are represented as vertical lines, two-phase regions as areas, and three-phase fields as horizontal lines. The vertical left- and right-hand axes represent the binary edge systems. In Fig. 1.42, the identical phase regions in the ternary isotherm and in the activity diagram at the same temperature are identified with the same color. The three-phase equilibria are shown as red triangles in the isothermal Section and as red horizontal lines in the activity diagram. In Fig. 1.43, the activity diagrams for all three species of the C–Si–Ta system are shown. Figure 1.44 shows the corresponding isothermal section.

The activity diagrams provide useful information about the formation of the reaction layer sequence when used together with the isothermal sections as follows. The example is from the Si/TaC/Cu diffusion barrier structure where the Si/TaC interface is studied. From the phase diagram, it is evident that the Si/TaC interface is not in equilibrium and a driving force for the formation of additional phases between the substrate and the TaC layer therefore exists (Fig. 1.44). Although there exists a TaC + $TaSi_2$ two-phase region in the phase diagram (Fig. 1.44), SiC must be formed to incorporate the carbon released after the formation of $TaSi_2$ in the reaction between Si and TaC, because of the mass balance requirement. The formation of SiC and $TaSi_2$ was confirmed with TEM investigations and therefore gives support to the assessed phase diagram. The reacted structure consisted of layers of SiC and $TaSi_2$ on top of the silicon substrate.

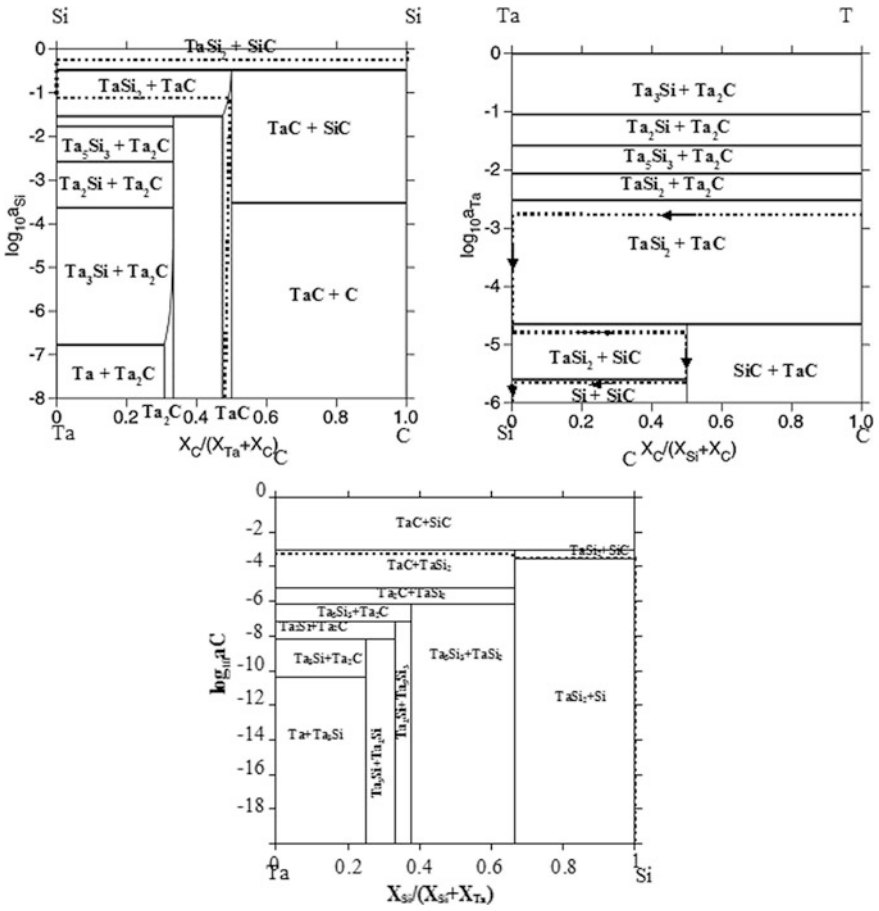

Fig. 1.43 Activity diagrams for C, Si, and Ta at 800 °C [14]

The original TaC was completely consumed during the reaction, since no traces of it could be found at 800 °C. The reaction sequence seemed to be Si/SiC/$TaSi_2$/TaC, in which the TaC was used completely to yield the final structure Si/SiC/$TaSi_2$. Silicon is expected to be the first species moving at this interface owing to the following reasons. Firstly, Si has been found to be the mobile species during the formation of $TaSi_2$ that occurs around 650 °C in the binary Ta–Si system by Si in diffusion, whereas the movement of Ta has not been observed under similar conditions. Secondly, chemical bonding between Ta and C in the TaC compound is expected to be strong, and breaking of these bonds, which is required for the release and subsequent diffusion of Ta, would require large amounts of energy. Owing to the facts stated above, the diffusion of tantalum or carbon in this system is not considered to be highly probable. Consequently, Si is anticipated to be the main diffusing species at the Si/TaC interface around 800 °C.

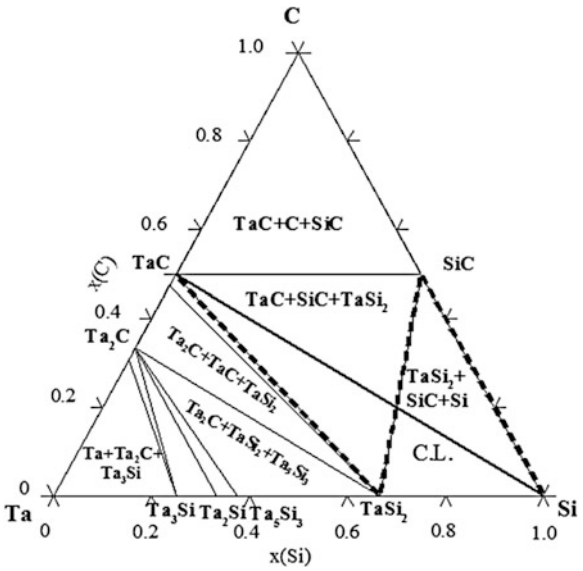

Fig. 1.44 Isothermal section at 800 °C from the C–Si–Ta system [14]

Whether the above-presented phase formation sequence is thermodynamically possible can be investigated with the help of Fig. 1.43. As can be seen from the calculated activity diagram, Si can move along its lowering activity in the proposed reaction sequence and therefore, diffusion of Si in this particular reaction sequence is allowed on thermodynamic grounds. The examination of the calculated activity diagrams for carbon and tantalum does not restrict the diffusion of these elements in the suggested reaction sequence either (Fig. 1.43). However, as already discussed, carbon and tantalum are strongly bonded to each other in the TaC compound and are not expected to move easily. Therefore, the reaction most likely starts by Si in diffusion into TaC (most probably via grain boundaries). This is followed by the formation of $TaSi_2$, which then leads to the accompanied dissociation of TaC. The released carbon is then available for the formation of SiC in the reaction with Si. This mechanism will finally yield the experimentally observed structure $Si/SiC/TaSi_2$.

1.15 The Use of Gibbs Energy Diagrams

In the following examples, the use of Gibbs energy diagrams is presented. The discussion follows largely that presented in the classical treatments of the subject by Hillert [10, 15].

In Fig. 1.45, a typical molar property diagram at a given temperature T_0 is shown. The diagram shows some of the basic properties of a molar property diagram. From Fig. 1.45, one can see, for example, how a Gibbs energy of a phase is defined ($g^{\alpha} = X_A^{\alpha}\mu_A^{\alpha} + X_B^{\alpha}\mu_B^{\alpha}$) with the help of chemical potentials, how the

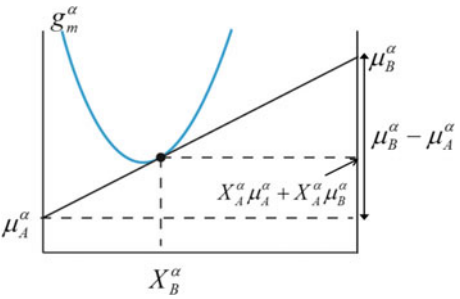

Fig. 1.45 Typical molar property diagram

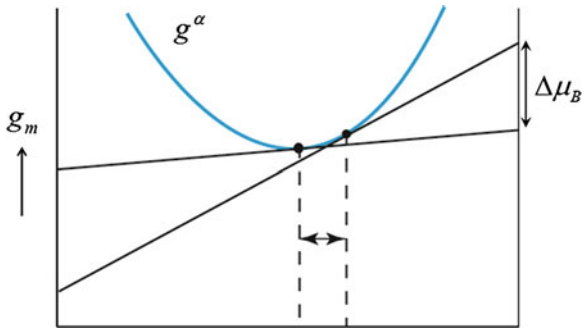

Fig. 1.46 Determination of the driving force for diffusion within a solution phase

chemical potentials for a species in a given phase are defined (from the end points of the tangent), that the slope of a tangent equals the chemical potential difference of B and A in the alpha phase $\left(\frac{dg^\alpha}{dX_\mathrm{B}} = \mu_\mathrm{B}^\alpha - \mu_\mathrm{A}^\alpha\right)$, and so on. These simple geometrical features of the molar diagrams can be used for a wide variety of applications [15].

The positive curvature of the Gibbs energy curve makes the phase stable against fluctuations in composition. The same feature of the curve also provides the driving force for the elimination of differences in composition within the phase (Fig. 1.46). Thus, this is the driving force for diffusion. Let us consider the situation where B atoms diffuse from a region of high concentration (more precisely activity) to a region of low concentration. Each individual region may be regarded as a reservoir of B with its own value of g_B, and the difference in g_B is identical to the decrease in Gibbs free energy when one mole of B is transferred. We make an assumption that the rate of transfer is proportional to the decrease in Gibbs free energy and the number of B atoms per volume $\frac{X_\mathrm{B}}{v_m}$ and inversely proportional to the transport distance Δy. With these assumptions, the expression for the flux of B atoms may be written as

$$J_\mathrm{B} = -\frac{M_\mathrm{B} X_\mathrm{B}}{v_m}\frac{\Delta g_\mathrm{B}}{v_m} = -\frac{M_\mathrm{B}}{v_m} X_\mathrm{B} \frac{dg_\mathrm{B}}{dX_\mathrm{B}}\frac{\Delta X_\mathrm{B}}{\Delta y} \tag{1.103}$$

The constant of proportionality, M_B, may be regarded as the mobility of the B atoms. By introducing the curvature of the g curve, we obtain

$$J_B = -\frac{M_B}{v_m} X_A X_B \frac{d^2 g}{dX^2} \frac{\Delta X_B}{\Delta v_m} \tag{1.104}$$

By considering the Fick's first law (see Chap. 3), the diffusion constant for B is recognized as

$$D_B = M_B X_A X_B \frac{d^2 g}{dX_B^2} \tag{1.105}$$

The mobility is thus multiplied by the thermodynamic factor. By using the activity or activity coefficient for B, the thermodynamic factor can be transformed to the shape as used in Chap. 3

$$X_A X_B \frac{d^2 g}{dX_B^2} = X_B \frac{dg_B}{dX_B} = \frac{dg_B}{d \ln X_B} = RT \frac{d \ln a_B}{d \ln X_B} = RT \left(1 + \frac{d \ln \gamma_B}{d \ln X_B}\right) \tag{1.106}$$

A similar derivation can be carried out also for component A, and the same factor is obtained

$$D_A = M_A X_A X_B \frac{d^2 g}{dX_B^2} \tag{1.107}$$

It is to be noted that in ternary systems, there are more than one thermodynamic factor. In a binary system, the Gibbs–Duhem equation (will be derived in Sect. 1.16) gives

$$X_A d\mu_A + X_B d\mu_B = 0$$

and

$$X_A d\mu_A = RT(dX_A + X_A d \ln \gamma_A)$$
$$X_B d\mu_B = RT(dX_B + X_B d \ln \gamma_B)$$

In a binary system, $X_A + X_B = 1$ and thus, $dX_A + dX_B = 0$ which finally gives

$$X_A \left(\frac{d \ln \gamma_A}{dX_A}\right) = X_B \left(\frac{d \ln \gamma_B}{dX_B}\right)$$

or

$$\frac{d\ln a_A}{d\ln X_A} = \frac{d\ln a_B}{d\ln X_B}$$

In a ternary system, Gibbs–Duhem equation is written as

$$X_A d\mu_A + X_B d\mu_B + X_C d\mu_C = 0$$

and it is immediately seen there must be more than one thermodynamic factor in a given ternary system. In fact, there are four factors of which three are independent.

van Loo et al. have derived [16] equations for the four thermodynamic factors in a ternary system as well as the relation between the three independent ones and the fourth which depends on the other three as follows.

$$\Theta_{11} = \left(\frac{d\ln a_1}{d\ln X_1}\right)_{p,T,X_2} \quad \Theta_{12} = \left(\frac{d\ln a_1}{d\ln X_2}\right)_{p,T,X_1}$$

$$\Theta_{21} = \left(\frac{d\ln a_2}{d\ln X_1}\right)_{p,T,X_2} \quad \Theta_{22} = \left(\frac{d\ln a_2}{d\ln X_2}\right)_{p,T,X_1}$$

$$\Theta_{21} = \frac{X_1}{(1-X_1)}\left[\frac{(1-X_2)}{X_2}\Theta_{12} + \Theta_{22} - \Theta_{11}\right]$$

By noting that the so-called phenomenological constant is related to the mobility by $L_B = M_B C_B$ and by remembering the relation between the chemical potential and the activity, the fluxes of elements A and B can be expressed as

$$\begin{aligned} J_A &= -L_A \frac{d\mu_A}{dx} \\ J_B &= -L_B \frac{d\mu_B}{dx} \end{aligned} \tag{1.108}$$

This equation will be utilized in Chap. 4.

One can also use Gibbs energy diagrams to obtain the driving force for diffusion of a particular species over a growing phase.

In Fig. 1.47, the common tangent construction defined above is used to determine the driving forces for diffusion of Cu through Cu_3Sn and Sn through Cu_6Sn_5. $\Delta\mu^{\varepsilon}_{Cu}$ is the chemical potential difference of Cu between interfaces Cu_3Sn/Cu and Cu_6Sn_5/Cu_3Sn, which drives the diffusion of Cu through Cu_3Sn and $\Delta\mu^{\eta}_{Sn}$ is the chemical potential difference of Sn between the interfaces Sn/Cu_6Sn_5 and Cu_6Sn_5/Cu_3Sn, which drives the diffusion of Sn through the Cu_6Sn_5 layer. It is easy to realize from Fig. 1.47 that changes in the stabilities of the η- and ε-phases

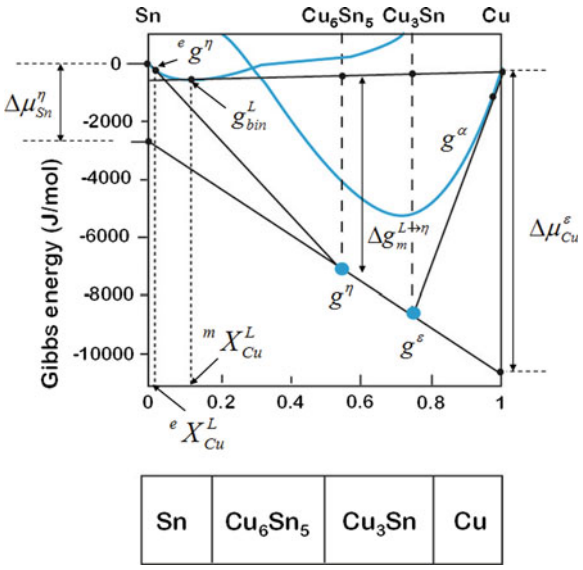

Fig. 1.47 Gibbs energy diagram from the Cu–Sn system at 235 °C

(in their Gibbs free energy) will change the values of $\Delta\mu^{\eta}_{\mathrm{Sn}}$ and $\Delta\mu^{\varepsilon}_{\mathrm{Cu}}$ and thus increase or decrease the driving forces for diffusion of components in the system.

From Fig. 1.47, other important features can also be extracted. For instance, the common tangent between the curves g^{L}_{bin} and g^{η} gives the equilibrium solubility of Cu to a liquid solder (L), which is given as ${}^{e}X^{L}_{\mathrm{Cu}}$. The equilibrium solubility is the amount of Cu that can be dissolved infinitely slowly to liquid solder before the η-phase comes into equilibrium with the liquid. The formation of the η-phase does not, however, occur with this composition, as the driving force is zero at this point (no supersaturation). In real cases, the dissolution of Cu does not take place infinitely slow and, therefore, the equilibrium solubility is generally exceeded. The solubility of Cu does not increase infinitely, but there is an upper limit for its value and this can also be determined from Fig. 1.47. When more and more Cu dissolves into liquid, eventually, a situation is faced where the dissolution of more Cu would lead to the precipitation of pure metallic Cu out of the supersaturated solder. This corresponds to the common tangent construction between the solder and pure Cu. The tangent point in the liquid curve at this metastable equilibrium gives the upper value of Cu that can be dissolved into liquid solder at any rate, i.e., the metastable solubility ${}^{m}X^{L}_{\mathrm{Cu}}$. When this value has been reached, also the driving force for the formation of the η-phase has reached its maximum (shown in the diagram as $\Delta g^{L\rightarrow\eta}$ in Fig. 1.47). Since the metastable solubility is directly related to the dissolution rate of a given metal to a solder in question, it provides important information about the formation of intermetallic compounds between different metals and solders. In many cases, its value is about 2–3 times larger than the equilibrium solubility [17–19].

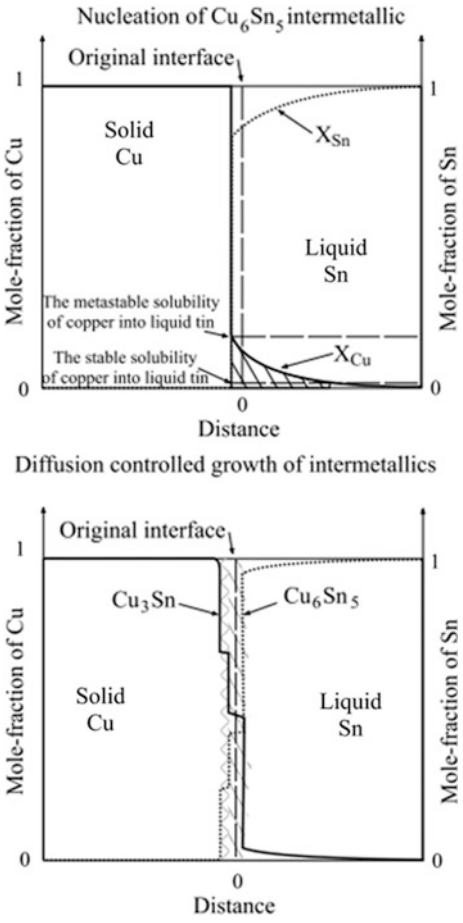

Fig. 1.48 Schematic presentation of the solid Cu/liquid Sn reaction couple after about 1 s (*upper figure*) and after several minutes (*lower figure*)

To get an idea about the relation between the above discussion and the actual phase formation in reaction couple where solid Cu is in contact with liquid Sn, it is helpful to consider the schematic presentation of the situation in Fig. 1.48. As Cu comes into contact with liquid Sn, it starts to dissolve rapidly. The equilibrium solubility of Cu_6Sn_5 to liquid Sn (${}^eX_L^{Cu}$) is achieved quickly (in fractions of second). Owing to the reasons explained above, the dissolution does not stop at this value but the dissolution of Cu continues until the ultimate limit, the metastable solubility (${}^mX_L^{Cu}$), is reached. At this point, the equilibrium between pure Cu and supersaturated liquid is achieved (equal chemical potential of Cu in both phases). This means that the dissolution of Cu must stop as there is no driving force for that anymore. At the same point, the maximum driving force for the formation of Cu_6Sn_5 is established (see Fig. 1.47). The composition profile of Cu is during these initial stages are shown by the hatched area in Fig. 1.49. As can be seen,

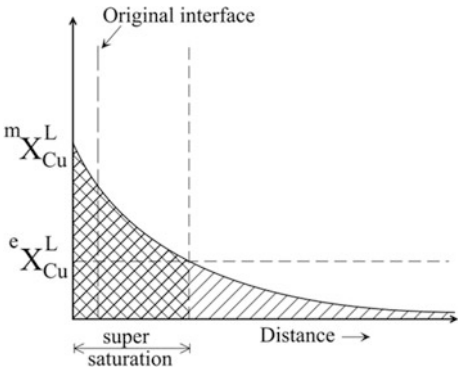

Fig. 1.49 Enlarged part of the solubility curves of the upper figure in Fig. 1.48

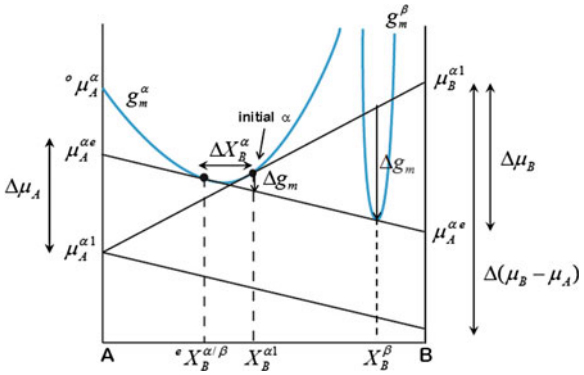

Fig. 1.50 Determination of a driving force for the nucleation of a new phase from supersaturated solid solution

there is a certain amount of Cu, the double hatched area, which exceeds the equilibrium solubility of Cu_6Sn_5 to liquid Sn. This is the extra amount of Cu that can be used to form Cu_6Sn_5 isothermally. It is evident from Fig. 1.49 that at the interface between Cu_6Sn_5 and the liquid Sn, the equilibrium solubility is established (where the second vertical dashed line from the left crosses the composition curve in Fig. 1.49).

The driving force for the precipitation can also be evaluated from the Gibbs phase diagram (Fig. 1.50). In Fig. 1.50, an alloy, α_1, which is inside the two-phase region $\alpha + \beta$ is shown. The Gibbs free energy of the system would decrease by precipitation of β, and the total driving force for the complete reaction in one mole of the alloy is given by the short arrow Δg The driving force for the formation of a very small quantity of β from a large quantity of α_1 is obtained by considering the tangent representing the supersaturated α-phase. The magnitude of the driving force (in nucleation stage) is given by the separation of the points at the two tangents as

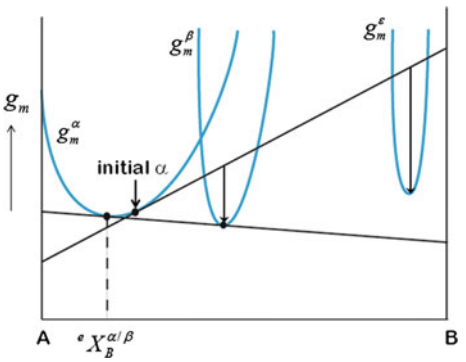

Fig. 1.51 Formation of a metastable phase

$$\begin{aligned}\Delta g &= X_A^\beta \mu_A^{\alpha 1} + X_B^\beta \mu_B^{\alpha 1} - g^\beta \\ g^\beta &= X_A^\beta \mu_A^{\alpha e} + X_B^\beta \mu_B^{\alpha e} \\ \Delta g &= X_A^\beta (\mu_A^{\alpha 1} - \mu_A^{\alpha e}) + X_B^\beta (\mu_B^{\alpha 1} - \mu_B^{\alpha e})\end{aligned} \tag{1.109}$$

For low supersaturations, one can introduce the curvature of the g^α curve. By comparing the triangles in Fig. 1.50, one obtains

$$\frac{\Delta g}{X_B^\beta - X_B^\alpha} = \frac{(\mu_B - \mu_A)}{1} \tag{1.110}$$

This can be further modified to obtain

$$\Delta g = \left(X_B^\beta - X_B^\alpha\right)\Delta(\mu_B - \mu_A) = \left(X_B^\beta - X_B^\alpha\right)\Delta\left(\frac{dg^\alpha}{dX_B}\right) \tag{1.111}$$

$$\Delta g = \frac{d^2 g^\alpha}{dX_B^2}\left(X_B^\beta - X_B^\alpha\right)\Delta X_B^\alpha \tag{1.112}$$

The last expression contains a factor $\left(x_B^\beta - x_B^\alpha\right)$ which is the difference in composition between the two phases. At the start of the precipitation, a new phase may be favored (higher driving force) if it differs much in composition even when it cannot be in stable equilibrium with the matrix phase. Thus, formation of a metastable phase (here ε) is favored (Fig. 1.51) according to the Ostwald rule.

One can also obtain quantitative numerical data about energy changes in a given system, by utilizing the simple geometric constructions shown above together with some simplified assumptions. Let us take one example from the important Cu–Sn system (Fig. 1.52). Consider the nucleation and growth of the η-phase, with $X_{Cu}^\eta = a$ and $X_{Sn}^\eta = b$ $(a + b = 1)$, out of supersaturated solder $^m X_{Cu}^L = c$. The driving force for the nucleation of the η-phase is given by $\Delta g^\eta = g_{tg}^L - g_{tg}^L$ (per mole of η). The two terms can be expanded as

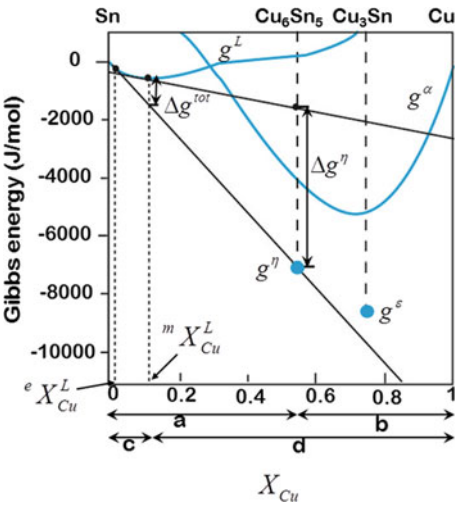

Fig. 1.52 Gibbs energy diagram from the Cu–Sn system at 235 °C

$$g^L_{tg} = X^\eta_{\mathrm{Cu}}\, {}^m\mu^L_{\mathrm{Cu}} + (1 - X^\eta_{\mathrm{Cu}})^m \mu^L_{\mathrm{Sn}} \tag{1.113}$$

and

$$g^L_{tg} = X^\eta_{\mathrm{Cu}}\, {}^e\mu^L_{\mathrm{Cu}} + (1 - X^\eta_{\mathrm{Cu}})^e \mu^L_{\mathrm{Sn}} \tag{1.114}$$

which gives

$$\Rightarrow \Delta g^\eta = X^\eta_{\mathrm{Cu}}\, {}^m\mu^L_{\mathrm{Cu}} + \left(1 - X^\eta_{\mathrm{Cu}}\right)^m \mu^L_{\mathrm{Sn}} - \left[X^\eta_{\mathrm{Cu}}\, {}^e\mu^L_{\mathrm{Cu}} + \left(1 - X^\eta_{\mathrm{Cu}}\right)^e \mu^L_{\mathrm{Sn}}\right] \tag{1.115}$$

and by using the definition of the chemical potential of a component, this gives

$$= RT\left[X^\eta_{\mathrm{Cu}} \ln\left(\frac{{}^m a^L_{\mathrm{Cu}}}{{}^e a^L_{\mathrm{Cu}}}\right) + X^\eta_{\mathrm{Sn}} \ln\left(\frac{{}^m a^L_{\mathrm{Sn}}}{{}^e a^L_{\mathrm{Sn}}}\right)\right] \tag{1.115}$$

If we simplify the treatment by assuming that the liquid behaves as a perfect solution, the activity values can be replaced by compositions, which give

$$\begin{aligned}
&\cong RT\left[X^\eta_{\mathrm{Cu}} \ln\left(\frac{{}^m X^L_{\mathrm{Cu}}}{{}^e X^L_{\mathrm{Cu}}}\right) + (1 - X^\eta_{\mathrm{Cu}}) \ln\left(\frac{1 - {}^m X^L_{\mathrm{Cu}}}{1 - {}^e X^L_{\mathrm{Cu}}}\right)\right] \\
&\cong 8.3145\ \mathrm{J/Kmol} \cdot 508\ \mathrm{K}\left[0.545 \ln\left(\frac{0.06}{0.018}\right) + (1 - 0.545) \ln\left(\frac{1 - 0.06}{1 - 0.018}\right)\right] \\
&= 2687.5\ \mathrm{J/mol}
\end{aligned} \tag{1.116}$$

Similarly, the change in Gibbs energy of the system owing to the precipitation of Cu_6Sn_5 can be expressed as

$$\Delta g^{\text{tot}} = g_{tg}^{L} - {}^{e}g_{tg}^{L} (= \Delta g^{L \to L+\eta}) \tag{1.117}$$

This can be written as

$$= RT \left[{}^{m}X_{\text{Cu}}^{L} \ln \left(\frac{{}^{m}a_{\text{Cu}}^{L}}{{}^{e}a_{\text{Cu}}^{L}} \right) + {}^{m}X_{\text{Sn}}^{L} \ln \left(\frac{{}^{m}a_{\text{Sn}}^{L}}{{}^{e}a_{\text{Sn}}^{L}} \right) \right] \tag{1.118}$$

and by again assuming perfect behavior

$$\begin{aligned} &\cong RT \left[{}^{m}X_{\text{Cu}}^{L} \ln \left(\frac{{}^{m}X_{\text{Cu}}^{L}}{{}^{e}X_{\text{Cu}}^{L}} \right) + \left(1 - {}^{m}X_{\text{Cu}}^{L}\right) \ln \left(\frac{1 - {}^{m}X_{\text{Cu}}^{L}}{1 - {}^{e}X_{\text{Cu}}^{L}} \right) \right] \\ &\cong 8.3145\,\text{J/Kmol} \cdot 508\,\text{K} \left[0.06 \ln \left(\frac{0.06}{0.018} \right) + (1 - 0.06) \ln \left(\frac{1 - 0.06}{1 - 0.018} \right) \right] \\ &= 131.6\,\text{J/mol} \end{aligned} \tag{1.119}$$

Hence, it can be concluded that these simple molar diagrams (Gibbs free energy diagrams) give an extensive amount of important information in an easily visualized form.

1.15.1 Effect of Pressure on the Phase Equilibrium

Related to the effects of pressure on the phase equilibrium, we shall consider two equations, the Laplace and the Kelvin equations. If a fluid interface is curved between two phases, then it turns out that the pressures on either side must be different. When the system is in equilibrium, every part of the surface must be in mechanical equilibrium (also in thermal and chemical). For a curved surface, the forces of surface tension are exactly balanced by the difference in pressure on the two sides of the interface. This is expressed by the Laplace equation

$$p^{\alpha} - p^{\beta} = \gamma \left(\frac{1}{r'} + \frac{1}{r''} \right) \tag{1.120}$$

where P stands for the pressure, γ is the surface tension, and r' and r'' are the radii of curvatures. By convention, positive values are assigned for the radii of curvature if they lie in phase α (see Fig. 1.53).

An important consequence of the Laplace equation concerns the effect of surface curvature on the vapor pressure of a liquid. This relationship is known as the Kelvin equation

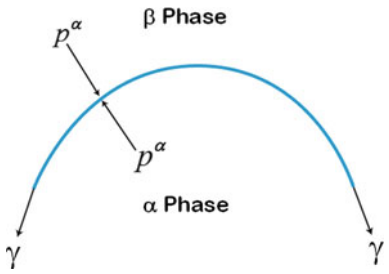

Fig. 1.53 Pressure difference across a curved surface

$$\ln\left(\frac{p^{c}}{p^{\infty}}\right) = \left(\frac{\gamma v_m^L}{RT}\right)\left(\frac{2}{r_m}\right) \tag{1.121}$$

where p^{c} and p^{∞} are the vapor pressures over the curved surface of mean curvature $r_m\left(\frac{1}{r_m} = \frac{1}{2}\left(\frac{1}{r'} + \frac{1}{r''}\right)\right.$ and a flat surface ($r = \infty$) and v_m^L is the molar volume of the liquid. There is a convention to assign a positive sign to r_m when it lies in the liquid phase and a negative sign when it lies in the vapor phase. Equation 1.121 can be used, for example, to rationalize capillary condensation or in the treatment of nucleation (Chap. 11). Condensation occurs when the actual vapor pressure exceeds the equilibrium vapor pressure. If the surface is curved, the Kelvin Eq. 1.121 shows that the actual pressure can be significantly lower than equilibrium pressure and thus, condensation in pores in the solid (if the liquid wets the solid) or between closed spaced solid particles may occur.

The effect pressure on the phase equilibrium can be investigated with Gibbs energy diagrams. According to the definition, the Gibbs free energy of a phase depends upon the pressure according to $g = g(0) + pv_m$ where 0 denotes the atmospheric pressure. As discussed above, for condensed phases, the pv_m term can often be neglected if the pressure is not exceptionally high. However, it plays an important role if the two phases in equilibrium are under different pressures. This occurs, as shown above, when the interface is curved and is caused by the surface tension (or energy) of the curved interfaces. Next, we shall briefly discuss how the equilibrium between two phases is changed by the introduction of increased pressure. The two g curves are displaced upward by the amounts $p^{\alpha}v_m^{\alpha}$ and $p^{\alpha}v_m^{\beta}$, respectively. This takes place even with phase compositions so well defined that they will not change (Fig. 1.54a). The change in g_B, for instance, can be evaluated as follows. By comparing the triangles in Fig. 1.54b, one obtains

$$\frac{g_B - p^{\beta}v_m^{\beta}}{g_B - p^{\alpha}v_m^{\alpha}} = \frac{X_A^{\beta}}{X_A^{\alpha}} \tag{1.122}$$

where ΔG_B equals $g_B(p^{\alpha}, p^{\beta}) - g_B(0)$. The above equation can be rearranged to give

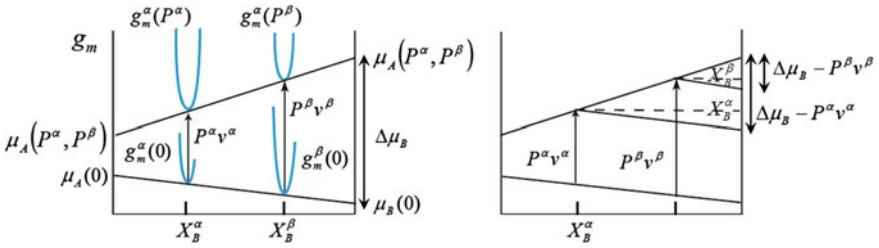

Fig. 1.54 Effect of pressure on phase equilibrium between two stoichiometric phases

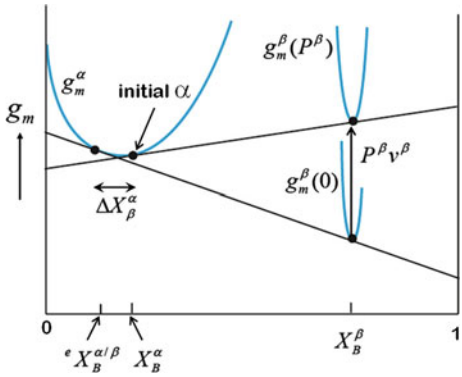

Fig. 1.55 Nucleation of β phase from α-matrix

$$g_{\mathrm{B}}(p^\alpha, p^\beta) - g_{\mathrm{B}}(0) = \frac{X_{\mathrm{A}}^\alpha p^\beta v_m^\beta - X_{\mathrm{A}}^\beta p^\alpha v_m^\alpha}{X_{\mathrm{A}}^\alpha - X_{\mathrm{A}}^\beta} \tag{1.123}$$

A similar equation can be derived also for g_{A}. When considering a spherical β particle in an α matrix, it is usually assumed that the matrix is under atmospheric pressure and one can therefore use $p^\alpha = 0$. One then obtains a diagram shown in Fig. 1.55. The compositional change, $\Delta X_{\mathrm{B}}^\alpha$ (for small values), can be written as

$$\Delta X_{\mathrm{B}}^\alpha = \frac{p^\beta v_m^\beta}{d^2 g^\alpha / dX_{\mathrm{B}}^2 \cdot \left(X_{\mathrm{B}}^\beta - X_{\mathrm{B}}^\alpha\right)} \tag{1.124}$$

By inserting $p^\beta = \frac{2\gamma}{r}$ and utilizing the regular solution model, one obtains

$$\Delta X_{\mathrm{B}}^\alpha = \frac{2\gamma v_m^\beta X_{\mathrm{A}}^\alpha X_{\mathrm{B}}^\alpha}{r\left(RT - 2L_{AB}^\alpha X_{\mathrm{A}}^\alpha X_{\mathrm{B}}^\alpha\right)\left(X_{\mathrm{B}}^\beta - X_{\mathrm{B}}^\alpha\right)} \tag{1.125}$$

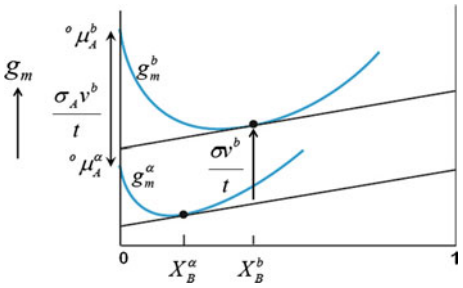

Fig. 1.56 Parallel tangent construction to investigate segregation

If both phases can vary in composition, the calculations become much more complicated.

It is also possible to use Gibbs energy diagrams to investigate the segregation of a given impurity to grain boundaries (Fig. 1.56). This involves a so-called constant volume condition. If we assume that the interface can be approximated as a thin layer of a homogeneous phase with constant thickness and its own Gibbs energy function as well as that the partial molar volumes of all the phases (including the interfacial phase) are independent of composition, we can use parallel tangent construction to find the interfacial composition. In this case, we consider exchange of atoms (A and B) between the interface and the bulk. The number of atoms at the interface is considered to be constant. Thus, if atom A leaves the interface and enters the bulk and atom B moves into opposite direction at the same time, the Gibbs free energy should not change

$$\mu_{\mathrm{A}}^{\alpha} - \mu_{\mathrm{A}}^{b} = \mu_{\mathrm{B}}^{\alpha} - \mu_{\mathrm{B}}^{b} \tag{1.127}$$

where α refers to the bulk phase and b to interface. This can be rewritten as

$$\mu_{\mathrm{B}}^{b} - \mu_{\mathrm{A}}^{b} = \mu_{\mathrm{B}}^{\alpha} - \mu_{\mathrm{A}}^{\alpha} \tag{1.128}$$

which gives the slopes for the interfacial phase and for the bulk phase

$$\frac{dg^{b}}{X_{\mathrm{B}}} = \frac{dg^{\alpha}}{X_{\mathrm{B}}} \tag{1.129}$$

For interphase segregation, where the volume is not necessarily fixed other approaches, like that of Gibbs surface excess model, must be utilized. Any change of γ due to an appreciable addition of B can be obtained directly from the molar Gibbs energy diagram. For instance, if one wants to estimate the maximum segregation to a grain boundary (which can possibly occur), the construction shown in Fig. 1.57 can be used. This is based on the fact that the maximum amount to segregate must certainly be less than the segregation needed in order to make the surface tension

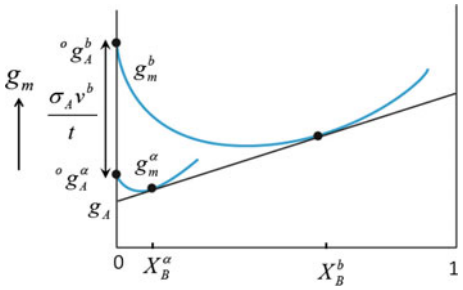

Fig. 1.57 The determination of the upper limit for segregation

to disappear, as this has never been observed experimentally. The surface tension will vanish when the two parallel tangents coincide as shown in Fig. 1.57. This gives the hypothetical upper limit for interfacial segregation. Several more advanced treatments of intergranular segregation have been published during recent decades [20–22].

1.15.2 Ternary Molar Gibbs Energy Diagrams

The molar Gibbs free energy diagrams for ternary systems can also be conveniently drawn, as shown in Fig. 1.58. In this case, the molar Gibbs energies of solution phases are represented by surfaces instead of curves and the common tangent construction is replaced by a common tangent plane. In Fig. 1.58, the ternary equivalent of the process shown in Fig. 1.18 is presented. As mentioned above, the chemical equilibrium condition of the equal value of the chemical potential of each component leads to the common tangent construction in a binary system and to the *common tangent plane* construction in a ternary system. In the latter case, the values for the chemical potentials are read from the intersections of the tangent plane with the three edges of the diagram. As shown in Fig. 1.58, the tangent plane is allowed to roll under the given Gibbs energy surfaces until a common tangent plane for the curves is established. Figure 1.58a shows the starting point of the process. The initial compositions of the phases are given by the points where the tangent plane touches the free energy surface of the given phase. The values for the chemical potentials for each component in a given phase are obtained for the intersection points of the corresponding tangent planes. As can be seen, the chemical potentials for components A, B, and C are hardly equal in the two phases to start with. Thus, there is driving force for diffusion of the components. The tangent plane drawn with green color belongs to the β-phase (blue curve) and that with red to the α-phase (red curve). The plane drawn with black lines shows the Gibbs energy for a purely mechanical mixture of A, B, and C. From the composition profile in Fig. 1.58a, it can be seen that no interdiffusion

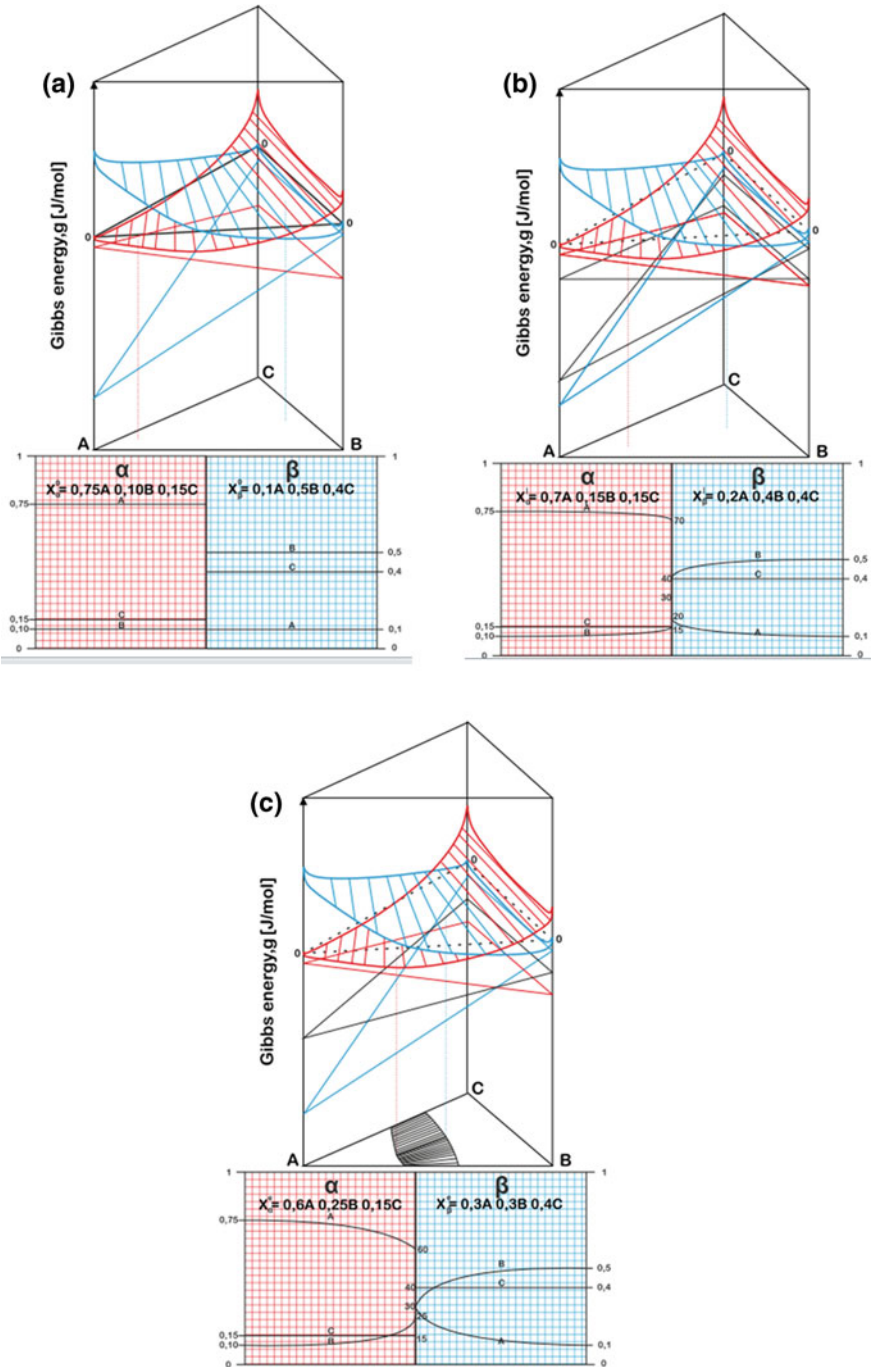

Fig. 1.58 **a** Ternary Gibbs energy diagram with composition profile showing the initial situation for the diffusion couple α/β. **b** Ternary Gibbs energy diagram with composition profile showing the situation for the diffusion couple α/β after some interdiffusion has taken place, but the equilibrium has not been reached. **c** Ternary Gibbs energy diagram with composition profile showing the final equilibrium situation for the diffusion couple α/β

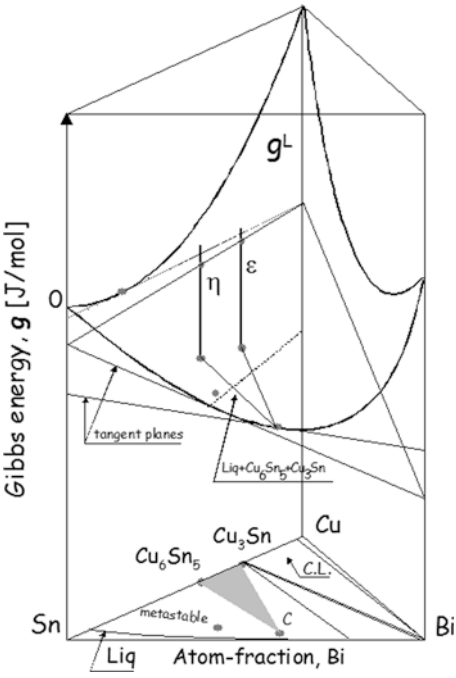

Fig. 1.59 Ternary molar Gibbs energy diagram from the BiCuSn system at 235 °C [17]

has taken place. As can be seen from Fig. 1.58b, the tangent planes start to roll under the Gibbs free energy surfaces and, consequently, the chemical potentials of the components start to change. It is evident that Fig. 1.58b represents an intermediate stage in the process as the chemical potentials for components A, B, and C are not yet equal in both phases. From the composition profile of the α/β-diffusion couple in Fig. 1.58b, it can be seen that the compositions at the interface have been changed. Further, it is noticed that only components A and B diffuses in this case and component *C* is immobile. The end-member compositions are unaffected by the diffusion process as required (See Chap. 3 for further discussion). The final equilibrium situation is given in Fig. 1.58c, in which the common tangent plane is shown. As can be seen, the chemical potentials for the components are now equal at each phase and thus, the chemical equilibrium condition is fulfilled.

Another example from a ternary Gibbs energy diagram is shown in Fig. 1.59 which represents the stability of phases in the BiCuSn system at 235 °C. There are two intermetallic compounds, (Cu_6Sn_5 (η) and Cu_3Sn (ε)), which enter the stable equilibrium at this temperature. A vertical section ($SnBi_{eut} \rightarrow Cu$) through this diagram is shown in Fig. 1.60. As can be seen, the section resembles the Gibbs energy diagram of the binary Cu-Sn system, but it is not exactly the same. The "tangent lines" drawn in the diagram (Fig. 1.60) are not identical to the tangent lines in Fig. 1.52, but are 2D sections through the corresponding tangent planes.

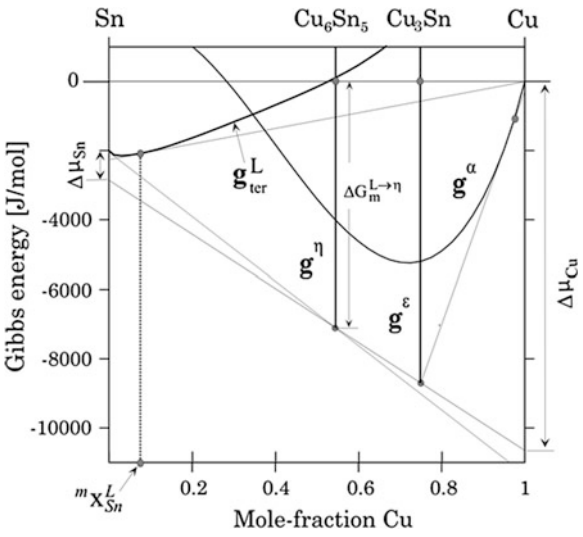

Fig. 1.60 A vertical section through the Gibbs energy diagram shown in Fig. 1.59 [17]

1.16 Interdependence of Chemical Potentials: Gibbs–Duhem Equation

In this section, we shall derive the Gibbs–Duhem relation, which will be useful in proceeding chapters to find the relation between diffusion under chemical potential gradient with the diffusion in the absence chemical potential gradient as the driving force. From our point of view, the application of Gibbs–Duhem equation to obtain the change in the chemical potential because of the change in composition of an alloy is the most important use of the general relation. For the sake of explanation, let us consider the free energy versus composition diagram, as shown in Fig. 1.61. First, we consider the point P and from the slope at that we can determine the chemical potential of elements A and B at that point as μ_A^P and μ_B^P, respectively. Now suppose we make a small change in the composition and move to the point Q. Again from the slope of the free energy at that point, we can find the chemical potential of elements as μ_A^Q and μ_B^Q. So it is apparent that the change in chemical potential of elements, A and B, because of the change in composition is $-d\mu_A = \left(\mu_A^Q - \mu_A^P\right)$ and $-d\mu_B = (\mu_B^Q - \mu_B^P)$, respectively. Further, from any point P or Q, it can be written that

$$-\frac{d\mu_A}{X_B} = \frac{d\mu_B}{X_A} = \frac{d(\mu_B - \mu_A)}{1} \tag{1.130}$$

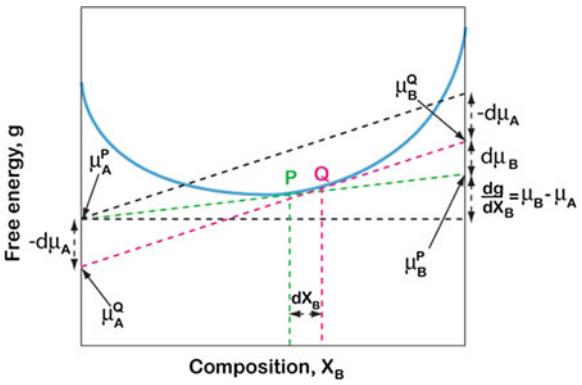

Fig. 1.61 The change in chemical potential because of the change in composition is shown to derive the Gibbs–Duhem equation

Further, from the slope, we can write

$$\frac{dg}{dX_B} = \frac{\mu_B - \mu_A}{1} \tag{1.131}$$

Combining Eqs. 1.130 and 1.131 and multiplying $X_A X_B$, the expression becomes

$$-X_A d\mu_A = X_B d\mu_B = X_A X_B \frac{d^2 g}{dX_B^2} dX_B \tag{1.132}$$

Further, it can be shown that

$$\frac{d^2 g}{dX_B^2} = \frac{d^2 g}{dX_A^2} \tag{1.133}$$

It follows that

$$X_A d\mu_A + X_B d\mu_B = 0 \tag{1.134}$$

Equation 1.134 is known as Gibbs Duhem equation. It illustrates clearly that chemical potentials, or any other partial thermodynamic properties [5], cannot be changed independently. On the contrary, for example, in a binary system considered here, when the one chemical potential is changed, the other one must change also. This is evident also in ternary systems as shown in Fig. 1.58a–c. Further, we can derive one another useful relation from Eq. 1.134. From Eqs. 1.132 and 1.133 follows

$$-X_A \frac{d\mu_A}{dX_B} = X_B \frac{d\mu_B}{dX_B} = X_A X_B \frac{d^2 g}{dX_B^2} = X_A X_B \frac{d^2 g}{dX_A^2} \tag{1.135}$$

and consequently,

$$\mu_B =^{\circ} \mu_B + RT \ln a_B =^{\circ} \mu_B + RT \ln \gamma_B X_B \tag{1.136a}$$

$$\mu_A =^{\circ} \mu_A + RT \ln a_A =^{\circ} \mu_A + RT \ln \gamma_A X_A \tag{1.136b}$$

From Eq. 1.136, the following expression can be obtained

$$\frac{d\mu_B}{dX_B} = RT\left[\frac{d\ln\gamma_B}{dX_B} + \frac{d\ln X_B}{dX_B}\right] = RT\left[\frac{1}{\gamma_B}\frac{d\gamma_B}{dX_B} + \frac{1}{X_B}\right] = \frac{RT}{X_B}\left[1 + \frac{d\ln\gamma_B}{d\ln\gamma_B}\right]$$
$$\frac{d\mu_B}{dX_B} = \frac{RT}{X_B}\frac{d\ln a_B}{d\ln X_B} \tag{1.137}$$

Similarly from Eq. 1.137, since $X_A + X_B = 1$, follows

$$\frac{d\mu_A}{dX_B} = -RT\left[\frac{d\ln\gamma_A}{dX_A} + \frac{d\ln X_A}{dX_A}\right] = -RT\left[\frac{1}{\gamma_A}\frac{d\gamma_A}{dX_A} + \frac{1}{X_A}\right] = \frac{RT}{X_B}\left[1 + \frac{d\ln\gamma_A}{d\ln\gamma_A}\right]$$
$$\frac{d\mu_A}{dX_B} = \frac{RT}{X_B}\frac{d\ln a_A}{d\ln X_A} \tag{1.138}$$

Using Eq. 1.137 in Eq. 1.138, we obtain

$$\frac{d\ln a_A}{d\ln X_A} = \frac{d\ln a_B}{d\ln X_B} = \frac{X_A X_B}{RT}\frac{d^2 g}{dX_A^2} = \frac{X_A X_B}{RT}\frac{d^2 g}{dX_B^2} \tag{1.139}$$

This is again the thermodynamic factor discussed in Sect. 1.15.

1.17 Molar Volume of a Phase and Partial Molar Volumes of the Species

Many times it is important to determine the molar volume of the phases and partial molar volume of the species. By definition, the molar volume, v_m, of a phase can be determined from

$$v_m = \frac{v_{cell}}{n_a} N_{Avo} \tag{1.140}$$

where $v_{cell}(m^3)$ is the volume of the unit cell determined from the known data on the lattice parameters available in the literature, N_0 is the Avogadro number (6.023×10^{23} mol^{-1}), and n_a is the number of atoms in the unit cell.

When virtually no structural vacancies are present in a unit cell, the number of atoms, n_a, in the last equation can be replaced by the number of lattice sites, n_s.

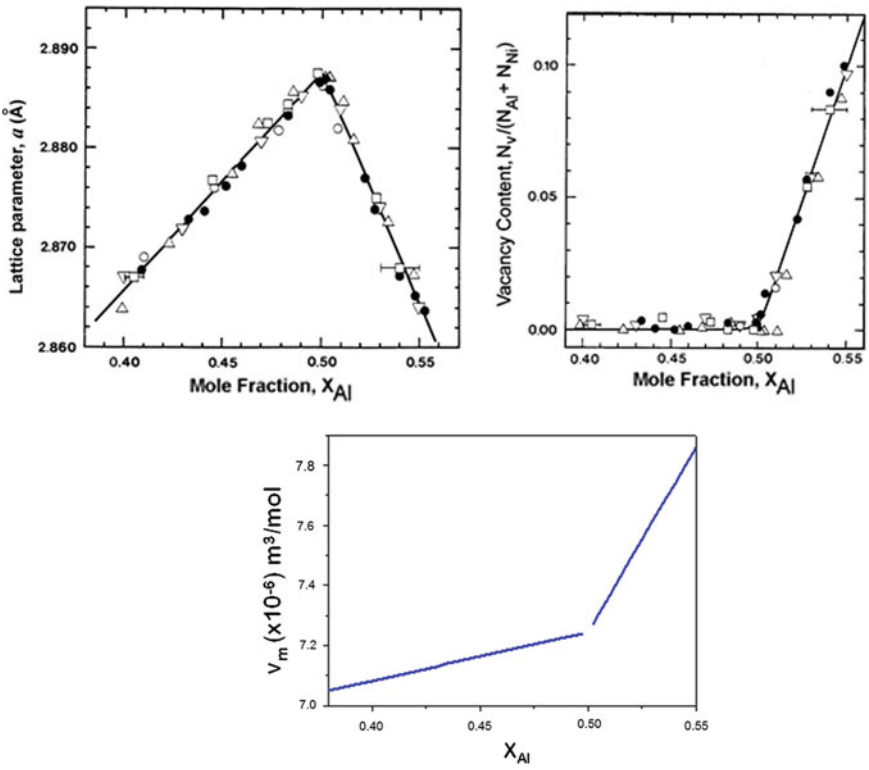

Fig. 1.62 The change in **a** lattice parameter and **b** vacancy concentration of NiAl phase and **c** molar volume of the phase (**a** and **b** are from [23])

We can neglect the amount of thermal vacancies, since this number is very small. On the other hand, when constitutional vacancies are created in the structure and if the number is appreciable, we should consider this for the calculation of molar volumes. In this case, we can write $n_a = n_s - n_V$, with n_V being the number of vacancies present in the unit cell.

So, when there are no structural vacancies present in the structure, the calculation of molar volume is rather straightforward. However, for further clarification, we like to extend our discussion to the calculation which contains structural vacancies. For this purpose, we consider the B2 NiAl phase in an Ni–Al system. The homogeneity range of the B2 phase is shown in Fig. 1.62. It can be seen that there is a wide homogeneity range on both sides of the stoichiometry. As will be discussed in Chap. 2, deviation from the homogeneity in the Ni-rich side is achieved by the Ni-antisite defects (Ni_{Al} that is Ni atom occupying the sublattice belongs to Al atom), whereas deviation in the Al-rich side is achieved by the presence of triple defect ($2V_{Ni} + Ni_{Al}$ composed of two vacancies in sublattice belonging to Ni atoms and one Ni atom occupying a site in a sublattice belonging to Al atoms).

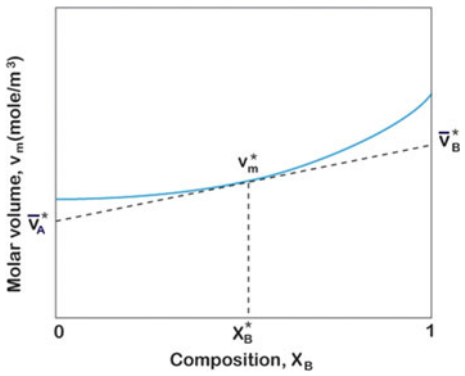

Fig. 1.63 The determination of partial molar volume of the species, *A* and *B* in a binary system is shown

So to calculate the molar volume in the Ni-rich side is straightforward and the number of lattice positions can be used to count the number of atoms. However, in the Al-rich side, we need to consider the number of antisites for the calculation of molar volume. The molar volume of the phase at different compositions can be calculated from the available data on the lattice parameter and vacancy concentration, as shown in Fig. 1.62a and b, respectively. The calculated molar volume of the phase is shown in Fig. 1.62c.

The partial molar volume of the species can be defined as the change in molar volume because of the addition of a very small amount of the species. The partial molar volume of the species A$(\bar{v}_A)$ and B$(\bar{v}_B)$ is related with the molar volume of a phase, or an alloy (v_m) is related by

$$v_m = X_A \bar{v}_A + X_B \bar{v}_B \tag{1.141}$$

Thus, the partial molar volume of the species at a particular composition, X_B^*, can be calculated by taking slope at v^* from the molar volume versus composition diagram, as shown in Fig. 1.63. The values $\bar{v}_A^*$ and $\bar{v}_B^*$ are the partial molar volumes of the species A and B, respectively, at X_B^*. This is a property diagram similar to that which was extensively used in Sect. 1.15 (the molar Gibbs energy diagram).

1.18 Few Standard Thermodynamic Relations

Derivations for a few relations can be found in [24]. We have previously shown that the mole fraction and the atomic fraction are the same in the systems we have considered. We commonly present the diffusion data with respect to atomic fraction or atomic percentage, and we shall use them for further derivations.

$$N_A + N_B = 1 \tag{1.142}$$

where N_A and N_B are the atomic fractions of A and B.

$$\begin{aligned} C_A &= \frac{X_A}{v_m} = \frac{N_A}{v_m} \\ C_B &= \frac{X_B}{v_m} = \frac{N_B}{v_m} \end{aligned} \tag{1.143}$$

where C_i is the concentration of species i and v_m is the molar volume at the composition of interest.

$$N_A \bar{v}_A + N_B \bar{v}_B = v_m \tag{1.144}$$

where ν_i is the partial molar volume of the species i. By utilizing (1.142 and 1.143), we get

$$C_A + C_B = \frac{N_A}{v_m} + \frac{N_B}{v_m} = \frac{(N_A + N_B)}{v_m} = \frac{1}{v_m} \tag{1.145}$$

On the other hand by substituting $N_i = C_i v_m$ from (1.143) to (1.144), we obtain

$$\begin{aligned} C_A v_m \bar{v}_A + C_B v_m \bar{v}_B &= v_m \\ v_m (C_A \bar{v}_A + C_B \bar{v}_B) &= v_m \\ C_A \bar{v}_A + C_B \bar{v}_B &= 1 \end{aligned} \tag{1.146}$$

Since the molar volumes also follow Gibbs–Duhem relation, which was presented in Sect. 1.16, we can write

$$X_A d\bar{v}_A + X_B d\bar{v}_B = 0 \quad \text{or} \quad N_A d\bar{v}_A + N_B d\bar{v}_B = 0 \tag{1.147}$$

By multiplying this with total concentration C, one gets $C(N_A d\bar{v}_A + N_B d\bar{v}_B) = 0$ $(C_A + C_B)(N_A d\bar{v}_A + N_B d\bar{v}_B) = 0$, and from (1.145), we see that $\left(\frac{1}{v_m}\right)(N_A d\bar{v}_A + N_B d\bar{v}_B) = 0$, which based on (1.143) reduces to

$$C_A d\bar{v}_A + C_B d\bar{v}_B = 0 \tag{1.148}$$

When taking total differential from (1.146), we get

$$C_A d\bar{v}_A + C_B d\bar{v}_B + \bar{v}_A dC_A + \bar{v}_B dC_B = 0$$

According to (1.148), the first two terms are zero and, thus,

$$\bar{v}_A dC_A + \bar{v}_B dC_B = 0 \tag{1.149}$$

When we consider that molar volume is not constant

$$dC_{\mathrm{A}} = \left(\frac{\bar{v}_{\mathrm{B}}}{v_m^2}\right) dN_{\mathrm{A}}$$
$$dC_{\mathrm{B}} = \left(\frac{\bar{v}_{\mathrm{A}}}{v_m^2}\right) dN_{\mathrm{B}} \tag{1.150}$$

References

1. K. Denbigh, The Principles of chemical equilibrium, 3rd ed., Cambridge University Press, Cambridge, U.K, 1978.
2. E.A. Guggenheim, Thermodynamics, Elsevier Science, The Netherlands, 1967.
3. D. Kondepudi and I. Prigogine, Modern Thermodynamics From Heat Engines to Dissipative Structures, Wiley, 1998.
4. P. Atkins and J. DePaula, Physical Chemistry, Macmillan Higher Education, 2009.
5. N. A. Gokcen, Thermodynamics, Techscience incorporated, 1975.
6. J.K. Kivilahti, Theory of metallic solutions, Otakustantamo, 1982, (in Finnish).
7. L. Darken and R. Gurry, Physical Chemistry of Metals, McGraw-Hill, (1953).
8. G.N. Lewis and M. Randall, Thermodynamics, revised by K. Pitzer and L. Brewer, McGraw-Hill, 1961.
9. D. Gaskell, Introduction to Metallurgical Thermodynamics, McGraw-Hill, Tokyo, 1973.
10. M. Hillert, Phase Equilibria, Phase Diagrams and Phase Transformations: Their Thermodynamic Basis, Cambridge Univ. Press, 1998.
11. H. Lukas, S. Fries, and B. Sundman (2007) Computational Thermodynamics- The Calphad Method, Cambridge University Press (2007).
12. Rönkä K., van Loo F.J.J. and. Kivilahti J.K, Metal. Mater. Trans. A, 29A (1998) 2951.
13. T. Mattila, V. Vuorinen and J.K. Kivilahti, J. of Mater. Res. 19 (2004) 3214.
14. Laurila T., Zeng K., Molarius J., Suni I., and Kivilahti J.K., Journal of Applied Physics 91 (2002) 5391.
15. Hillert M., "The Uses of Gibbs Free Energy-Composition Diagrams", in Lectures on the Theory of Phase Transformations, (Ed. H.I. Aaronson, The Metallurgical Society of the AIME, (1975)).
16. C. Cserhati, U. Ugaste, M. van Dal, N. Lousberg, A. Kodentsov, and F.J.J. van Loo, Defect and Diffusion Forum 194-199 (2001) 189.
17. T. Laurila, V. Vuorinen and J.K Kivilahti, Materials Science and Engineering – R, R49, (1-2), pp. 1-60, (2005).
18. Laurila T, Vuorinen V. and Paulasto-Kröckel M, Materials Science and Engineering – R, R68 (2010) 1-38.
19. R. Wang and Y. Kim, Metall Trans 5 (1974) 1973.
20. E. Hondros and M. Seah, Metall. Trans. A, 8A (1977) 1363.
21. M. Guttmann, Metall. Trans. A 8A (1977) 1383.
22. E. Guggenheim, Trans. Faraday Soc, 36 (1940) 397.
23. Y.A. Chang and J.P. Neumann, Prog. Solid State Chem. 14 (1982) 221.
24. L. Trimble, D. Finn and A. Cosgarea, Acta Metallurgica 13 (1965) 501.